UNIVERSITAT DE BARCELONA

On the validity of the $\Delta I = 1/2$ Isospin Rule and the Block–Dalitz Model in Hypernuclear Non–mesonic Weak Decay

Òscar Hernández Martín

Master's Thesis

advisors:
Assumpta Parreño, Àngels Ramos

Departament de Física Quàntica i Astrofísica
and Institut de Ciències del Cosmos,
Universitat de Barcelona, E–08028 Barcelona, Spain

November 29, 2020

Abstract

A study of the non–mesonic weak decay of light hypernuclei is performed on the basis of the Block–Dalitz approach which allows one to extract the elementary $\Lambda N \to nN$ decay amplitudes and rates without detailed knowledge of the microscopic interaction mechanism. The present work analyses the validity of this approach using decay rates calculated within a one–meson–exchange transition potential supplemented by a two–pion–exchange mechanism. It is found that although the Block–Dalitz model is a reliable approximation for predicting the decay rates of s–shell hypernuclei, it fails to reproduce the ${}^{5}_{\Lambda}$He asymmetry parameter. Possible $\Delta I = 3/2$ isospin contributions to the non–mesonic decay rates are also investigated within the factorization approximation. Unfortunately, the experimental data are still of limited precision and therefore, it is not possible to extract the degree of violation of the $\Delta I = 1/2$ isospin rule. The present study introduces improvements on preceding theoretical models and, together with forthcoming J–PARC data on the non–mesonic decay of four–body hypernuclei, it will play an important role in establishing the detailed spin–isospin dependence of the $\Lambda N \to nN$ process as well as in the design of theoretical models.

Acknowledgment

M'agradaria agrair a les meves tutores, l'Assumpta i l'Àngels, la seva amable ajuda i guia en la realització d'aquest treball. No hauria estat possible sense elles. També m'agradaria agrair a les meves amigues i amics tota l'ajuda i estima que m'han donat en tota la meva formació acadèmica. Per últim, però no menys important, agrair el suport incondicional de la meva família. Gràcies de tot cor.

Contents

1 Introduction

The strangeness quantum number, S, is conserved in processes mediated by the strong and electromagnetic interactions, but not in those involving the weak force. Baryons which contain this quantum number are called hyperons. The Λ baryon is the lightest hyperon, composed by u, d and s quarks and plays an important role in a variety of processes involving strangeness. For instance, hyperons may appear in the inner core of neutron stars and they are important players in their evolution and balance, which is given by the weak interactions. The mass of the Λ particle is $m_\Lambda = 1115.68$ MeV and it has zero charge and isospin. With a mean free path and a lifetime of the order of 10 cm and 10^{-10} seconds, respectively, hyperons decay through weak processes (except the Σ^0 which decay via electromagnetic processes) which do not conserve parity, isospin or strangeness quantum number.

A hypernucleus is a bound system which contains nucleons (N) and one or more strange baryons (Y). An important point to describe the hypernuclear structure is the knowledge of the YN and YY interactions in the same way that the NN interaction serves to know the nuclear structure. Although we could obtain more direct information of the YN and YY interaction from cross section measurements, these are very difficult due to the short hyperon mean free path. For this reason, quantitative information of these interactions comes mainly from the study of production and decay of hypernuclei. The existence of these systems gives a new vision to the traditional nuclear physics, as for example the possibility of new selection rules and states with new symmetries. In fact, the study of strange nuclei have opens the door to studies of other exotic systems, as the ones in the charm sector. In addition, a precise knowledge of the baryon–baryon interactions in the strange sector would allow to determine the amount of flavor SU(3) symmetry breaking due to the different values of the quark masses in the light u, d and s sector.

Hypernuclear physics was born in 1952 when Marian Danysz and Jerzy Pniewski discovered the first hypernucleus. They observed a delayed disintegration of a heavy fragment when they were working with emulsion chamber experiments [1]. These observations based on emulsion and bubble chambers motivated new experiments of hypernuclear production. With the advent of particle accelerators, beams of particles (usually kaons and pions) collide with a nucleon producing hyperons among the fragments of these collisions, which are then captured by a nucleus. Different reaction mechanisms are used: strangeness exchange reactions such as $n(\pi^-, K^-)\Lambda$, and associated strangeness production processes such as the hadronic $n(\pi^+, K^+)\Lambda$ reaction or the electroproduction $n(e, e'K+)\Lambda$ reaction. In these processes, hypernuclei can be created in some excited state but they reach their ground state via mechanisms mediated by the strong interaction, the electromagnetic one or by particle emission [2].

The Λ decay in free space proceeds mainly via the mesonic mode, $\Lambda \to N\pi$, in which a meson (pion, in this case) and a nucleon are detected in the final

state. This decay mode is larger than the semi–leptonic and weak radiative ones by a factor of 10^3, so the Λ hyperon decays via two different mesonic channels: $\Lambda \to p + \pi^-$ (63.9%) and $\Lambda \to n + \pi^0$ (35.8%) [3]. The experimental ratio for the free decay rates, $\Gamma^{\rm free}_{\pi^-}/\Gamma^{\rm free}_{\pi^0} \approx 1.78$, is very close to 2 and strongly suggests the dominance of $\Delta I = 1/2$ isospin transitions over the $\Delta I = 3/2$ ones, which is commonly known as the $\Delta I = 1/2$ rule for weak processes. Although this rule is well established experimentally and it turns to be valid for different processes that involve strangeness (such as the decay of the kaon meson [4]), its dynamical origin is not yet understood. Neither is it if the $\Delta I = 3/2$ suppression is a universal feature of all weak decay processes. In case of finding a significant relevance of $\Delta I = 3/2$ terms in the strangeness physics sector it would be the first indication of violation of the $\Delta I = 1/2$ selection rule. Such experimental evidence has not been found yet.

When the Λ particle is embedded in a nuclear medium, the mesonic decay mode becomes Pauli blocked because the final nucleon momentum ($p_N \approx 100$ MeV/c) is smaller than the Fermi one ($k_F \approx 270$ MeV/c). As we shall see in the following, although this mode is blocked in infinite nuclear matter, it can occur in finite nuclei under different circumstances, being less important as the mass number increases [7]. The same medium which is responsible for the suppression of the mesonic mode is also responsible for the appearance of a new decay mode, the weak non–mesonic decay which becomes dominant in hypernuclei with $A \geq 5$. Hence, except for the very lightest ones, Λ–hypernuclei decay mainly through the non–mesonic decay, in which mesons are not detected in the final state and involves decay channels induced by one ($\Lambda N \to nN$) and two ($\Lambda NN \to nNN$) nucleons, the two nucleon–induced channel representing the $10 - 15\%$ of the total non–mesonic weak decay rate [5].

Relevant quantities for comparison between theory and experiment are the total decay width, which can be expressed in terms of the mesonic and non–mesonic decay widths, the ratio between the neutron–induced ($\Lambda n \to nn$) and proton–induced ($\Lambda p \to np$) decays, Γ_n/Γ_p, and the asymmetry in the angular distribution of the nucleons from the weak decay of hypernuclei. This asymmetry arises from the interference between the parity–conserving (PC) and parity–violating (PV) amplitudes on the weak decay mechanism, as we will see in Section 3. The total decay rate of a Λ–hypernucleus is then:

$$\Gamma_{\rm T} = \Gamma_{\rm M} + \Gamma_{\rm NM} \ , \tag{1}$$

where

$$\Gamma_{\rm M} = \Gamma_{\pi^-} + \Gamma_{\pi^0} \ , \quad \Gamma_{\rm NM} = \Gamma_p + \Gamma_n + \Gamma_2 \ , \tag{2}$$

where Γ_2 stands for the two–nucleon induced channel ($\Lambda nn \to nnn$, $\Lambda np \to nnp$, $\Lambda pp \to npp$).

Although it is true that the total width is well reproduced by different models, one of the problems that hypernuclear studies had to face for many years was to

reconcile experimental and theoretical values for the Γ_n/Γ_p and for the asymmetry parameter [2,6–8]. There were many efforts devoted to provide a theoretical explanation of the large experimental values obtained for this ratio. These experimental results were quite scarce and not precise, so they presented large uncertainties due to, in part, the difficulty of detecting the products of non–mesonic decay, especially the neutrons. Essentially, two kinds of approaches are available for predicting the decay rates and the asymmetry parameters of Λ–hypernuclei. The first one consists in a finite nucleus formalism where by using a weak coupling scheme and a shell model approach, the many–body transition amplitude is expressed in terms of the two–body amplitudes calculated using a meson–exchange potential. Other approaches include a many–body technique in which the calculation is performed in infinite nuclear matter and then it is extended to finite nuclei through the local density approximation. [6, 9].

Given the impossibility of generating stable hyperon beams, hypernuclear decay offers us the best scenario to study the weak $\Lambda N \to nN$ interaction. Moreover, using the change of strangeness as a signature, this mechanism allows us to extract more information than the strangeness 0 counterpart, the weak NN interaction, since one can explore not only the the parity–violating part of baryon–baryon interaction but also the parity–conserving one.

The non–mesonic decay can be understood in terms of the free–space mechanism, where the virtual pion emitted at the weak vertex, $\Lambda N\pi$, is absorbed by a nucleon in the system. Although this one–pion-exchange process (OPE) generates good estimations for the total non–mesonic decay rate, the model fails to reproduce the Γ_n/Γ_p ratio. The reason lies in the tensor dominance of the pion-exchange mechanism, which favors the p–induced process leading to np pairs in the final state. Due to the large momentum of the final nucleon ($k \approx$ 400MeV/c), it is advisable to include not only long–range contributions (those generated by the pion) but also short–range contributions generated by heavier mesons. The OPE model was generalized to a one–meson–exchange model (OME) including the mesons of the pseudoscalar (η, π, K) and the vector octets (ρ, w and K^*) [10]. Although the OME model describes the non–mesonic rates and the ratio Γ_n/Γ_p satisfactorily, it predicts a too large and negative asymmetry parameter. Fortunately, recently these problems were resolved [8]. The degree of development reached in the last years permitted to achieve a reasonable agreement between theory [11–23] and experiment [24–32]. In particular, within a finite nucleus framework which adopted a OME model supplemented by a chirally motivated (correlated plus uncorrelated) two–pion exchange models (TPE), it was possible to reproduce the asymmetry and the decay rates of ${}^{5}_{\Lambda}$He and ${}^{5}_{\Lambda}$C [11]. As we will see in the following, the correlated ($2\pi/\sigma$) and uncorrelated (2π) two–pion exchanges drastically modify the asymmetry parameter while exerting a moderate effect on the decay rates. However, although the OME+TPE model was able to reproduce the measured observables of non–mesonic decay, the discrepancies between various models fall within the large error bars of the experimental data, meaning that the weak decay of hy-

pernuclei is not yet properly understood.

Other models have been developed to address some of the observed discrepancies between theory and experiments. Among them, hybrid models combining quark and meson degrees of freedom [33] or calculations based on effective field theories [34].

In the present work, we will study the weak non–mesonic decay based on the OME and OME+TPE models for different hypernuclei using the finite nucleus approach. The Λ particle can interact with the nucleons of the s, p or higher shells, involving a relative angular momentum of the ΛN pair $L \neq 0$. In our case, we will consider s–shell hypernuclei since it has the merit of considerably reducing the number of possible states for the initial state (and thus the final state) by considering the ΛN pair in a relative angular momentum of $L = 0$. Possible violations of the $\Delta I = 1/2$ rule are discussed using the phenomenological Block–Dalitz model, whose limits of applicability have not been discussed to date. Although this approach starts from a contact interaction which does not consider the long–range effects of the exchange model, we will see that it will be extremely good in reproducing the decay rates of light hypernuclei in terms of a few elementary spin–isospin rates for the $\Lambda n \to nn$ and $\Lambda p \to np$ processes without detailed knowledge of the microscopic interaction mechanism.

This work is organized as follows. In Section 2 we briefly detail the main characteristics of the mesonic and the non–mesonic weak decay, as well as the finite nucleus formalism used for the calculation of the decay rates and asymmetries. The weak transition potential is based on one–meson–exchange and one–meson–exchange plus two–pion–exchange. In Section 3 the approach of Block–Dalitz to the non–mesonic weak decay of s–shell hypernuclei is discussed. Numerical results obtained with the finite nucleus calculation for the decay rates and the asymmetries of four– and five–body hypernuclei are presented in Section 4, together with a discussion on the reliability of the Block–Dalitz model. Moreover, possible violations of the selection isospin rule $\Delta I = 1/2$ are investigated by adopting the factorization approximation of Ref. [35]. Finally, some concluding remarks are given in Section 5.

2 Hypernuclear weak decay

In order to discuss the weak decay modes of hypernuclei, it is convenient to introduce the Fermi gas model. This model defines the properties of an infinite system of non–interacting identical fermions which obey the Pauli exclusion principle. In the isospin picture, nuclear matter is made up of nucleons (proton and neutron are two states of the same particle, the nucleon) with mono–particular states described by plane wave functions. The energy and the single–particle nucleon wave function read:

$$\Phi_{\vec{k}} = \frac{1}{\sqrt{V}} e^{i\vec{k}\vec{r}} \chi^s_{m_s} \chi^t_{m_t} \ , \qquad E = \frac{\hbar^2 k^2}{2m_N} \ , \tag{3}$$

where the two χ's denote the spin and isospin states. According to the Pauli principle, each nucleon in this system occupies a different mono–particular state with one of the two possible values of the third spin component, $m_s \pm 1/2$ and one of the two possible values of isospin, $m_t \pm 1/2$. The maximum value of $|\vec{k}|$ corresponding to the occupied states in the ground state is the Fermi momentum, k_F. Therefore, the density reads:

$$\rho(r) = \sum_{k<k_F} |\Phi_{\vec{k}}|^2 = \frac{2}{3\pi^2} k_F^3 \ . \tag{4}$$

Using the normal nuclear matter density, $\rho(r) \approx \ 0.16$ fm^{-3}, one obtains $k_F = 270$ MeV/c .

The Λ hyperon production takes place by collision reactions between different kind of mesons (pions and kaons) and a nucleus by means of processes such as the $n(K^-, \pi^-)\Lambda$ and $n(\pi^+, K^+)\Lambda$ reactions. The creation of Λ–hypernuclei requires that the Λ particle created in these reactions remains in the nuclear system. As we already mentioned, the free Λ decays mainly via two mesonic weak decay modes ($\Lambda \to \pi^- p, \pi^0 n$). Using energy–momentum conservation, it is possible to evaluate the Q–value and the final momentum:

$$m_\Lambda \approx \sqrt{\vec{p}^2 + m_\pi^2} + \sqrt{\vec{p}^2 + m_N^2} \ , \tag{5}$$

$$Q \approx m_\Lambda - m_\pi - m_N \approx 35 \text{ MeV} \ , \tag{6}$$

$$p \approx 100 \text{ MeV/c} \ . \tag{7}$$

Inside the hypernucleus, the hyperon and the nucleon feel the action of attractive mean fields U_N and U_Λ, which come from the NN and ΛN interactions, respectively. The binding energies of the recoil nucleon ($B_N \simeq -8$ MeV) and of the Λ ($B_\Lambda \geq -27$ MeV) affect the above expressions [36]. $Q_{\rm bound} = Q + B_\Lambda - B_N$ is smaller than the free Q–value and hence tends to reduce p.

Since the Fermi momentum is $k_F \approx 270$ MeV/c, the mesonic weak decay process becomes Pauli blocked due to the fact that final momentum ($\vec{p}$) is not large

enough to access unoccupied stated in nuclear matter. This Pauli blocking is logically much larger if one considers the Λ and N binding energy. Although the mesonic weak decay is strictly forbidden in infinite nuclear matter it can occur in finite nuclei due to different reasons. Firstly, the density distribution of a finite nucleus makes the Fermi momentum to become r–dependent (namely a local Fermi momentum) and it is smaller at the nuclear surface, allowing more available states for the final nucleon as compared to infinite nuclear matter. Secondly, the final nucleon wave function can have larger momentum components due to the momentum distribution of the Λ wave function in a final hypernucleus. Finally, the final pion feels an attraction by the nuclear medium and, thus, it has a smaller energy than the free one which leaves the final nucleon with a larger energy and has more chances to exceed Pauli blocking. This increase can be of one or two orders of magnitude for heavy hypernuclei whereas is smaller for light and medium ones with respect to the value obtained without the medium distortion [7, 36].

Nevertheless, at the end, these effects do not prevent a strong decrease of the mesonic weak decay as the mass number increases. However, the same medium which is responsible for the Pauli blocking is also responsible for the non–mesonic weak decay. In this new mechanism pions do not appear in the final state. Proceeding as in the previous case, the final nucleon momentum and the Q–value are:

$$m_\Lambda + m_N \approx \sqrt{\vec{p}^2 + m_N^2} + \sqrt{\vec{p}^2 + m_N^2} \ , \tag{8}$$

$$Q \approx m_\Lambda - m_N = 175 \text{ MeV} \ , \tag{9}$$

$$p \approx 415 \text{ MeV/c} \ , \tag{10}$$

for one–nucleon– ($\Lambda N \to nN$) and

$$m_\Lambda + 2m_N \approx 3\sqrt{\vec{p}^2 + m_N^2} \ , \tag{11}$$

$$Q \approx m_\Lambda - m_N = 175 \text{ MeV} \ , \tag{12}$$

$$p \approx 340 \text{ MeV/c} \tag{13}$$

for two–nucleon–induced processes ($\Lambda NN \to nNN$).

As we can see, the final momentum is larger than the Fermi one, so the produced nucleons are almost free from Pauli blocking. In case of assuming a finite nucleus, the transition will even be more favorable. As a consequence, the non–mesonic decay mode dominates over the mesonic one for all but the s–shell hypernuclei. For very light systems the two decay modes are competitive.

2.1 Non–mesonic decay rate

In this section, we describe the hypernuclear weak decay rates in terms of the initial and final wave function and the two–body mechanism, which involves the weak and the strong interactions.

The decay rate for a hypernucleus decaying non–mesonically in finite nuclei is written in terms of a transition amplitude, $\mathcal{M}_{fi}$, from an initial hypernuclear state $({}^{A}_{\Lambda}Z)$ to a final state, which is divided into two final free nucleons (1 and 2) and a residual nucleus state (R) composed by (A - 2) particles [37]. The finite nucleus approach has been used only for describing one–nucleon–induced decays in such a way that:

$$\Gamma_1 = \int \frac{d^3k_1}{(2\pi)^3} \int \frac{d^3k_2}{(2\pi)^3} \sum_{\substack{M_{3I}(R) \\ (1)(2)}} (2\pi)\delta(M_H - E_R - E_1 - E_2) \times \frac{1}{2J_I + 1} \mid \mathcal{M}_{fi} \mid^2 \ , \tag{14}$$

where M_H, E_R, E_1 and E_2 are the mass of the initial hypernucleus, the energy of the residual state and the energies of the final nucleons, respectively. The integrals in the momentum space cover the momenta $\vec{k_1}$ and $\vec{k_2}$ of the two final outgoing nucleons. In this expression, the integration over the momentum of the residual nucleus has already been performed using momentum conservation. Since we consider the case in which we do not measure the final polarization and we do not know the initial one, we average over the initial hypernucleus spin projections (M_{3I}) and sum over all final spin projection quantum numbers $((R), (1), (2))$.

The nuclear transition amplitude is expressed as:

$$\mathcal{M}_{fi} = \langle F \mid M \mid I \rangle = \langle \Phi_{\vec{k}_1 m_{s_1} t_{3_1}, \vec{k}_2 m_{s_2} t_{3_2}} \cdot \Phi_R^{A-2} \mid \hat{O}_{\Lambda N \to nN} \mid {}^{A}_{\Lambda} Z \rangle \ , \tag{15}$$

where $\hat{O}_{\Lambda N \to nN}$ is the two–body operator acting over all initial ΛN pairs. For the purpose of describing this matrix element in terms of the two–body transition, the final state has been decomposed in products of two–nucleon (NN) $\Phi_{\vec{k}_1 m_{s_1} t_{3_1}, \vec{k}_2 m_{s_2} t_{3_2}}$ wave functions and a residual core Φ_R^{A-2} one.

Following the approach used in Ref. [10] and in order to evaluate the decay rate in terms of the two–body amplitudes involving a ΛN pair in the initial state and a NN pair in the final state, it is necessary to decouple the Λ–particle and the interacting nucleon from the nuclear system. The starting point is the weak coupling scheme in which the Λ–particle in the $\alpha_\Lambda = n_\Lambda l_\Lambda s_\Lambda j_\Lambda m_\Lambda$ orbit couples only to the nuclear–$(A-1)$ core wave function in its ground state:

$$\begin{aligned} |{}^{A}_{\Lambda} Z\rangle \equiv & |{}^{A}_{\Lambda} Z\rangle^{J_I, M_{3I}}_{T_I, T_{3I}} = \mid \alpha_\Lambda \rangle \otimes \mid A-1 \rangle \\ & = \sum_{m_\Lambda M_C} \langle j_\Lambda m_\Lambda J_C M_C \mid J_I M_{3I} \rangle \mid (n_\Lambda l_\Lambda s_\Lambda) j_\Lambda m_\Lambda \rangle \otimes \mid J_C M_C T_I T_{3I} \rangle \ , \end{aligned} \tag{16}$$

where the initial hypernuclear total angular momentum and isospin are denoted by J_I and T_I, with third projections and M_{3I} and T_{3I}, respectively. The quantum numbers of the Λ baryon are $n_\Lambda = 0$, $l_\Lambda = 0$, $s_\Lambda = \frac{1}{2}$, $j_\Lambda = \frac{1}{2}$ and $t_\Lambda = 0$ and those of the nuclear core are denoted by J_C, $T_C = T_3$, M_C and T_{3I}.

Now, the nuclear core $(A-1)$ can be written in terms of the product of a nucleon in a $\alpha_N = n_N l_N s_N j_N m_N$ orbit and a residual nuclear system composed by $(A-2)$–particles. This can be achieved by using the technique of the coefficients of fractional parentage which maintains the antisymmetry character of this residual system [38]:

$$
\begin{aligned}
\mid J_C M_C T_I T_{3I}\rangle &= \sum_{J_R T_R j_N} \langle J_C T_I \{\mid J_R T_R, j_N t_N\rangle [\mid J_R T_R\rangle \times \mid (n_N l_N s_N) j_N t_N\rangle]^{J_C M_C}_{T_I T_{3I}} \\
&= \sum_{J_R T_R j_N} \langle J_C T_I \{\mid J_R T_R, j_N t_N\rangle \\
&\times \sum_{M_R m_N} \sum_{T_{3R} t_{3i}} (J_R j_N J_C, M_R m_N M_C)(T_R t_N T_I, T_{3R} t_{3i} T_{3I}) \\
&\times \mid J_R M_R\rangle \mid T_R T_{3R}\rangle \mid (n_N l_N s_N) j_N m_N\rangle \mid t_N t_{3i}\rangle,
\end{aligned}
\tag{17}
$$

where we denote with the subscript R the quantum numbers of the residual nuclear core, and $\langle J_c M_I \{\mid J_R T_R, j_N t_N\rangle$ are the coefficients of fractional parentage.

It is convenient, at this point, to define the total momentum, $\vec{P} \equiv \vec{k}_1 + \vec{k}_2$, and relative momentum, $\vec{k} \equiv (\vec{k}_1 - \vec{k}_2)/2$, of the two outgoing final nucleons in such a way that, if we also work in a coupled two–body spin and isospin basis, the the nuclear transition amplitude can be expressed as the following form:

$$
\mathcal{M}_{fi} = \langle \Phi_R^{A-2}; \vec{P}\vec{k} S M_S T T_3 \mid \hat{O}_{\Lambda N \to nN} \mid^A_\Lambda Z\rangle \ . \tag{18}
$$

2.1.1 Two–body Spin-Isospin states

In order to establish a connection with the two–body operator in the amplitude of Eq. (18), it is convenient to work in the coupled basis. We may add the spin angular momentum $\vec{s}_1 = 1/2$ of a single–particle to the spin angular momentum $\vec{s}_2 = 1/2$ to of another single–particle. The total spin angular momentum is $\vec{S} = \vec{s_1} + \vec{s_2} = 1/2 \otimes 1/2 = 1 \oplus 0$. To these quantum numbers, the corresponding isospin ones are added. The isospin adds an extra degree of freedom which is analogous to spin. By definition, the proton state is $t = 1/2$ and $t_3 = 1/2$ and the neutron state is then, $t = 1/2$ and $t_3 =$ -1/2, where t_3 is the isospin third component. Thus, for a system of two interacting nucleons, the total isospin operator is given by $\vec{T} = \vec{t_1} + \vec{t_2} = 1/2 \otimes 1/2 = 1 \oplus 0$.

The two nucleon total wave function is:

$$
\Psi(1,2) = \phi_{coord}(1,2) \chi^S_{M_S}(1,2) \chi^T_{T_3}(1,2) \ , \tag{19}
$$

where $\chi^S_{M_S}$ and $\chi^T_{T_3}$ are the total spin and isospin wave functions with third projections M_S and T_3 respectively. Regarding the two–body radial wave function $\phi(1,2)$, we will discuss the details later.

In the coupled scheme, the two nucleons can be either in isospin triplet ($T = 1$) or singlet ($T = 0$) and in spin triplet ($S = 1$) or singlet ($S = 0$). The total spin wave function are:

$$\begin{aligned}
&\chi^S_{M_S}(1,2;S=1,M_S=1) = \chi^s_\uparrow(1)\chi^s_\uparrow(2) \ , \\
&\chi^S_{M_S}(1,2;S=1,M_S=0) = \frac{1}{\sqrt{2}}(\chi^s_\uparrow(1)\chi^s_\downarrow(2) + \chi^s_\downarrow(2)\chi^s_\uparrow(1)) \ , \\
&\chi^S_{M_S}(1,2;S=1,M_S=-1) = \chi^s_\downarrow(1)\chi^s_\downarrow(2) \ , \\
&\chi^S_{M_S}(1,2;S=0,M_S=0) = \frac{1}{\sqrt{2}}(\chi^s_\uparrow(1)\chi^s_\downarrow(2) - \chi^s_\downarrow(2)\chi^s_\uparrow(1)) \ ,
\end{aligned} \tag{20}$$

and isospin wave functions are:

$$\begin{aligned}
&\chi^T_{T_3}(1,2;T=1,T_3=1) = \chi^t_p(1)\chi^t_p(2) \ , \\
&\chi^T_{T_3}(1,2;T=1,T_3=0) = \frac{1}{\sqrt{2}}(\chi^t_p(1)\chi^s_n(2) + \chi^t_n(2)\chi^t_p(1)) \ , \\
&\chi^T_{T_3}(1,2;T=1,T_3=-1) = \chi^t_n(1)\chi^t_n(2) \ , \\
&\chi^T_{T_3}(1,2;T=0,T_3=0) = \frac{1}{\sqrt{2}}(\chi^t_p(1)\chi^t_n(2) - \chi^t_n(2)\chi^t_p(1)) \ .
\end{aligned} \tag{21}$$

Note that spin and isospin triplet states are symmetric while singlets are antisymmetric. By convention, we use the spectroscopic notation. The quantum state is denoted as ${}^{2S+1}L_J$ being $\vec{J} = \vec{L} + \vec{S}$ the total angular momentum.

Then, let us now show the available states for each ΛN and NN pair of the $\Lambda N \to NN$ transition.

ΛN initial state :

As we already mentioned, the benefit of light hypernuclei, meaning s–shell hypernuclei, is the fact that the ΛN pair is in $L = 0$. As just discussed, the total spin state can be in spin–triplet or spin–singlet state.

Thus, only ${}^1S_0$ and ${}^3S_1$ states are possible.

NN final state :

The total angular momentum conservation ($\Delta J = 0$) in the non–mesonic weak transition implies certain restrictions for the available final NN state. The action of the central potential ($\Delta L = 0, \Delta S = 0$), tensor ($\Delta L = 2, \Delta S = 2$) and PV ($\Delta L = 1, \Delta S = 1$) terms makes that the only allowed transitions are the following:

$$\begin{aligned}
&{}^1S_0 \to {}^1S_0 \qquad {}^1S_0 \to {}^3P_0 \\
&{}^3S_1 \to {}^3S_1 \qquad {}^3S_1 \to {}^3D_1 \\
&{}^3S_1 \to {}^1P_1 \qquad {}^3S_1 \to {}^3P_1
\end{aligned}$$

Table 1: Amplitudes for the $\Lambda N \to nN$ decay in s–shell hypernuclei. The spectroscopic notation $^{2S+1}L_J$ is used. I_f is the isospin of the final NN pair. PC and PV denotes parity–conserving and parity–violating channels, respectively.

Amplitude	Channel	I_f	Parity
a_p, a_n	$^1S_0 \to {}^1S_0$	1	PC
b_p, b_n	$^1S_0 \to {}^3P_0$	1	PV
c_p	$^3S_1 \to {}^3S_1$	0	PC
d_p	$^3S_1 \to {}^3D_1$	0	PC
e_p	$^3S_1 \to {}^1P_1$	0	PV
f_p, f_n	$^3S_1 \to {}^3P_1$	1	PV

As we already discussed, the final states in these process are np and nn pairs. The constraint from the Pauli principle requires that the total wave function must be completely antisymmetric. For the two nucleon system, the isospin T can either be 1 or 0. If we use $+1$ to represent a symmetric wave function and -1 to represent an antisymmetric one, then, the isospin wave function has a symmetry factor $(-1)^{T+1}$ and the spin wave function has $(-1)^{S+1}$. With regard to the space wave function, states with L=even are symmetric while L=odd are antisymmetric, being L the orbital angular momentum of the relative motion. Therefore, the orbital wave function has the $(-1)^L$ symmetry factor. To sum up, the total symmetry factor is $(-1)^{L+T+S}$ which has to be -1. Hence, $L+S+T$ must be odd. Now, we will analyse the symmetric (S) and antisymmetric (A) properties of the available final states in order to assign them to the np and/or nn states.

$$\begin{aligned}
^1S_0 \to &\quad S=0\ (\mathrm{A})\ \mathrm{L}=0\ (\mathrm{S}) &&\to I_f=1\ (\mathrm{S}) \\
^3P_0 \to &\quad S=1\ (\mathrm{S})\ \mathrm{L}=1\ (\mathrm{A}) &&\to I_f=1\ (\mathrm{S}) \\
^3S_1 \to &\quad S=1\ (\mathrm{S})\ \mathrm{L}=0\ (\mathrm{S}) &&\to I_f=0\ (\mathrm{A}) \\
^3D_1 \to &\quad S=1\ (\mathrm{S})\ \mathrm{L}=2\ (\mathrm{S}) &&\to I_f=0\ (\mathrm{A}) \\
^3P_1 \to &\quad S=1\ (\mathrm{S})\ \mathrm{L}=1\ (\mathrm{A}) &&\to I_f=1\ (\mathrm{S}) \\
^1P_1 \to &\quad S=0\ (\mathrm{A})\ \mathrm{L}=1\ (\mathrm{A}) &&\to I_f=0\ (\mathrm{A})
\end{aligned} \tag{22}$$

To sum up, the available $\Lambda N \to nN$ transition channels are given in Table 1 together with their main properties. For each transition there is an elementary $\Lambda N \to nN$ decay amplitude and the subscript n and p denotes the neutron–induced channel and proton–induced one, respectively. Note that $\Lambda n \to nn$ process has final states with isospin $I_f = 1$ only, while for $\Lambda p \to np$ both $I_f = 1$ and $I_f = 0$ are allowed.

The non–mesonic decay rate becomes

$$\Gamma_{\mathrm{NM}} = \Gamma_n + \Gamma_p \ , \tag{23}$$

where the partial decay rates are written as

$$\Gamma_i = \int \frac{d^3P_T}{(2\pi)^3} \int \frac{d^3k_r}{(2\pi)^3}(2\pi)\delta(M_H - E_R - E_1 - E_2) \sum_{S,M_S} \sum_{J_R,M_R} \sum_{T_R,T_{3R}} \frac{1}{2J_I+1}$$
$$\times \sum_{M_I} \mid (T_R \frac{1}{2} T_I, T_{3R} t_{3i} T_{3I}) \mid^2 \times \mid \sum_{T,T_3} (\frac{1}{2}\frac{1}{2} T, t_1 t_2 T_3) \sum_{m_\Lambda M_C} (j_\Lambda J_C J_I, m_\Lambda M_C M_I)$$
$$\times \sum_{j_N} \sqrt{S(J_C T_I; J_R T_R, j_N t_{3i})} \sum_{M_R m_N} (J_R j_N J_C, M_R m_N M_C)$$
$$\times \sum_{m_{l_N} m_{s_N}} (l_N \frac{1}{2} j_N; m_{l_N} m_{s_N} m_N) \sum_{m_{l_\Lambda} m_{s_\Lambda}} (l_N \frac{1}{2} j_\Lambda, m_{s_\Lambda} m_{s_N} m_\Lambda)$$
$$\times \sum_{S_0 M_{S_0}} (\frac{1}{2}\frac{1}{2} S_0; m_{s_\Lambda} m_{s_N} S_{M_0}) \sum_{T_0 T_{3_0}} (\frac{1}{2}\frac{1}{2} T_0, -\frac{1}{2} t_{3i} T_{3_0})$$
$$\times t_{\Lambda N \to NN}(S, M_S, T, T_3, S_0, M_{S_0}, T_0, T_{3_0}, l_\Lambda, l_N, \vec{P}_T, \vec{k}_r) \mid^2 \quad , \tag{24}$$

with $t_1 = -1/2$, $t_2 = 1/2$, $t_{3i} = 1/2$ for the p–induced rate and $t_1 = -1/2$, $t_2 = -1/2$, $t_{3i} = -1/2$ for the n–induced one. We denote the initial ΛN system with spin S_0 and isospin T_0 and the final antisymmetric NN state with spin S and isospin T. We note that Eq. (24) is written in terms of the two–body transition, $t_{\Lambda N \to NN}$, which contains the details of the non–mesonic weak decay process. In Eq. (24) the Λ–particle is assumed to be in a $t_\Lambda = 1/2$, $t_{3_\Lambda} = -1/2$ state, which is a practical way to impose the phenomenological $\Delta I = 1/2$ isospin rule observed in weak hadronic processes. Moreover, we write the coefficients of fractional parentage as spectroscopic factors, $S(J_C T_I; J_R T_R, j_N t_{3i}) \equiv (A-1)\langle J_C T_I \{ \mid J_R T_R, j_N t_N \rangle^2$ [10].

2.1.2 $\Delta I = 1/2$ rule

The $\Delta I = 1/2$ isospin rule reflects the dominance of the $\Delta I = 1/2$ transitions over the $\Delta I = 3/2$ ones. In the mesonic decay of a free Λ ($t_\Lambda = 0$) into a nucleon ($t_N = 1/2$) and a pion ($t_\pi = 1$), both $T = 1/2$ and $T = 3/2$ isospin final state are possible. Using isospin coupling algebra and the Clebsch–Gordan coefficients, it is possible to evaluate the relative importance of the two mesonic channels for each ΔI value.

$$|n\rangle|\pi^0\rangle \equiv |\frac{1}{2} - \frac{1}{2}\rangle|10\rangle = \sqrt{\frac{1}{3}}|\frac{1}{2}, 1; \frac{1}{2}, -\frac{1}{2}\rangle + \sqrt{\frac{2}{3}}|\frac{1}{2}, 1; \frac{3}{2}, -\frac{1}{2}\rangle \ , \tag{25}$$

$$|p\rangle|\pi^-\rangle \equiv |\frac{1}{2}\frac{1}{2}\rangle|1\text{ - }1\rangle = -\sqrt{\frac{2}{3}}|\frac{1}{2}, 1; \frac{1}{2}, -\frac{1}{2}\rangle + \sqrt{\frac{1}{3}}|\frac{1}{2}, 1; \frac{3}{2}, -\frac{1}{2}\rangle \ . \tag{26}$$

Denoting by $\Gamma^{\rm free}_{\pi^0}$ the mesonic $\Lambda \to n + \pi^0$ decay width and by $\Gamma^{\rm free}_{\pi^-}$ the mesonic $\Lambda \to p + \pi^-$ ones, the ratio of rates for $\Delta I = 1/2$ yields:

$$\frac{\Gamma^{\rm free}_{\pi^-}}{\Gamma^{\rm free}_{\pi^0}} \approx \frac{\mid \langle \pi^- p | \hat{T}_{1/2,\text{-}1/2} | \Lambda \rangle \mid^2}{\mid \langle \pi^0 n | \hat{T}_{1/2,\text{-}1/2} | \Lambda \rangle \mid^2} = \left| \frac{\sqrt{2/3}}{\sqrt{1/3}} \right|^2 = 2 \ , \tag{27}$$

while for $\Delta I = 3/2$ processes one finds:

$$\frac{\Gamma^{\rm free}_{\pi^-}}{\Gamma^{\rm free}_{\pi^0}} \approx \frac{\mid \langle \pi^- p | \hat{T}_{3/2,\text{-}1/2} | \Lambda \rangle \mid^2}{\mid \langle \pi^0 n | \hat{T}_{3/2,\text{-}1/2} | \Lambda \rangle \mid^2} = \left| \frac{\sqrt{1/3}}{\sqrt{2/3}} \right|^2 = \frac{1}{2} \ , \tag{28}$$

where the $\hat{T}_{1/2}$ and $\hat{T}_{3/2}$ operators change 1/2 and 3/2 units of isospin, respectively. Experimentally the ratio of the relevant widths is $\Gamma^{\rm free}_{\pi^-}/\Gamma^{\rm free}_{\pi^0} \approx 1.78$ [2]. As we can see above, only in the first case seems the experimental prediction to be recovered, although there is room for some amount of $\Delta I = 3/2$ contributions.

2.1.3 Initial ΛN wave function

Although the total hypernuclear system has been decomposed in terms of angular momentum coupling between the ΛN pair and the $(A$ - 2) nuclear core, it is still necessary to know the initial and final two–body wave functions. As for the Λ and N wave functions in the initial state, we use the solutions of a harmonic oscillator potential, with appropriate values of the oscillator parameters b_Λ and b_N that are adjusted to reproduce the binding energy of the Λ–particle in the considered hypernucleus and the form factor for the $(A$–1)–particle core, respectively. For ${}^{5}_{\Lambda}$He we use $b_\Lambda = 1.85$ fm and $b_N = 1.39$ fm, while $b_\Lambda = 2.04$ fm and $b_N = 1.54$ fm are taken for ${}^{4}_{\Lambda}$He and ${}^{4}_{\Lambda}$H. Working in the center of mass frame system, the initial Λ and N wave functions can be written in terms of relative (rel) and center of mass (CM) harmonic oscillator wave functions describing the ΛN system as:

$$\Phi^{\Lambda}_{100}(\frac{\vec{r}_1}{b})\Phi^{N}_{100}(\frac{\vec{r}_2}{b}) = \Phi^{rel}_{100}(\frac{\vec{r}}{\sqrt{2}b})\Phi^{CM}_{100}(\frac{\vec{R}}{\sqrt{2}b}) \ , \tag{29}$$

where $b = \frac{b_\Lambda + b_N}{2}$ is the average oscillator parameter. Consequently, the two–body transition in Eq. (24) can be factorized in terms of other transition amplitudes, which depend on relative (N_r,L_r) and CM (N_R,L_R) principal and orbital angular momentum quantum numbers of the ΛN and NN systems:

$$t_{\Lambda N \to NN} = \sum_{N_r L_r N_R L_R} X(N_r L_r N_R L_R l_\Lambda l_N) t^{N_r L_r N_R L_R}_{\Lambda N \to NN} \ , \tag{30}$$

where $X(N_r L_r N_R L_R, l_\Lambda l_N)$ are called the Moshinky brackets. For $l_\Lambda = l_N = 0$ the value is $X(101000) = 1$ [39].

Using this approach, the initial nucleon and Λ are assumed to be independent but there is a correlation between them due to the action of the strong interaction. To take this initial interactions into account, the harmonic oscillator wave function is replaced by a correlated ΛN wave function which is obtained by multiplying the uncorrelated Λ and N wave functions by a function that is adjusted to microscopic G–matrix calculations in nuclear matter. For the baryon–baryon strong interactions we take the Nijmegen soft–core model, version NSC97f [40], which has been used with success in hypernuclear structure and decay calculations. We follow the Ref. [10], where the correlation function is parametrized as:

$$f_{\Lambda N}(r) = (1 - \exp\{-r^2/a^2\})^n + br^2 \exp\{-r^2/c^2\} \ , \tag{31}$$

with $a = 0.5$ fm, $b = 0.25$ fm, $c = 1.28$ fm and $n = 2$.

2.1.4 Final NN wave function

The final wave function of the two outgoing free nucleons can be written as

$$\langle \vec{r}_1 \vec{r}_2 \mid \vec{k}_1 \vec{k}_1 s_1 m_{s_1} s_2 m_{s_2} t_1 m_{t_1} t_2 m_{t_2} \rangle = e^{i\vec{k}_1 \vec{r}_1} e^{i\vec{k}_2 \vec{r}_2} \chi^{s_1}_{m_{s_1}} \chi^{s_2}_{m_{s_2}} \chi^{t_1}_{m_{t_1}} \chi^{t_2}_{m_{t_2}} \tag{32}$$

where the four χ's are the spin and isospin states. We use relative and CM coordinates in such a way that the final state is rewritten as follows:

$$\langle \vec{R}\vec{r} \mid \vec{P}\vec{k} S M_S T M_T \rangle = e^{i\vec{P}\vec{R}} e^{i\vec{k}\vec{r}} \chi^S_{M_S} \chi^T_{T_3}, \tag{33}$$

where $\chi^S_{M_S}$ and $\chi^T_{T_3}$ are the aforementioned total spin and isospin wave function, respectively. In order to incorporate the antisymmetrization of the two–nucleon wave function, it is necessary to include the exchange of their coordinates and quantum numbers. This involves exchanging $\vec{k} \rightarrow$ -$\vec{k}$ and adding the factor $(-1)^{S+T}$. Therefore, Eq. (33) is rewritten as:

$$\langle \vec{R}\vec{r} \mid \vec{P}\vec{k} S M_S T M_T \rangle = \frac{1}{\sqrt{2}} e^{i\vec{P}\vec{R}} \left(e^{i\vec{k}\vec{r}} - (-1)^{S+T} e^{-i\vec{k}\vec{r}} \right) \chi^S_{M_S} \chi^T_{M_T} \ . \tag{34}$$

Moreover, it is also possible to incorporate interaction effects between the two outgoing nucleons by substituting the plane wave function by a distorted wave function, which is the solution of the Lippmann–Schwinger equation with an appropriate NN potential. The Lippmann–Schwinger equation is

$$\mid \Phi^{(\pm)} \rangle = \mid \phi \rangle + \frac{1}{E - H_0 \pm i\epsilon} V \mid \Phi^{(\pm)} \rangle \ , \tag{35}$$

where $\mid \phi \rangle$ represents a solution of the free Hamiltonian H_0, E is the energy of the two final nucleon state represented by $\mid \Phi^{(\pm)} \rangle$. The plus (minus) signs denotes states at infinite time before (after) the interaction. Multiplying Eq. (35) by the potential V and defining $V \mid \Phi^{(\pm)} \rangle \equiv T^{\pm} \mid \phi \rangle$, one obtains the T–matrix equation.

$$T^{\pm} = V + V G_0^{\pm} T^{\pm}, \tag{36}$$

Table 2: Possible $^{2S+1}L_J$ channels in the weak decay (WD) of s–shell hypernuclei incorporating the strong final state interaction (FSI)

$\Lambda N(L_r)$	WD	NN (L')	FSI	NN (L)
$^1S_0$	$\longrightarrow$	$^1S_0$	$\longrightarrow$	$^1S_0$
$^3S_1$	$\longrightarrow$	$^3S_1$	$\longrightarrow$	$^3S_1$, $^3D_1$
$^3S_1$	$\longrightarrow$	$^3D_1$	$\longrightarrow$	$^3D_1$, $^3S_1$
$^1S_0$	$\longrightarrow$	$^3P_0$	$\longrightarrow$	$^3P_0$
$^3S_1$	$\longrightarrow$	$^1P_1$	$\longrightarrow$	$^1P_1$
$^3S_1$	$\longrightarrow$	$^3P_1$	$\longrightarrow$	$^3P_1$

where $G_0^{\pm} = (E - H_0 \pm i\epsilon)^{-1}$ is the free–space Green's function. Once the T–matrix equation has been solved and using the previous equations and definitions, the correlated NN wave function (Φ) is obtained. We will denote as $\Phi_{\vec{k}}$ in the relative and center of mass coordinates. Therefore, the free wave function $e^{i\vec{k}\vec{r}}$, which is a solution of Schrödinger equation, is replaced by the correlated wave function of the two nucleons $\Phi_{\vec{k}}$.

In Table 2 we present all the possible final states starting from ΛN initial states with $L = 0$ and considering the final state interaction after the action of the weak transition potential. The strong interaction conserves, among other properties, parity $(-1)^L$ and total angular momentum ($\Delta J = 0$). Specifically, the tensor component ($\Delta L = 2$) of the strong final state interaction produces a mixing between $^3S_1$ and $^3D_1$ NN final state whereas the central part ($\Delta L = 0$) does not produce an overlap between different channels.

Based on these considerations, the matrix elements of Eq. (30) are:

$$\begin{aligned} t_{\Lambda N\to NN}^{N_rL_rN_RL_R} &= \frac{1}{\sqrt{2}}\int d^3R \int d^3r e^{-i\vec{P}\cdot\vec{R}}\Phi^*_{\vec{k}}(\vec{r})\chi^{\dagger S}_{M_S}\chi^{\dagger T}_{T_3}V(\vec{r})\Phi^{CM}_{N_RL_R}\left(\frac{\vec{R}}{b/\sqrt{2}}\right) \\ &\times \Phi^{rel}_{N_rL_r}\left(\frac{\vec{r}}{\sqrt{2}b}\right)\chi^{S_0}_{M_{S_0}}\chi^{T_0}_{T_{3_0}} \\ &= (2\pi)^{3/2}\Phi^{CM}_{N_RL_R}\left(\vec{P}\frac{b}{\sqrt{2}}\right)t_{rel}\ , \end{aligned} \tag{37}$$

with $\Phi^{CM}_{N_RL_R}\left(\vec{P}\frac{b}{\sqrt{2}}\right)$ is the Fourier transform of the ΛN center of mass oscillator wave function and

$$t_{rel} = \frac{1}{\sqrt{2}}\int d^3r \Phi^*_{\vec{k}}(\vec{r})\chi^{\dagger S}_{M_S}\chi^{\dagger T}_{T_3}V(\vec{r})\Phi^{rel}_{N_rL_r}\left(\frac{\vec{r}}{\sqrt{2}b}\right)\chi^{S_0}_{M_{S_0}}\chi^{T_0}_{T_{3_0}}\ . \tag{38}$$

2.2 Weak Transition Potential

The weak transition potential is built from the exchange of virtual mesons belonging to the ground state pseudoscalar (π, ρ, K) and vector octets (K^*, ω, η) [10], to which we add the uncorrelated (2π) and correlated ($2\pi/\sigma$) two–pion–exchange [11]. One of the merits of this weak potential was that for the first time it was possible to reproduce the experimental data of both the asymmetry parameters and the decay rates for ${}^{5}_{\Lambda}$He and ${}^{12}_{\Lambda}$C. In this work we show the final expressions of the transition potentials.

The one-meson exchange contributions are obtained from the corresponding Feynman amplitudes, displayed in Figure 1, conveniently Fourier transformed to coordinate space. In order to account for the finite size of the hadrons involved in the transition, form factors are included at the weak and strong vertices of these amplitudes. More details are given in Ref. [10]. We note that, while the baryon–baryon strong coupling constants are taken from the model NSC97f, in the present work we employ monopole–type form factors at the meson–baryon–baryon vertices, typical of the Juelich BB interaction models [41] with similar cut–off values, instead of the exponential–type form–factor of the Nijmegen models adopted in [11]. This new procedure gives rise to similar results as those obtained in Ref. [11] and has the advantage of permitting a more straightforward comparison with the parameters employed by other models in the literature.

Within the OME model, the decomposition of the weak interaction potential for the $\Lambda N \to nN$ transition is given in the following way:

$$V(\vec{r}) = \sum_i V_i(\vec{r}) = \sum_i \sum_\alpha V_\alpha^{(i)}(r) \hat{O}_\alpha \hat{I}_\alpha^{(i)}, \tag{39}$$

where the index i runs over all exchanged mesons and the index α over the different spin–space operational structures. The spin operators $\hat{O}_\alpha$ are:

$$\hat{O}_\alpha = \begin{cases} \hat{1} & \text{central spin-independent (C)} \\ \vec{\sigma}_1 \cdot \vec{\sigma}_2 & \text{central spin-dependent (SS)} \\ S_{12}(\vec{r}) = 3(\vec{\sigma}_1 \cdot \vec{r})(\vec{\sigma}_2 \cdot \vec{r}) - \vec{\sigma}_1 \cdot \vec{\sigma}_2 & \text{tensor (T)} \\ \vec{\sigma}_2 \cdot \vec{r} & \text{PV for pseudoescalar mesons} \\ (\vec{\sigma}_1 \times \vec{\sigma}_2) \cdot \vec{r} & \text{PV for vector mesons} \end{cases}$$

and the isospin operators $\hat{I}_\alpha^{(i)}$ are:

$$\hat{I}_\alpha^{(i)} = \begin{cases} \hat{1} & \text{isoescalar mesons } (\eta, \omega) \\ \vec{\tau}_1 \cdot \vec{\tau}_2 & \text{isovector mesons } (\pi, \rho) \\ \text{linear combination of } \hat{1} \text{ and } \vec{\tau}_1 \cdot \vec{\tau}_2 & \text{isodoublet mesons } (K, K^*) \end{cases}$$

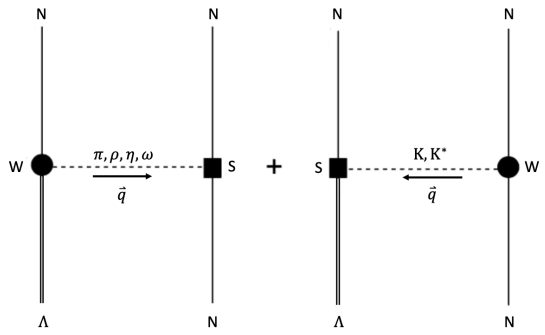

Figure 1: Feynman diagrams corresponding to the weak $\Lambda N \to NN$ transition amplitudes mediated by the exchange of the non–strange $(\pi, \rho, \eta, \omega)$ and the strange (K, K^*) mesons. The circle and the square stand for a weak and a strong vertex, respectively.

The different pieces of $V_\alpha^{(i)}$ can be written in terms of Yukawa or Yukawa–like functions multiplied by certain factors, $K_\alpha^{(i)}$, which contain weak and strong coupling constants:

$$V_C^{(i)}(r) = K_C^{(i)} \frac{\exp^{-\mu_i r}}{4\pi r} \equiv K_C^{(i)} V_C(r, \mu_i) \ , \tag{40}$$

$$V_{SS}^{(i)}(r) = K_{SS}^{(i)} \frac{1}{3} \left[\mu_i^2 \frac{\exp^{-\mu_i r}}{4\pi r} - \delta(r) \right] \equiv K_{SS}^{(i)} V_{SS}(r, \mu_i) \ , \tag{41}$$

$$V_T^{(i)}(r) = K_T^{(i)} \frac{1}{3} \mu_i^2 \exp^{-\mu_i r} \left(1 + \frac{3}{\mu_i r} + \frac{3}{(\mu_i r)^2} \right) \equiv K_T^{(i)} V_T(r, \mu_i) \ , \tag{42}$$

$$V_{PV}^{(i)}(r) = K_{PV}^{(i)} \mu_i \exp^{-\mu_i r} \left(1 + \frac{1}{\mu_i r} \right) \equiv K_{PV} V_{PV}(r, \mu_i) \ , \tag{43}$$

where μ_i denotes the mass of the different mesons. The expressions for $K_\alpha^{(i)}$ are given in [10].

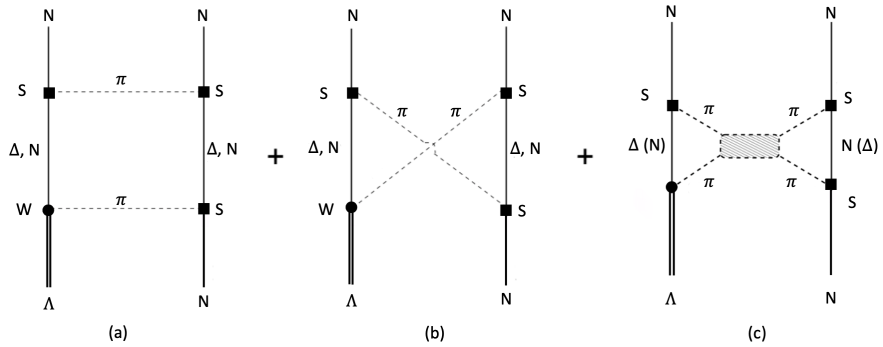

Figure 2: Uncorrelated [(a) and (b)] and correlated [(c)] two–pion–exchange Feynman diagrams corresponding to the weak $\Lambda N \to NN$ transition amplitudes. The circle and the square stand for a weak and a strong vertex, respectively.

This OME potential is supplemented by chirally motivated contributions of uncorrelated (2π) and correlated ($2\pi/\sigma$) two–pion–exchange mechanism. The relevant diagrams are shown in Fig. 2. The two–pion–exchange (TPE) interaction takes place only in the scalar–isoscalar channel. This is due to the fact that the ρ meson is already represented in the OME mechanism and, therefore, the vector–isovector channel ($2\pi/\rho$) is not implemented here. Also, the intermediate NN states are not considered in these diagrams to avoid double counting when including the NN strong correlations. Furthermore, we note that the full TPE potential is of pure parity–conserving nature.

Once the expression for the potential is known, what remains to be done in Eq. (38) is to perform a partial–wave expansion of the final wave function, so that the relative $\Lambda N \to nN$ amplitude t_{rel} in Eq. (38) can be written as follows:

$$\begin{aligned} t_{rel} = \frac{1}{\sqrt{2}} \sum_i \sum_\alpha \sum_{LL'J} & 4\pi i^{-L'} \langle LM_L SM_S | JM_J \rangle Y_{LM_L}(\hat{k}_r) \\ & \times \langle L_r M_{L_r} S_0 M_{S_0} | JM_J \rangle \langle (L'S) JM_J | \hat{\mathcal{O}}_\alpha | (L_r S_0) JM_J \rangle \\ & \times \langle TT_3 | \hat{\mathcal{I}}^i_\alpha | T_0 T_{3_0} \rangle \int r^2 dr \Phi^{*^J}_{LL'}(k_r, r) V^i_\alpha(r) \\ & \times \Phi^{rel}_{N_r L_r}(r/\sqrt{2}b) \ , \end{aligned} \tag{44}$$

where the function $\Phi^{*^J}_{LL'}(k_r, r)$ is the scattering solution of the two final nucleons moving under the influence of the strong interaction. The explicit expressions for the expectation value of the spin–space piece of $\hat{\mathcal{O}}_\alpha$ can be found in Appendix B.

2.3 Decay rate asymmetry

Λ–hypernuclei can be created with a certain degree of polarization depending on the kinematic conditions employed in the production reactions. This means that the hypernucleus has a total angular momentum (J_I) in a preferred direction in space, known as polarization axis. J_I comes from the addition between the spin of the Λ–particle and the nuclear core angular momentum, J_C. The two dominant decay mechanisms are the proton– and neutron–induced decay, where we have added a vector index in the Λ to indicate that the hypernucleus is polarized:

$$\vec{\Lambda}p \to np$$
$$\vec{\Lambda}n \to nn$$

Protons from the proton–stimulated decay are emitted asymmetrically with respect the polarization axis of Λ–hypernuclei. We denote as θ the angle between the direction of the outgoing protons and the polarization axis. This asymmetric emission means that the number of protons emerging in a certain direction (θ) is different from the number of protons in the opposite direction ($180^\circ + \theta$). As we will see later, this asymmetry comes from the interference between the PC and PV amplitudes. Therefore, the study of polarized hypernuclei provides us with extra information on the non–mesonic weak decay, such as the relative phases between PC and PV amplitudes, which puts additional restrictions to the theoretical models. In principle, there is also an asymmetry with respect to the neutrons emitted in the proton–stimulated decay, but its measurement is hard to reach. In addition to this, it should be pointed out that there is no neutron–asymmetry from neutron–stimulated decay because one can not distinguish the two final neutrons.

From now on we will focus on the asymmetry generated in the accessible $\vec{\Lambda}p \to np$ process. It is obtained from the intensity of protons emitted along a direction forming an angle θ with respect to the hypernuclear polarization axis [37]:

$$\begin{aligned} I(\theta, J_I) \equiv Tr[\mathcal{M}\rho(J_I)\mathcal{M}^\dagger](\theta) = \sum_{F,M,M'} \langle F;\theta|\mathcal{M}|I;J_I,M_I\rangle \\ \times \langle I;J_I,M_I|\rho(J_I)|I;J_I,M'\rangle\langle I;J_I,M'|\mathcal{M}^\dagger|F;\theta\rangle \ , \end{aligned} \tag{45}$$

where $\mathcal{M}$ is the operator describing the elementary transition, $|I;J_I,M_I\rangle$ is the initial hypernuclear state, M_I denoting the third component of the total hypernuclear spin J_I and $|F;\theta\rangle$ is the final state, which is composed by the residual nucleus and the two outgoing nucleons, and $\rho(J_I)$ is the density matrix of the polarized hypernucleus. For pure vector polarization perpendicular to the plane of the $n(K^+,\pi^+)\Lambda$ reaction producing the hypernucleus, the density matrix is given in Ref. [7] as:

$$\rho(J) = \frac{1}{2J+1}[1 + P_y(J_I)S_y\frac{3}{J_I+1}] \ , \tag{46}$$

where P_y is the hypernuclear polarization, which depends on the kinematics and dynamics of the hypernuclear production reaction, and S_y is the J–spin operator along the polarization axis. From Eq. (46) one can obtain the proton distribution in the following form:

$$I(\theta, J_I) = I_0(J_I)[1 + \mathcal{A}(\theta, J_I)] = I_0(J_I)[1 + P_y(J_I)A_p(\theta, J_I)] \ , \tag{47}$$

where I_0 is the isotopic intensity for an unpolarized hypernucleus and A_p is the hypernuclear asymmetry parameter which read:

$$I_0(J_I) = \frac{Tr(\mathcal{M}\mathcal{M}^\dagger)}{2J_I + 1} \equiv \Gamma_p \ , \tag{48}$$

$$\mathcal{A}(\theta, J_I) = P_y(J_I)\frac{3}{J_I + 1}\frac{Tr(\mathcal{M}S_y\mathcal{M}^\dagger)(\theta)}{Tr(\mathcal{M}\mathcal{M}^\dagger)} \ . \tag{49}$$

It is clear that, by construction, we can write down two properties of $I(\theta, J_I)$ and $\mathcal{A}(\theta, J_I)$.

$$\int_0^\pi d\theta I(\theta, J_I) = I_0(J_I) \ . \tag{50}$$

$$\int_0^\pi d\theta \mathcal{A}(\theta, J_I) = 0 \ . \tag{51}$$

From the last equation, the function $\mathcal{A}(\theta, J_I)$ can be expressed as a series of odd powers of $\cos\theta$. If we truncate to first order in the expansion, we have:

$$\mathcal{A}(\theta, J_H) = C\cos\theta \ . \tag{52}$$

It is clear that if the hypernucleus is generated without polarization, there is no asymmetry in the protons emitted in proton-stimulated decay. This means that $\mathcal{A}(\theta, J_H) = 0$. For this reason, and as shown in Eq. (47), the constant C can be expressed as a product of the hypernucleus polarization, P_y times a remainder quantity, called by exclusion as the asymmetry parameter, A_p.

$$C \equiv P_y A_p \ . \tag{53}$$

Using these considerations, the Eq. (47) is rewritten as follows:

$$I(\theta, J_I) = I_0(J_I)[1 + \mathcal{A}(\theta, J_I)] = I_0(J_I)[1 + P_y(J_I)A_p(J_I)\cos(\theta)] \ . \tag{54}$$

The shell model weak–coupling scheme allows rewriting the asymmetry in terms of the polarization of the hyperon spin, p_Λ and the so–called intrinsic asymmetry parameter, a_Λ:

$$\mathcal{A} = P_y A_p \cos(\theta) = p_\Lambda a_\Lambda \cos(\theta) \ . \tag{55}$$

This is as if we considered that the process responsible for the appearance of the asymmetry is the elementary process $\vec{\Lambda}p \to np$ taking place in the nuclear medium. In other words, the polarization and the asymmetry parameter of the entire hypernucleus are referred to as those of the elemental decay process.

This representation implies that the asymmetry parameter should be practically independent of the decaying hypernucleus. Several calculations [2, 6, 10, 11, 15, 17, 37, 42] of the asymmetry parameter of different hypernuclei show only moderate dependence on the hypernuclear structure. Although this property is also supported by experimental data [28], one has to note that there are still large error bars.

Using the weak–coupling scheme, the relation between the hypernuclear and the Λ polarization is:

$$p_\Lambda = \begin{cases} -\frac{J}{J+1} P_y & \text{if } J = J_C - \frac{1}{2} \\ P_y & \text{if } J = J_C + \frac{1}{2} \end{cases} \tag{56}$$

From Eq. (55) it then follows:

$$a_\Lambda = \begin{cases} -\frac{J+1}{J} A_p & \text{if } J = J_C - \frac{1}{2} \\ A_p & \text{if } J = J_C + \frac{1}{2} \end{cases} \tag{57}$$

where a_Λ can be reinterpreted as an intrinsic value of the process as mentioned above. Note that, for example, in case of ${}^{5}_{\Lambda}\vec{\mathrm{He}}$, $J = 1/2$ and J_C=0, the intrinsic asymmetry parameter is $a_\Lambda = A_p({}^{5}_{\Lambda}\vec{\mathrm{He}})$. Note also that $a_\Lambda = A_p = 0$ if $J = 0$. In relation to this last result, the four–body hypernuclei have $J = 0$ and, therefore, the asymmetry parameter vanish in this approach.

In Appendix C one can find the expression of the asymmetry parameter for s–shell hypernuclei in terms of the elementary amplitudes appearing in Table 1. From all these considerations we can rewrite Eq. (54) as:

$$I(\theta, J_I) = I_0(J_I)\left[1 + p_\Lambda a_\Lambda \cos\theta\right] \ . \tag{58}$$

Experimentally, the asymmetry is determined by measuring $I(0^\circ)$ and $I(180^\circ)$ as:

$$a_\Lambda = \frac{1}{p_\Lambda} \frac{I(0^\circ, J_I) - I(180^\circ, J_I)}{I(0^\circ, J_I) + I(180^\circ, J_I)} \ . \tag{59}$$

3 Block–Dalitz model for s–shell hypernuclei

An approach was proposed by Block and Dalitz [43] which allows one to determine the neutron– and proton–induced decays in terms of a few rates for the elementary process $\Lambda N \to nN$ in s–shell hypernuclei. As we will see in this chapter, the relationship between this elementary rates is affected by the isospin change involved in the non–mesonic weak decay. In principle, both $\Delta I = 1/2$ and $\Delta I = 1/3$ transitions are possible, but most of the models impose the phenomenological $\Delta I = 1/2$ rule observed in hadronic weak processes. In previous works these rates were determined phenomenologically by fitting the available data on s–shell hypernuclei for total and partial decay widths [44–49]. The usual outcome was the large error bars prevent from drawing any definitive conclusions. For this reason, more precise measurements of the decay rates are necessary, especially for four–body hypernuclei, in order to obtain reliable conclusions on the identification of possible violation of the $\Delta I = 1/2$ selection rule. Fortunately, an upcoming experiment at J-PARC will measure these decay rates more precisely [50].

The Block–Dalitz approach obtains the decay rates employing simple arguments. In terms of classical physics, the interaction probability of a particle which crosses an infinite homogeneous system is $dP = ds/\lambda$, where ds is the thickness, $\lambda = 1/(\sigma\rho)$ is the mean free path of this particle, σ is the cross section and ρ is the particle density of the homogeneous system. In this way, one can evaluate the width for the non–mesonic weak decay by:

$$\Gamma_{\rm NM} = \frac{dP_{\Lambda N \to nN}}{dt} = \frac{ds}{\lambda dt} = \sigma\rho\frac{ds}{dt} = \sigma\rho v \ , \tag{60}$$

where v is the speed of Λ particle in the rest frame of the system. Within a semiclassical approximation for a finite nuclei one can evaluate the width by performing an average over spin and isospin states. In addition, if one assumes the zero range approximation of the non–mesonic process, the decay rate is proportional to the overlap between the Λ and nuclear densities [2].

$$\Gamma_{\rm NM} = \langle\sigma v\rangle \int d(\vec{r})\rho(\vec{r}) \mid \psi_\Lambda(\vec{r}) \mid^2 = \langle\sigma v\rangle\rho_A \ , \tag{61}$$

being ρ_A the nuclear density normalized to the mass number $A = Z + N$ at the position of the Λ particle and $\psi_\Lambda(\vec{r})$ is the Λ wave function normalized to unity. Consequently, in the Block and Dalitz approach, the non–mesonic width $\Gamma_{\rm NM} = \Gamma_n + \Gamma_p$ of the hypernucleus ${}^{A+1}_{\Lambda}Z$ turns out to be factorized into a density–dependent factor (ρ_A) and a term incorporating the dynamics of the non–mesonic decay [43].

$$\Gamma({}^{A+1}_{\Lambda}Z) = \overline{R}({}^{A+1}_{\Lambda}Z)\rho_A = \frac{N\overline{R}_n({}^{A+1}_{\Lambda}Z) + Z\overline{R}_p({}^{A+1}_{\Lambda}Z)}{A}\rho_A \ , \tag{62}$$

where $\overline{R}$ denotes a rate (per unit nucleon density at the Λ position) average over spin and isospin and is given in the second equality in Eq. (62) in terms of

spin–averaged rates $\overline{R}_n$ and $\overline{R}_p$ for the neutron– and proton–induced processes, respectively.

For s–shell hypernuclei the ΛN pair is in the $L = 0$ relative orbital angular momentum state and the possible $\Lambda N \to nN$ transition channels are given in Table 1. Now, we may introduce the Block–Dalitz rates R_{NJ} for spin–singlet ($J = 0 \Rightarrow R_{n0}$ and R_{p0}) and spin–triplet ($J = 1 \Rightarrow R_{n1}$ and R_{p1}) elementary $\Lambda N \to nN$ interactions in terms of the rates associated to the partial–wave transitions and the elementary amplitudes of Table 1 in such a way that:

$$\begin{aligned} R_{n0} &= R_n(^1S_0) + R_n(^3P_0) = |a_n|^2 + |b_n|^2 \ , \\ R_{n1} &= R_n(^3P_1) = |f_n|^2 \ , \\ R_{p0} &= R_p(^1S_0) + R_p(^3P_0) = |a_p|^2 + |b_p|^2 \ , \\ R_{p1} &= R_p(^3S_1) + R_p(^3D_1) + R_p(^1P_1) + R_p(^3P_1) \\ &= |c_p|^2 + |d_p|^2 + |e_p|^2 + |f_p|^2 \ . \end{aligned} \tag{63}$$

The quantum numbers of the final state being reported in brackets. Observe that the $\overline{R}$ is the spin–isospin average of the R_{NJ} rates. The non–mesonic decay widths of s–shell hypernuclei are thus easily derived using angular momentum coupling as one can see in Appendix A:

$$\Gamma_{\rm NM}(^3_\Lambda{\rm H}) = (3R_{n0} + R_{n1} + 3R_{p0} + R_{p1})\,\frac{\rho_2}{8} \ , \tag{64}$$

$$\Gamma_{\rm NM}(^4_\Lambda{\rm H}) = (R_{n_0} + 3R_{n_1} + 2R_{p_0})\,\frac{\rho_3}{6} \ , \tag{65}$$

$$\Gamma_{\rm NM}(^4_\Lambda{\rm He}) = (2R_{n0} + R_{p0} + 3R_{p1})\,\frac{\rho_3}{6} \ , \tag{66}$$

$$\Gamma_{\rm NM}(^5_\Lambda{\rm He}) = (R_{n0} + 3R_{n1} + R_{p0} + 3R_{p1})\,\frac{\rho_4}{8} \ . \tag{67}$$

In these relations it has been taken into account that the total hypernuclear angular momentum is $J_I = 0$ for $^4_\Lambda$H and $^4_\Lambda$He and $J_I = 1/2$ for $^3_\Lambda$He and $^5_\Lambda$He [5]. Note that, for both $^4_\Lambda$H and $^4_\Lambda$He rates, the same density factor ρ_3 has been used. We observe, for example, that only the spin–singlet interactions is effective for neutron–induced transitions in $^4_\Lambda$He whereas only the proton–induced ones for $^4_\Lambda$H.

Within the Block–Dalitz model the intrinsic Λ asymmetry parameter is given by

$$a_\Lambda = \frac{2\sqrt{3}\,\mathcal{R}e\left[a_p e_p^* - \frac{1}{\sqrt{3}} b_p(c_p^* - \sqrt{2}d_p^*) + f_p(\sqrt{2}c_p^* + d_p^*)\right]}{|a_p|^2 + |b_p|^2 + 3(|c_p|^2 + |d_p|^2 + |e_p|^2 + |f_p|^2)} \ , \tag{68}$$

as is shown in detail in Appendix C. Although the above equation is only valid for the $\vec{\Lambda}p \to np$ free space process, it makes evident that the asymmetry is due to the interference between parity–conserving (a_p, c_p and d_p) and parity–violating (b_p, e_p and f_p) $\vec{\Lambda}p \to np$ elementary amplitudes with the same value

of np intrinsic spin S. As we shall see in the following, this expression has an approximate validity for the proton–induced decay of ${}^{5}_{\Lambda}$He.

As we discussed at the beginning of this section, the Block–Dalitz phenomenological model (i.e, Eqs. (64)–(67)) makes use of a few assumptions, which should be verified before one employs this model for predictions or extrapolations to other hypernuclei. The decays are treated incoherently on the stimulating nucleons and a local point–like Λ–N interaction is assumed, thus interference effects originated from antisymmetrization of the two–nucleon final state commented in Section 2.1.4, are neglected. The use of a point–like interaction allows to write the decay rates in a simple and factorized form as in Eq. (62), although it could be an inadequate approximation since the long–range meson exchange (via pion and kaon mesons) gives a dominant contribution to the non–mesonic decay [11]. Moreover, the calculation employs an average nuclear density at the position of the Λ particle (here, the same density is employed for ${}^{4}_{\Lambda}$He and ${}^{4}_{\Lambda}$H). In addition, processes induced by two nucleons or more are not taken into account in this model, although their relevance has been established both theoretically [20, 51, 52] and experimentally [30–32]. Despite of all of this, one could argue that some assumptions can be expected to be quite satisfactory. First, hypernuclear structure effects are expected to be unimportant due to the high momentum of the outgoing nucleons. Secondly, the experimental data are still quite limited and not precise since it is difficult to detect the products of the non–mesonic decay, especially for the neutron–induced one. This would imply that the above approximations could be enough for interpreting the present data. Finally, multinucleon induced decays are quite negligible in the light system studied here. Section 4.1 will be devoted study the reliability of Block–Dalitz approach by means of a finite nucleus calculation of the R_{NJ} elementary rates.

The non–mesonic weak transition occurs mainly with a $\Delta I = 1/2$ isospin change. If we assume pure $\Delta I = 1/2$ transitions, the following relations hold among the rates and elementary amplitudes for transitions to $I_f = 1$ states:

$$R_n({}^1S_0) = 2R_p({}^1S_0)\ ,\quad R_n({}^3P_0) = 2R_p({}^3P_0)\ ,\quad R_n({}^3P_1) = 2R_p({}^3P_1)\ . \tag{69}$$

$$a_n = \sqrt{2}a_p\ ,\qquad b_n = \sqrt{2}b_p\ ,\qquad f_n = \sqrt{2}f_p\ . \tag{70}$$

These relations have been obtained from the Clebsch–Gordan coefficients and the Wigner–Eckart theorem. By definition, we may assume that $R_n({}^{2S+1}L_J)$ and $R_p({}^{2S+1}L_J)$ differ only by the isospin factors (for a given ${}^{2S+1}L_J$). The $\Delta I = 1/2$ isospin change is represented by the $\hat{T}^J_{1/2}$ operator with ΔT^J_3 = -1/2. Then, for instance, the spin–averaged rates for the ${}^1S_0 \to {}^1S_0$ neutron–induced transition is

$$\begin{aligned} R_n({}^1S_0) &= \mid \langle nn \mid \hat{T}^{J=0}_{1/2} \mid \Lambda n\rangle \mid^2 = \mid \langle 1\text{ - }1 \mid \hat{T}^{J=0}_{1/2} \mid \frac{1}{2}\text{ - }\frac{1}{2}\rangle \mid^2 \\ &= \mid \langle \frac{1}{2}\text{ - }\frac{1}{2}\ \frac{1}{2}\text{ - }\frac{1}{2} \mid 1\text{ - }1\rangle\langle 1 \mid\mid \hat{T}^{J=0}_{1/2} \mid\mid \frac{1}{2}\rangle \mid^2 = \mid \langle 1 \mid\mid \hat{T}^{J=0}_{1/2} \mid\mid \frac{1}{2}\rangle \mid^2\ , \end{aligned} \tag{71}$$

and for the proton–induced is

$$\begin{aligned} R_p(^1S_0) =& \mid \langle np \mid \hat{T}^{J=0}_{1/2} \mid \Lambda p \rangle \mid^2 = \mid \langle 10 \mid \hat{T}^{J=0}_{1/2} \mid \frac{1}{2}\frac{1}{2} \rangle \mid^2 \\ =& \mid \langle \frac{1}{2}\frac{1}{2}\ \frac{1}{2}\ -\ \frac{1}{2} \mid 10 \rangle \langle 1 \mid\mid \hat{T}^{J=0}_{1/2} \mid\mid \frac{1}{2} \rangle \mid^2 = \frac{1}{2} \mid \langle 1 \mid\mid \hat{T}^{J=0}_{1/2} \mid\mid \frac{1}{2} \rangle \mid^2 \ . \end{aligned} \tag{72}$$

Note that, although the np pair can be either in isospin $I_f = 0$ and $I_f = 1$, due to the antisymmetry issues summarized in Eq. (22), the $^1S_0$ np state is an isotriplet state ($I_f = 1$) with $I_3 = 0$ (via Eq. (21)). Then, the ratio is

$$\frac{R_n(^1S_0)}{R_p(^1S_0)} = 2 \ . \tag{73}$$

In consequence, the following expressions are valid

$$\begin{aligned} R_{n0} &= R_n(^1S_0) + R_n(^3P_0) = 2R_p(^1S_0) + 2R_p(^3P_0) \ , \\ R_{n1} &= R_n(^3P_1) = 2R_p(^3P_1) \ . \end{aligned} \tag{74}$$

The isospin–dependence of the $\Lambda N \to nN$ process is summarized by the following ratios:

$$\frac{R_{n0}}{R_{p0}} = \frac{2\left(R_p(^1S_0) + R_p(^3P_0)\right)}{R_p(^1S_0) + R_p(^3P_0)} = 2 \ , \tag{75}$$

$$\frac{R_{n1}}{R_{p1}} = \frac{2R_p(^3P_1)}{R_p(^3S_1) + R_p(^3D_1) + R_p(^1P_1) + R_p(^3P_1)} \leq \frac{R_{n0}}{R_{p0}} = 2 \ . \tag{76}$$

Therefore,

$$\frac{R_{n1}}{R_{p1}} \leq \frac{R_{n0}}{R_{p0}} = 2 \tag{77}$$

The procedure is analogous in case of considering that the non–mesonic weak decay occurs with pure $\Delta I = 3/2$ isospin change. The transition operator will be $\hat{T}^J_{3/2}$ with $\Delta T^J_3 =$ -1/2. The following relations hold for a pure $\Delta I = 3/2$ transitions.

$$R_n(^1S_0) = \frac{1}{2}R_p(^1S_0) \ , \quad R_n(^3P_0) = \frac{1}{2}R_p(^3P_0) \ , \quad R_n(^3P_1) = \frac{1}{2}R_p(^3P_1) \ . \tag{78}$$

$$a_n = \sqrt{\frac{1}{2}}a_p \ , \qquad b_n = \sqrt{\frac{1}{2}}b_p \ , \qquad f_n = \sqrt{\frac{1}{2}}f_p \ . \tag{79}$$

In a consequence of above expressions, the factor 2 in Eq. (77) are replaced by 1/2 and one can obtains:

$$\frac{R_{n1}}{R_{p1}} = \frac{R_{n0}}{R_{p0}} = \frac{1}{2} \tag{80}$$

Now, let us show how the previous inequalities are modified in case of the transition does not occur purely. This implies that the transition occurs with a

mixture between $\Delta I = 1/2$ and $\Delta I = 3/2$ isospin change. The study proceeds by introducing the ratios:

$$\delta_0 = \frac{\langle I_f = 1||\hat{T}^{J=0}_{3/2}||I_i = \frac{1}{2}\rangle}{\langle I_f = 1||\hat{T}^{J=0}_{1/2}||I_i = \frac{1}{2}\rangle} \equiv \frac{A^{J=0}_{3/2}(I_f = 1)}{A^{J=0}_{1/2}(I_f = 1)} \tag{81}$$

$$\delta_1 = \frac{\langle I_f = 1||\hat{T}^{J=1}_{3/2}||I_i = \frac{1}{2}\rangle}{\langle I_f = 1||\hat{T}^{J=1}_{1/2}||I_i = \frac{1}{2}\rangle} \equiv \frac{A^{J=1}_{3/2}(I_f = 1)}{A^{J=1}_{1/2}(I_f = 1)} \tag{82}$$

between the $\Delta I = 3/2$ and $\Delta I = 1/2$ $\Lambda N \to nN$ reduced transition amplitudes with total angular momentum $J = 0$ and $J = 1$ for $I_f = 1$ final state, respectively, and

$$\epsilon = \frac{\langle I_f = 0||\hat{T}^{J=1}_{1/2}||I_i = \frac{1}{2}\rangle}{\langle I_f = 1||\hat{T}^{J=1}_{1/2}||I_i = \frac{1}{2}\rangle} \equiv \frac{A^{J=1}_{1/2}(I_f = 0)}{A^{J=1}_{1/2}(I_f = 1)} \tag{83}$$

between the $\Delta I = 1/2$ transition amplitudes with total angular momentum $J = 1$ having isospin $I_f = 0$ and $I_f = 1$ in the final state. Note that, in this case, the reduced transition amplitude $A^{J=1}_{1/2}(I_f = 0)$ contains the sum of all contributions with $I_f = 0$, meaning $|A^{J=1}_{1/2}(I_f = 0)|^2 \approx R(^3S_1) + R(^3D_1) + R(^1P_1)$ while $A^{J=1}_{1/2}(I_f = 1)$ only contains the $R(^3P_1)$ contribution.

In general, we may define the transition operator $\hat{T}^J$ as a sum of $\Delta I = 1/2$ and $\Delta I = 3/2$ contributions, $\hat{T}^J = \hat{T}^J_{1/2} + \hat{T}^J_{3/2}$. Thus, one gets:

$$\frac{R_{n0}}{R_{p0}} = \frac{\delta_0^2 - 4\delta_0 + 4}{2\delta_0^2 + 4\delta_0 + 2}\ , \tag{84}$$

$$\frac{R_{n1}}{R_{p1}} = \frac{\delta_1^2 - 4\delta_1 + 4}{2\delta_1^2 + 4\delta_1 + 2 + 2\epsilon^2}\ , \tag{85}$$

where Eq. (84) has been obtained from:

$$\begin{aligned} R_{n0} &= \left|\langle 1\text{ - }1 \mid \hat{T}^{J=0} \mid \frac{1}{2}\text{ - }\frac{1}{2}\rangle\right|^2 = \left|\langle 1\text{ - }1 \mid \hat{T}^{J=0}_{1/2} \mid \frac{1}{2}\text{ - }\frac{1}{2}\rangle + \mid \langle 1\text{ - }1 \mid \hat{T}^{J=0}_{3/2} \mid \frac{1}{2}\text{ - }\frac{1}{2}\rangle\right|^2 \\ &= \left|\langle \frac{1}{2}\text{ - }\frac{1}{2}\,\frac{1}{2}\text{ - }\frac{1}{2} \mid 1\text{ - }1\rangle A^{J=0}_{1/2}(I_f = 1) + \langle \frac{1}{2}\text{ - }\frac{1}{2}\,\frac{3}{2}\text{ - }\frac{1}{2} \mid 1\text{ - }1\rangle A^{J=0}_{3/2}(I_f = 1)\right|^2 \\ &= \left|A^{J=0}_{1/2}(I_f = 1) - \frac{1}{2}A^{J=0}_{3/2}(I_f = 1)\right|^2 = \left|A^{J=0}_{1/2}(I_f = 1)\right|^2 \left|1 - \frac{\delta_0}{2}\right|^2\ , \end{aligned}$$

$$
\begin{aligned}
R_{p0} &= \left| \langle 10 \mid \hat{T}^{J=0} \mid \frac{1}{2}\frac{1}{2} \rangle \right|^2 = \left| \langle 10 \mid \hat{T}^{J=0}_{1/2} \mid \frac{1}{2}\frac{1}{2} \rangle \rangle \right|^2 + \left| \langle 10 \mid \hat{T}^{J=0}_{3/2} \mid \frac{1}{2}\frac{1}{2} \rangle \right|^2 \\
&= \left| \langle \frac{1}{2}\frac{1}{2}\ \frac{1}{2}\frac{1}{2} \mid 10 \rangle A^{J=0}_{1/2}(I_f = 1) + \langle \frac{1}{2}\frac{1}{2}\ \frac{3}{2}\frac{1}{2} \mid 10 \rangle A^{J=0}_{3/2}(I_f = 1) \right|^2 \\
&= \left| \frac{1}{\sqrt{2}} A^{J=0}_{1/2}(I_f = 1) + \frac{1}{\sqrt{2}} A^{J=0}_{3/2}(I_f = 1) \right|^2 \\
&= \frac{1}{2} \left| A^{J=0}_{1/2}(I_f = 1) \right|^2 |1 + \delta_0|^2 \ ,
\end{aligned}
$$

whereas Eq. (85) by means of the following steps:

$$
\begin{aligned}
R_{n1} &= \left| \langle 1\text{ - }1 \mid \hat{T}^{J=1} \mid \frac{1}{2}\text{ - }\frac{1}{2} \rangle \right|^2 = \left| \langle 1\text{ - }1 | \hat{T}^{J=0}_{1/2} | \frac{1}{2}\text{ - }\frac{1}{2} \rangle + \langle 1\text{ - }1 | \hat{T}^{J=0}_{3/2} | \frac{1}{2}\frac{1}{2} \rangle \right|^2 \\
&= \left| \langle \frac{1}{2}\text{ - }\frac{1}{2}\ \frac{1}{2}\text{ - }\frac{1}{2} \mid 1\text{ - }1 \rangle A^{J=1}_{1/2}(I_f = 1)) + \langle \frac{1}{2}\text{ - }\frac{1}{2}\ \frac{3}{2}\text{ - }\frac{1}{2} | 1\text{ - }1 \rangle A^{J=1}_{3/2}(I_f = 1) \right|^2 \\
&= \left| A^{J=1}_{1/2}(I_f = 1) - \frac{1}{2} A^{J=1}_{3/2}(I_f = 1) \right|^2 = \left| A^{J=1}_{1/2}(I_f = 1) \right|^2 \left| 1 - \frac{\delta_1}{2} \right|^2 \ ,
\end{aligned}
$$

$$
\begin{aligned}
R_{p1} &= \left| \langle 00 \mid \hat{T}^{J=1} \mid \frac{1}{2}\frac{1}{2} \rangle \right|^2 + \left| \langle 10 \mid \hat{T}^{J=1} \mid \frac{1}{2}\frac{1}{2} \rangle \right|^2 \\
&= \left| \langle 00 \mid \hat{T}_{1/2} + \hat{T}_{3/2} \mid \frac{1}{2}\frac{1}{2} \rangle \right|^2 + \left| \langle 10 \mid \hat{T}_{1/2} + \hat{T}_{3/2} \mid \frac{1}{2}\frac{1}{2} \rangle \right|^2 \\
&= \left| \langle 00 | \hat{T}_{1/2} | \frac{1}{2}\frac{1}{2} \rangle + \langle 00 | \hat{T}_{3/2} | \frac{1}{2}\frac{1}{2} \rangle \right|^2 + \left| \langle 10 | \hat{T}_{1/2} | \frac{1}{2}\frac{1}{2} \rangle + \langle 10 | \hat{T}_{3/2} | \frac{1}{2}\frac{1}{2} \rangle \right|^2 \\
&= \left| \langle \frac{1}{2}\frac{1}{2}\ \frac{1}{2}\text{ - }\frac{1}{2} \mid 00 \rangle A^{J=1}_{1/2}(I_f = 0) \right|^2 \\
&+ \left| \langle \frac{1}{2}\frac{1}{2}\ \frac{1}{2}\text{ - }\frac{1}{2} \mid 10 \rangle A^{J=1}_{1/2}(I_f = 1) + \langle \frac{1}{2}\frac{1}{2}\ \frac{3}{2}\text{ - }\frac{1}{2} \mid 10 \rangle A^{J=1}_{3/2}(I_f = 1) \right|^2 \\
&= \left| \frac{1}{\sqrt{2}} A^{J=1}_{1/2}(I_f = 0) \right|^2 + \left| \frac{1}{\sqrt{2}} (A^{J=1}_{1/2}(I_f = 1) + A^{J=1}_{3/2}(I_f = 1)) \right|^2 \\
&= \frac{1}{2} \left| (A^{J=1}_{1/2}(I_f = 1) \right|^2 \left(|\epsilon|^2 + \mid 1 + \delta_1 \mid^2 \right) \ .
\end{aligned}
$$

By using Eqs. (64)–(67) and Eq. (84)–(85) together with the available data of decay rates one can extract the spin and isospin structure of the $\Lambda N \to nN$ interaction without needing a detailed of knowledge of the hypernuclear structure or the weak transition interaction. Such an approach had been employed in various works [44–48]. The subsequent analysis of Ref. [49], performed with the most recent available data at that moment, was not able to provide clearer indications either on the spin–isospin structure of the non–mesonic weak decay and the possible violation of the $\Delta I = 1/2$ rule.

Let us be more specific. Eqs. (84)–(85) provide a isospin–dependence of the Block–Dalitz rates for the $\Lambda N \to nN$ process. Starting from Eqs. (64)-(67), the relation between spin–singlet and spin–triplet decay rates can be rewritten in terms of the measurable non–mesonic decay widths:

$$\begin{aligned} \frac{\Gamma_n(^3_\Lambda\mathrm{H})}{\Gamma_p(^3_\Lambda\mathrm{H})} &= \frac{3R_{n0}+R_{n1}}{3R_{p0}+R_{p1}}\ , \qquad \frac{\Gamma_n(^4_\Lambda\mathrm{H})}{\Gamma_p(^4_\Lambda\mathrm{H})} = \frac{R_{n0}+3R_{n1}}{2R_{p0}} \\ \frac{\Gamma_n(^4_\Lambda\mathrm{He})}{\Gamma_p(^4_\Lambda\mathrm{He})} &= \frac{2R_{n0}}{R_{p0}+3R_{p1}}\ , \qquad \frac{\Gamma_n(^5_\Lambda\mathrm{He})}{\Gamma_p(^5_\Lambda\mathrm{He})} = \frac{R_{n0}+3R_{n1}}{R_{p0}+R_{p1}} \end{aligned} \tag{86}$$

By using the above equations, the isospin–dependence of the R_{NJ} rates is summarized by the ratios R_{n0}/R_{p0} and R_{n_1}/R_{p_1} and it can be rewritten in terms of the measurable decay rates of four–body $^4_\Lambda$H and $^4_\Lambda$He hypernuclei.

$$\frac{R_{n0}}{R_{p0}} = \frac{\Gamma_n(^4_\Lambda\mathrm{He})}{\Gamma_p(^4_\Lambda\mathrm{H})}\ . \tag{87}$$

$$\frac{R_{n1}}{R_{p1}} = \frac{2\Gamma_n(^4_\Lambda\mathrm{H}) - \Gamma_\mathrm{n}(^4_\Lambda\mathrm{He})}{2\Gamma_p(^4_\Lambda\mathrm{He}) - \Gamma_\mathrm{p}(^4_\Lambda\mathrm{H})}\ . \tag{88}$$

In addition, the spin–dependence of the R_{NJ} rates can be summarized by the following ratios:

$$\frac{R_{n1}}{R_{n0}} = \frac{1}{3}\left(2\frac{\Gamma_n(^4_\Lambda\mathrm{H})}{\Gamma_n(^4_\Lambda\mathrm{He})} - 1\right) \tag{89}$$

$$\frac{R_{p1}}{R_{p0}} = \frac{1}{3}\left(2\frac{\Gamma_p(^4_\Lambda\mathrm{He})}{\Gamma_p(^4_\Lambda\mathrm{H})} - 1\right) \tag{90}$$

However, the amount of information that can be extract from the spin–isospin dependence of the elementary non–mesonic process directly from the available hypernuclear data will depend, to a large extend, on the reliability of the Block–Dalitz model. The test of this model is discussed in Section 4.1.

To conclude, from the previous identities a few expressions that depend on the Γ_p and Γ_n observables of the considered s–shell hypernuclei can be extracted. These expressions turn out to be useful for testing the Block–Dalitz approach and can be easily obtained from Eqs. (86). One finds:

$$\frac{\Gamma_n(^4_\Lambda\mathrm{H})}{\Gamma_p(^4_\Lambda\mathrm{He})} = \frac{\Gamma_n(^5_\Lambda\mathrm{He})}{\Gamma_p(^5_\Lambda\mathrm{He})}\ , \tag{91}$$

$$\frac{\Gamma_p(^4_\Lambda\mathrm{H})}{\Gamma_p(^4_\Lambda\mathrm{He})} \leq 2\ , \tag{92}$$

$$\frac{\Gamma_n(^4_\Lambda\mathrm{He})}{\Gamma_n(^4_\Lambda\mathrm{H})} \leq 2\ , \tag{93}$$

$$\frac{\Gamma_n(^4_\Lambda\mathrm{He})}{\Gamma_p(^4_\Lambda\mathrm{He})} \leq 2\frac{\Gamma_n(^5_\Lambda\mathrm{He})}{\Gamma_p(^5_\Lambda\mathrm{He})} \leq 4\frac{\Gamma_n(^4_\Lambda\mathrm{H})}{\Gamma_p(^4_\Lambda\mathrm{H})}\ , \tag{94}$$

where Eq. (91) could be directly verified if the data of $\Gamma_n(^4_\Lambda\mathrm{He})$ and $\Gamma_p(^4_\Lambda\mathrm{H})$ were available. In particular, it provides an important restriction for four– and five–body hypernuclei that can be directly checked by experimentalists.

3.1 Pure $\Delta I = 1/2$ and $\Delta I = 3/2$ transitions

We have already mentioned the characteristics in case of assuming that the $\Lambda N \to nN$ transition occurs with a $\Delta I = 1/2$ and $\Delta I = 3/2$ pure isospin change. For pure $\Delta I = 1/2$, Eqs. (84) and (85) taking $\delta_0 = 0$ and $\delta_1 = 0$ give:

$$\frac{R_{n1}}{R_{p1}} = \frac{2}{1+\epsilon^2} \leq \frac{R_{n_0}}{R_{p_0}} = 2 \ . \tag{95}$$

For pure $\Delta I = 3/2$ one has ($\delta_0 \to \infty$ and $\delta_1 \to \infty$):

$$\frac{R_{n1}}{R_{p1}} = \frac{R_{n0}}{R_{p0}} = \frac{1}{2} \ . \tag{96}$$

We note that, although the ratio $R_{n0}/R_{p0} = 2$ is implied by the $\Delta I = 1/2$, R_{n0}/R_{p0} also equals 2 for a particular mixture of $\Delta I = 1/2$ and $\Delta I = 3/2$ transitions (using $\delta_0 = -4$ in Eq. (84)). Similarly occurs for pure $\Delta I = 3/2$ transitions, with the ratio R_{n0}/R_{p0} taking a value of $1/2$ for a specific combination of $\Delta I = 1/2$ and $\Delta I = 3/2$ transitions. Therefore, a result with $R_{n0}/R_{p0} = 2$ does not necessarily imply the validity of the $\Delta I = 1/2$ rule, although a result different from 2 would certainly imply the violability of this selection rule.

Two equalities among the hypernuclear decay rates can be obtained from Eq. (95) and Eqs. (64)–(67) for pure $\Delta I = 1/2$ transitions:

$$\frac{R_{n0}}{R_{p0}} \equiv \frac{\Gamma_n({}^4_\Lambda\mathrm{He})}{\Gamma_p({}^4_\Lambda\mathrm{H})} = 2 \ , \tag{97}$$

which can be equivalently rewritten as:

$$\frac{R_{n0}}{R_{p0}} \equiv \frac{\dfrac{\Gamma_n}{\Gamma_p}({}^4_\Lambda\mathrm{H})\dfrac{\Gamma_n}{\Gamma_p}({}^4_\Lambda\mathrm{He})}{\dfrac{\Gamma_n}{\Gamma_p}({}^5_\Lambda\mathrm{He})} = 2 \ . \tag{98}$$

4 Results

4.1 On the reliability of the Block–Dalitz model

In this section we show how a finite calculation of four– and five–body hypernuclei allows one to study the reliability of the Block–Dalitz approach.

First, we evaluate the amplitudes for the proton–induced non–mesonic decay of ${}^{5}_{\Lambda}$He with the shell model calculation. The results are given in Table 3 and, as we previously commented, we have employed two weak transition potentials: the one–meson–exchange (OME) and one–meson–exchange plus two–pion–exchange (OME+TPE) models that were built imposing the $\Delta I = 1/2$ transitions rule. The non–vanishing neutron–induced amplitudes, equally as in Eq. (70), verify:

$$A_n = \sqrt{2}A_p, \qquad B_n = \sqrt{2}B_p, \qquad F_n = \sqrt{2}F_p. \tag{99}$$

Within the shell–model approach, the partial non–mesonic decay rates of ${}^{5}_{\Lambda}$He read:

$$\begin{aligned} \Gamma_n({}^{5}_{\Lambda}\mathrm{He}) = &\quad |A_n|^2 + |B_n|^2 + |F_n|^2 = 2(|A_p|^2 + |B_p|^2 + |F_p|^2) \ , \\ \Gamma_p({}^{5}_{\Lambda}\mathrm{He}) = &\quad |A_p|^2 + |B_p|^2 + |C_p|^2 + |D_p|^2 + |E_p|^2 + |F_p|^2 \ . \end{aligned} \tag{100}$$

Before proceeding, it is necessary to discuss the difference between the uppercase amplitudes shown here and the lowercase ones, which were introduced in the previous chapter. The uppercase amplitudes include the effect of the realistic NN final state interaction (FSI) and details of the hypernuclear structure. For this reason, uppercase amplitudes are denoted as hypernuclear amplitudes. As we commented in Section 2.1.4, FSI introduce a mixing between the ${}^3S_1$ and ${}^3D_1$ NN final state after the action of the weak transition because other transitions mediated by the strong interaction are possible. This mixing only affects the parity–conserving amplitudes C_p and D_p because the tensor component ($\Delta L = 2$) of the NN strong interaction couples relative angular states having the same parity and total angular momentum. These amplitudes are modified as follows:

$$\begin{aligned} C_p &= C_p({}^3S_1 \to {}^3S_1 \to {}^3S_1) + C_p({}^3S_1 \to {}^3D_1 \to {}^3S_1) \ , \\ D_p &= D_p({}^3S_1 \to {}^3S_1 \to {}^3D_1) + D_p({}^3S_1 \to {}^3D_1 \to {}^3D_1) \ , \end{aligned}$$

where the first arrow in each amplitude denotes the weak transition $\Lambda p \to np$ and the second one denotes the strong transition $np \to np$. It is expected that, by introducing a TPE central potential such as the one of Ref. [11], their effects would only be seen on the A_p and C_p amplitudes. However, as we can see in Table 3, the TPE mechanism also modifies the tensor transition amplitude D_p due to the mixing mentioned above.

In order to obtain a relationship between the elementary amplitudes of the Block–Dalitz model (a_p to f_p) and the hypernuclear amplitudes (A_p to F_p), it

Table 3: Proton–induced non–mesonic weak decay amplitudes for ${}^{5}_{\Lambda}$He obtained with the one–meson–exchange (OME) and one–meson–exchange plus two–pion–exchange (OME+TPE) finite nucleus approach.

	OME	OME+TPE
$A_p : {}^1S_0 \to {}^1S_0$	-0.1057	$+0.0823$
$B_p : {}^1S_0 \to {}^3P_0$	$+0.0056$	$+0.0056$
$C_p : {}^3S_1 \to {}^3S_1$	-0.1818	$+0.0739$
$D_p : {}^3S_1 \to {}^3D_1$	-0.1483	-0.2772
$E_p : {}^3S_1 \to {}^1P_1$	$+0.4593$	$+0.4593$
$F_p : {}^3S_1 \to {}^3P_1$	$+0.2045$	$+0.2045$

is convenient to express Eq. (67) as follows:

$$\begin{aligned} \Gamma_n({}^{5}_{\Lambda}\mathrm{He}) = &\quad 2(|a_p|^2 + |b_p|^2 + |f_p|^2)\frac{\rho_4}{8} \ , \\ \Gamma_p({}^{5}_{\Lambda}\mathrm{He}) = &\quad (|a_p|^2 + |b_p|^2 + |c_p|^2 + |d_p|^2 + |e_p|^2 + |f_p|^2)\frac{\rho_4}{8} \ . \end{aligned} \tag{101}$$

From Eq. (100) and (101) one immediately obtains the elementary Block–Dalitz amplitudes from the calculated hypernuclear ones:

$$\begin{aligned} &a_p = A_p\sqrt{\frac{8}{\rho_4}} \ , \quad b_p = B_p\sqrt{\frac{8}{\rho_4}} \ , \quad c_p = C_p\sqrt{\frac{8}{3\,\rho_4}} \ , \\ &d_p = D_p\sqrt{\frac{8}{3\,\rho_4}} \ , \quad e_p = E_p\sqrt{\frac{8}{3\,\rho_4}} \ , \quad f_p = F_p\sqrt{\frac{8}{3\,\rho_4}} \ . \end{aligned} \tag{102}$$

Therefore, by construction, with the Block–Dalitz amplitudes of Eq. (102) one reproduces the ${}^{5}_{\Lambda}$He calculated decay rates, as can seen in Table 5 when comparing the Block–Dalitz results with those of the OME (lines OME and OME–BD) and the OME+TPE (lines OME+TPE and OME+TPE–BD) models.

The decay amplitudes of Table 3 together with the Block–Dalitz approach allows one to extend the prediction to the other s–shell hypernuclei. The procedure is the following: by comparing Eqs. (100) with Eq. (67) one first obtains the R_{NJ} rates and, subsequently, these rates are employed in Eqs. (64)–(66) to obtain the decay widths for ${}^{3}_{\Lambda}$H, ${}^{4}_{\Lambda}$H and ${}^{4}_{\Lambda}$He.

The results for the R_{NJ} rates obtained with the OME and OME+TPE models are reported in Table 4, where the value $\rho_4 = 0.045$ fm^{-3}, evaluated in Ref. [47] through a quark model based Λ wave–function and a Gaussian nuclear density that reproduced the experimental mean square radius of ^{4}He, has been taken.

The isospin–dependence of the $\Lambda N \to nN$ process is summarized by the ratios R_{n0}/R_{p0} and R_{n1}/R_{n1}. The first one equals 2 for both models due to the

Table 4: Elementary $\Lambda N \to nN$ Block–Dalitz decay rates R_{NJ} (in units of fm^{-3}) obtained with the one–meson–exchange (OME) and one–meson–exchange plus two–pion–exchange (OME+TPE) weak potential models enforcing the $\Delta I = 1/2$ isospin rule.

Model	R_{n0}	R_{p0}	R_{n1}	R_{p1}	$\frac{R_{n0}}{R_{p0}}$	$\frac{R_{n1}}{R_{p1}}$	$\frac{R_{n1}}{R_{n0}}$	$\frac{R_{p1}}{R_{p0}}$
OME	3.98	1.99	4.96	18.24	2.00	0.27	1.24	9.16
OME+TPE	2.42	1.21	4.96	19.86	2.00	0.25	2.05	16.41

enforced $\Delta I = 1/2$ rule. The second one gives, via Eq. (95), $|\epsilon| = 2.53$ for the OME while $|\epsilon| = 2.65$ for the OME+TPE potential. These results imply that, by inspecting the definition of the parameter ϵ in Eq. (83), the $\Lambda N \to nN$ reduced amplitudes into isospin 0 and 1 final states are of the same order of magnitude, that is, the $\Delta I = 1/2$ transition gives the same probability of leaving the final state in a isosinglet–state or in a isotriplet–state. The spin–dependence of the $\Lambda N \to nN$ process is instead summarized by the ratios R_{n1}/R_{n0} and R_{p1}/R_{p0}. We observe that the TPE terms contribute in the same amount in both ratios, almost doubling their value compared to the OME result. This is due to the fact that the TPE terms decrease the central amplitude A_p and, therefore, reduce the value of R_{n0} and R_{p0} with the same factor. On the other hand, the calculation predicts the dominance of the spin–triplet channels , especially for the proton–induced transitions and the OME+TPE model.

As we previously mentioned, the R_{NJ}'s values adjusted for the five–body hypernuclei ${}^{5}_{\Lambda}$He allows one to obtain the Block–Dalitz decay rates to three– and four–body hypernuclei. In this work we limit to ${}^{4}_{\Lambda}$H and ${}^{4}_{\Lambda}$He since for hypertriton (${}^{3}_{\Lambda}$H) there is still no data available on non–mesonic decay rates, which complicates the discussion of the results. Moreover, a realistic theoretical approach implies knowing the exact solution of a three–body problem. Let us point out that the lifetime of the ${}^{3}_{\Lambda}$H has been a controversial observable for many years, since several experiments have claimed it to be as much as 30% shorter [53–55] than the lifetime of the free Λ, which is the value that one expects due to loosely bound Λ in the hypertriton. Although some theoretical works assigned a possible explanation to the effect of pion final–state interactions [56], recent experiments [57] have obtained a value within 1σ of the free Λ lifetime, being also compatible with the result obtained in a recent theoretical study that employs state–of–the–art nuclear and hypernuclear hamiltonians, considers ΣNN admixtures in the wave–function and accounts for pion distortion [58]. The non–mesonic decay channels of the hypertriton have been theoretically established to represent only about 1.5% of the total decay rate [59] and would not help in explaining an hypothetical smaller lifetime than that of the free Λ.

The results for four–body hypernuclei have been obtained from Eqs. (65)–(66)

and are summarized in Table 5 (lines OME–BD and OME+TPE–BD) together with the results of the finite nucleus calculations (lines OME and OME+TPE). The value employed for the density ρ_3 ($= 0.0259$ fm^{-3}) has been fixed in order to reproduce the OME+TPE finite nucleus prediction for $\Gamma_{\rm NM}({}^{4}_{\Lambda}{\rm He})$.

From Table 5, we observe that the OME and OME+TPE models predict similar values for both the Γ_n and Γ_p rates of ${}^{5}_{\Lambda}$He, while this does not hold for Γ_n in ${}^{4}_{\Lambda}$He and Γ_p in ${}^{4}_{\Lambda}$H. This is due to the fact that the OME+TPE model reduces the spin–singlet rates R_{n0} and R_{p0} in relation to those of the OME model, while taking approximately equal values for R_{n1} and R_{p1} in both models. The lack of spin–triplet R_{n1} contribution in $\Gamma_n({}^{4}_{\Lambda}{\rm He})$ and R_{p1} in $\Gamma_n({}^{4}_{\Lambda}{\rm H})$ but present in $\Gamma_p({}^{4}_{\Lambda}{\rm He})$ and $\Gamma_p({}^{4}_{\Lambda}{\rm H})$, respectively, aggravates the effect. On the contrary, this does not take place in ${}^{5}_{\Lambda}$He because the spin–triplet contributions dominate in the rates $\Gamma_n({}^{5}_{\Lambda}{\rm He})$ and $\Gamma_p({}^{5}_{\Lambda}{\rm He})$.

The decay rates obtained with the Block–Dalitz model for four–body hypernuclei are very similar to the ones calculated within the finite nucleus calculation. Despite the fact that no assumptions were made on the dynamics of the $\Lambda N \to nN$ interaction mechanism and in view of the results obtained in Table 5, we conclude that the Block–Dalitz model can be used to infer directly from the experimental hypernuclear rates the spin–isospin dependence of the non–mesonic weak decay. We think that this result is especially important in view of the forthcoming E22 J–PARC experiment [50].

In contrast to what is obtained for the decay rates, Table 5 shows that the Block–Dalitz model is unable to reproduce the asymmetry parameter obtained with the finite nucleus calculation for ${}^{5}_{\Lambda}$He. We have seen that the two approaches turn out to predict different contributions for all the interference terms building up the asymmetry. Note that the asymmetry parameter a_Λ in the Block–Dalitz model is given by Eq. (68) which is strictly valid only for the $\vec{\Lambda}p \to np$ free space process and the effects of the FSI and the hypernuclear structure have not been included.

In view of the results in Table 5, we may conclude that by looking at the decay rates there is a reasonable agreement between the finite nucleus OME and OME+TPE results and the available data. However, the OME badly fails in reproducing the experimental asymmetry parameter for ${}^{5}_{\Lambda}$He. We note that the negative value of the asymmetry in the OME model comes mainly from the interference between the A_p and E_p amplitudes and the sum of interferences of the F_p amplitude with the C_p and D_p ones. On the other hand, the TPE mechanism transforms the negative interferences A_pE_p, B_pC_p and F_pC_p into positive contributions that cancel the negative interferences F_pD_p and B_pD_p. In consequence, the large and negative a_Λ in the OME model becomes a positive value in the OME+TPE one.

The OME+TPE model corrects the OME defect to reproduce a_Λ but it seems to slightly imbalance the decay rates. Specifically, the OME+TPE model predicts

Table 5: The s–shell hypernuclei non–mesonic weak decay rates (in units of the free Λ decay width, $\Gamma_\Lambda = 3.8 \times 10^9$ s^{-1}) and intrinsic asymmetry parameters predicted by the finite nucleus calculation and the Block–Dalitz model (BD) for the one–meson–exchange (OME) and one–meson–exchange plus two–pion–exchange (OME+TPE) weak potential models. Results are shown for pure $\Delta I = 1/2$ decays and by including $\Delta I = 3/2$ contributions evaluated with the factorization approximation of Ref. [35]. Comparison with the most recent data is also given

		${}^{5}_{\Lambda}$He			
Model	Γ_n	Γ_p	$\Gamma_{\rm NM} = \Gamma_n + \Gamma_p$	Γ_n/Γ_p	a_Λ
OME	0.106	0.319	0.425	0.332	-0.516
OME–BD	0.106	0.319	0.425	0.332	-0.605
OME $\Delta I = 3/2$	0.086–0.145	0.308–0.367	0.425–0.453	0.236–0.468	-0.761– -0.162
OME+TPE	0.097	0.342	0.439	0.284	+0.070
OME+TPE–BD	0.097	0.342	0.439	0.284	+0.111
OME+TPE $\Delta I = 3/2$	0.084–0.129	0.335–0.383	0.439–0.468	0.220–0.381	-0.249–+0.346
KEK–E462 [25, 26]			0.424±0.024	0.45±0.11±0.03	
KEK–E462 [28]					$0.07 \pm 0.08^{+0.08}_{-0.00}$
		${}^{4}_{\Lambda}$He			
Model	Γ_n	Γ_p	$\Gamma_{\rm NM} = \Gamma_n + \Gamma_p$	Γ_n/Γ_p	
OME	0.032	0.248	0.280	0.128	
OME–BD	0.034	0.245	0.279	0.140	
OME $\Delta I = 3/2$	0.004–0.086	0.241–0.282	0.276–0.328	0.014–0.359	
OME+TPE	0.016	0.267	0.283	0.062	
OME+TPE–BD	0.021	0.262	0.283	0.080	
OME+TPE $\Delta I = 3/2$	0.001–0.059	0.263–0.294	0.281–0.324	0.003–0.220	
BNL07 [29]	≤ 0.035	0.180 ± 0.028	0.177 ± 0.029	≤ 0.19	
BNL98 [60]	0.04 ± 0.02	0.16 ± 0.02	0.20 ± 0.03	0.25 ± 0.13	
KEK98 [61]	$0.01^{+0.04}_{-0.01}$	0.16 ± 0.02	0.17 ± 0.05	$0.06^{+0.28}_{-0.06}$	
		${}^{4}_{\Lambda}$H			
Model	Γ_n	Γ_p	$\Gamma_{\rm NM} = \Gamma_n + \Gamma_p$	Γ_n/Γ_p	
OME	0.080	0.016	0.095	4.992	
OME–BD	0.081	0.017	0.099	4.734	
OME $\Delta I = 3/2$	0.066–0.107	2E-4–0.084	0.093–0.150	0.785–411.292	
OME+TPE	0.072	0.008	0.080	8.764	
OME+TPE–BD	0.075	0.010	0.086	7.264	
OME+TPE $\Delta I = 3/2$	0.064–0.093	0.001–0.064	0.079–0.128	1.008–117.359	
BNL98 [60]			0.17 ± 0.11		

a relative large value of $\Gamma_p({}^{5}_{\Lambda}\mathrm{He})$, thus increasing the value of $\Gamma_{\rm NM}({}^{5}_{\Lambda}\mathrm{He})$ and reducing $\Gamma_n/\Gamma_p({}^{5}_{\Lambda}\mathrm{He})$ away from the central value of the experimental results. However, one has to note that in several cases the available data are of limited

precision, lacking or even missing. For this reason and despite the scarcity experimental data, we may conclude that the OME+TPE model obtains results approximately in accordance with the experimental data. Future experimental data on the decay rates and Γ_n/Γ_p ratio, especially in four–body hypernuclei will be of utmost importance in order to infer the best potential model for the $\Lambda N \to nN$ weak decay. Furthermore, an improvement of experimental data could represent an important advance on the discussion of the reliability of the Block–Dalitz model, since as we previously commented, Eqs. (91)–(94) turn out to be useful for testing it.

4.2 Four–body hypernuclei and test of the $\Delta I = 1/2$

The results discussed so far have been obtained enforcing the $\Delta I = 1/2$ isospin rule for all the meson–baryon weak couplings involved in the meson–exchange weak transition potential (OME and OME+TPE). As we previously mentioned, the transition $\Lambda N \to nN$ is assumed to proceed via the exchange of virtual pseudoescalar and vector mesons. The transition involves a weak ($\mathcal{H}^W_{BB'M}$) and a strong vertex ($\mathcal{H}^S_{BB'M}$). Now, we study possible contributions of the $\Delta I = 3/2$ terms to the non–mesonic weak decay. The $BB'M$ weak couplings for the $\Delta I = 3/2$ transitions are negligible for pions and this result is generalized to the entire pseudoscalar octet. Therefore, the weak vertices that will be modified to include the violation of the $\Delta I = 1/2$ rule are $\Lambda N\rho$, ΛNK^* and $\Lambda N\omega$. Unfortunately, these couplings are not known experimentally. They will be obtained from the factorization approximation, in which each $BB'M$ vertex is factorized into the product of baryon–to–baryon and vacuum–to–meson matrix elements of quarks currents. The $\Delta I = 3/2$ $\Lambda N\omega$ coupling vanishes in the factorization approximation [62] . In order to take into account the limitations of this approximation, we allow for a variation of up to a factor ± 3 (s_M) in the $\Delta I = 3/2$ ρ and K^* couplings. Since the relative sign between the $\Delta I = 1/2$ and $\Delta I = 3/2$ amplitudes is not predicted within this approach we allow for both possibilities. For details on the factorization approximation we refer to Refs. [35, 62].

The results for the decay rates and the asymmetry parameter of four– and five–body hypernuclei are also given in Table 5 for the OME and OME+TPE models including $\Delta I = 3/2$ contributions. The range of variability of the $\Delta I = 3/2$ contributions depends on these scaling factors s_ρ and $s_{K^*} \in [-3, +3]$. From Table 5 we see that the effect of $\Delta I = 3/2$ contributions is moderate in all the decay rates except for $\Gamma_n(^4_\Lambda\mathrm{He})$, $\Gamma_p(^4_\Lambda\mathrm{H})$ and the asymmetry parameter. A comparison between our results and the experimental data can inform us about possible violations of the $\Delta I = 1/2$ rule. Unfortunately, as we mentioned in Section 4.1, the available data are scarce or still present large experimental error bars and therefore, it is not appropriate to draw conclusions yet. We hope that the future E22 experiment at J–PARC [50] can obtain improved data, especially for $^4_\Lambda$He and $^4_\Lambda$H.

Table 6: Predictions for the isospin ratios R_{n0}/R_{p0} and corresponding value of $\delta_0 \equiv A_{3/2}^{J=0}(I_f = 1)/A_{1/2}^{J=0}(I_f = 1)$ obtained with the OME+TPE model introducing different $\Delta I = 3/2$ contributions. The value of δ_0 is obtained from Eq. (84).

s_ρ	s_{K^*}	R_{n0}/R_{p0}	δ_0
-3	-3	0.18	0.88
-3	0	3.89	-0.21
-3	3	9.68	-0.44
0	-3	0.07	1.18
0	0	2	0
0	3	7.29	-0.38
3	-3	0.01	1.56
3	0	0.83	0.31
3	3	3.74	-0.20

We have seen in Section 3.1 that the available data of $\Gamma_n(^4_\Lambda\mathrm{He})$ and $\Gamma_n(^4_\Lambda\mathrm{H})$ are especially useful for testing the $\Delta I = 1/2$ isospin selection rule. As we see in Eq. (97), the ratio R_{n0}/R_{p0} can be obtained by the OME and OME+TPE finite nucleus calculation as $\Gamma_n(^4_\Lambda\mathrm{He})/\Gamma_\mathrm{p}(^4_\Lambda\mathrm{H})$ and can be expressed, via Eq. (84), as a function of the ratio δ_0 of Eq. (81) between the $\Delta I = 3/2$ and $\Delta I = 1/2$ $\Lambda N \to nN$ reduced amplitudes for isospin 1 final states. In Table 6 we show the numerical values of R_{n0}/R_{p0} and δ_0 obtained for the different contributions of the s_ρ and s_{K^*} scaling factors. Pure $\Delta I = 1/2$ transitions corresponds to $\delta_0 = 0$, $R_{n0}/R_{p0} = 2$ and $s_{K^*} = s_\rho = 0$. As we mentioned, $R_{n0}/R_{p0} = 2$ does not imply that the $\Delta I = 1/2$ rule is valid but deviations from this value are clearly signal of the violation of this selection rule. By a simple inspection of Figure 3 and Table 6 we conclude that the R_{n0}/R_{p0} is very sensitive to the $\Delta I = 3/2$ contributions.

We have seen that the ratio R_{n1}/R_{p1} is not sensitive to the $\Delta I = 3/2$ transitions. This is due to the fact that the only transition with total spin $J = 1$ that leaves the final state with $I_f = 1$ (note that $\hat{T}_{3/2}$ acting on an $I = 1/2$ initial state cannot leave the final state at $I_f = 0$) is the one corresponding to the parity–violating (PV) amplitude F, $^1S_1 \to {}^3P_1$. The PV operator for vector mesons is given in Section 2.2 and has the following form: $\hat{\mathcal{O}}_{\mathrm{PV}} = (\vec{\sigma}_1 \times \vec{\sigma}_2) \cdot \vec{r}$. With the quantum numbers of the initial (L_r,S_0) and final state (L,S) we see that the vector mesons (ρ and K^*) do not contribute to this amplitude because the $9j$ symbol appearing in this matrix element is equal to 0, so (See Appendix B.4):

$$\langle (LS)JM_J|\hat{\mathcal{O}}|(L_rS_0)JM_J)\rangle = 0 \ . \tag{103}$$

This is the reason why the ratio R_{n1}/R_{p1} is insensitive to $^1S_1 \to {}^3P_1$ $\Delta I = 3/2$ contributions. Based on these conclusions, we will study the degree of violation of the $\Delta I = 1/2$ rule in terms of the parameter δ_0, which measures the strength

of $\Delta I = 3/2$ contributions.

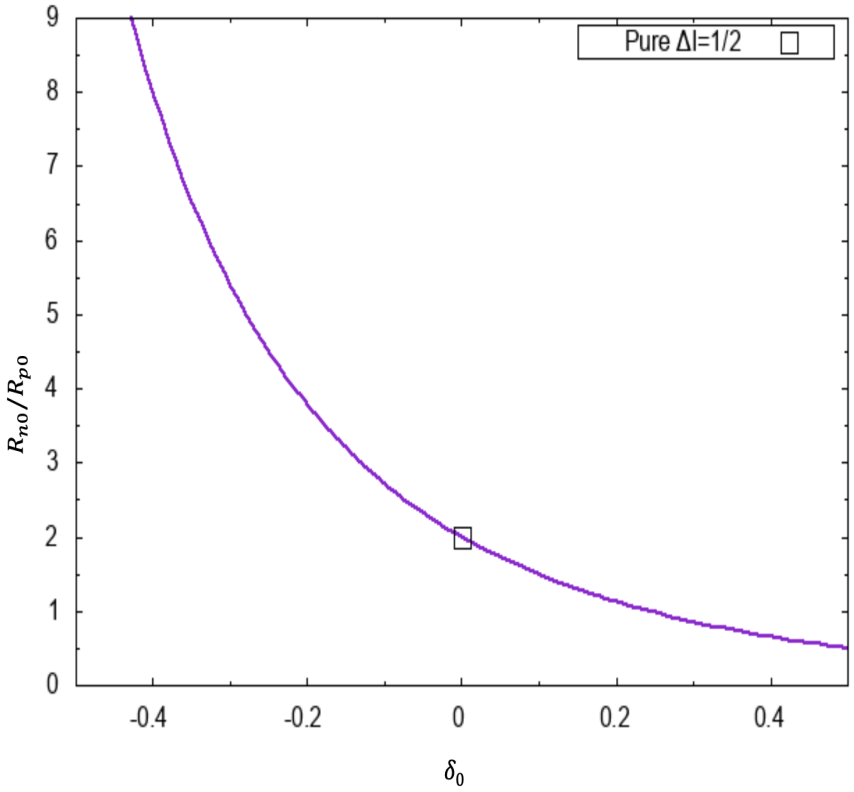

Figure 3: The ratio R_{n0}/R_{p0} is given versus $\delta_0 = A^{J=0}_{3/2}(I_f = 1)/A^{J=0}_{1/2}(I_f = 1)$.

The following figures show the dependence of the the asymmetry parameter, the total non–mesonic decay rate and the Γ_n/Γ_p ratio of ${}^{5}_{\Lambda}$He on the amount of $\Delta I = 1/2$ violation, measured by the parameter δ_0, for the OME and OME+TPE models. The experimental value together with the margin of error (faded grey box) are also shown. In Figure 4 it can be seen that the asymmetry parameter is very sensitive to the meson–exchange model. As we already commented, the OME+TPE model transforms the large and negative value of the OME model into a positive value, more aligned with the experimental result. The $\Delta I = 3/2$ maintain the positive sign of the asymmetry parameter as long as $\delta_0 \geq -0.17$. Moreover, the asymmetry parameter becomes relatively sensitive to δ_0 and changes from -0.3 to 0.2 in OME+TPE and from -0.3 to -0.6 in OME for the considered δ_0 range.

As for the total rate $\Gamma_{\rm NM}$ and Γ_n/Γ_p ratio, we observe in Figure 5 and Figure 6,

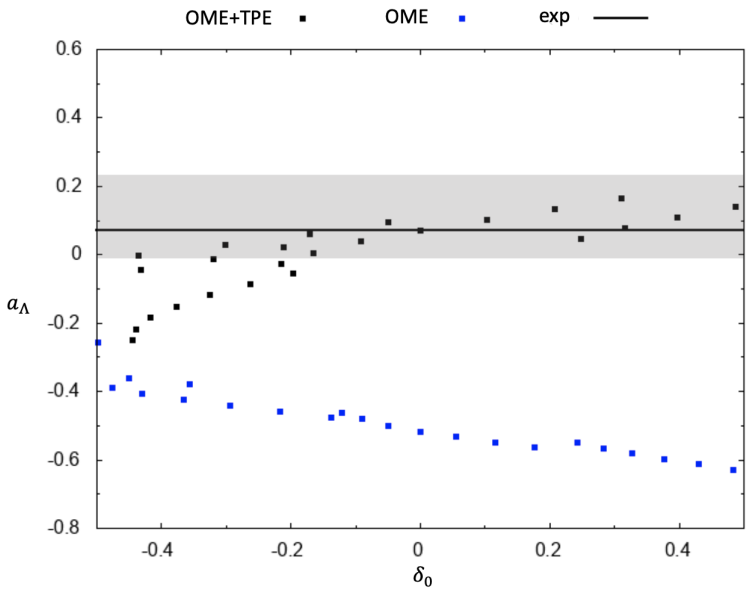

Figure 4: The asymmetry parameter a_Λ of ${}^{5}_{\Lambda}$He obtained with OME and OME+TPE model is given versus $\delta_0 = A^{J=0}_{3/2}(I_f = 1)/A^{J=0}_{1/2}(I_f = 1)$. Faded grey box represents the margin of error of the experimental central value represented by the continuous line (exp).

respectively, that they are relatively insensitive to the model, while Γ_n/Γ_p is moderately sensitive to δ_0.

To finalize, we conclude that more precise data of the hypernuclear decay observables are needed in order to learn about the details of the non–mesonic weak decay. In this respect, the asymmetry parameter stands out for being strongly sensitive to the model, and the present measured value has already discarded some of the existing models in the literature. In order to learn about the $\Delta I = 1/2$ isospin rule, it is necessary to obtain R_{n0}/R_{p0} with good precision because a deviation of the value 2 would indicate the presence of $\Delta I = 3/2$ terms. Thanks to the Block–Dalitz model validated in the present work, we can identify the former ratio to the ratio $\Gamma_n({}^{4}_{\Lambda}\mathrm{He})/\Gamma_p({}^{4}_{\Lambda}\mathrm{H})$, built up from the rates of light hypernuclei. A forthcoming experiment in J–PARC that focuses in the measurement of the non–mesonic rates of light hypernuclei will being new light to this subject.

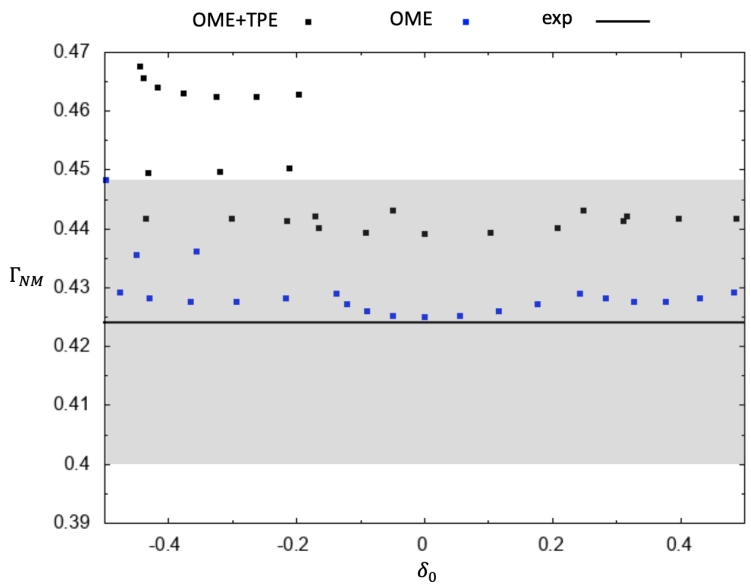

Figure 5: The total decay rate $\Gamma_{\rm NM}$ of ${}^{5}_{\Lambda}$He obtained with OME and OME+TPE model is given versus $\delta_0 = A^{J=0}_{3/2}(I_f = 1)/A^{J=0}_{1/2}(I_f = 1)$. Faded grey box represents the margin of error of the experimental central value represented by the continuous line (exp).

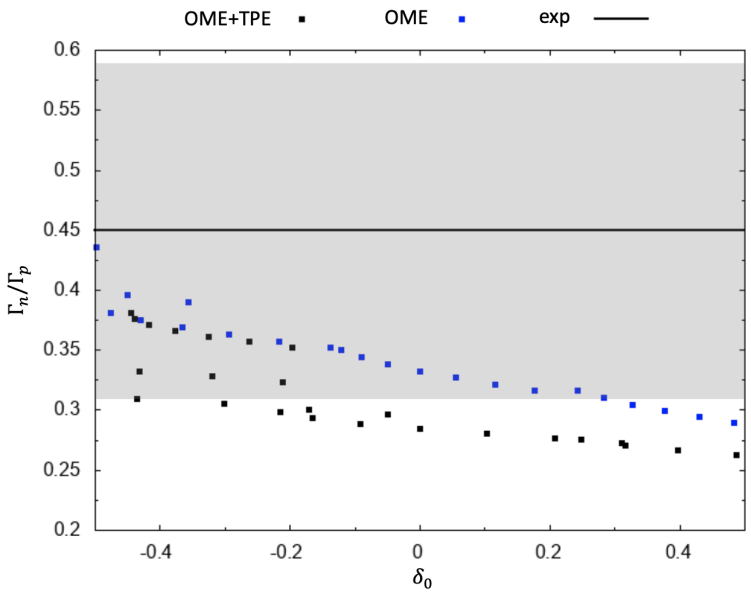

Figure 6: The ratio Γ_n/Γ_p of ${}^{5}_{\Lambda}$He obtained with OME and OME+TPE model is given versus $\delta_0 = A^{J=0}_{3/2}(I_f = 1)/A^{J=0}_{1/2}(I_f = 1)$. Faded grey box represents the margin of error of the experimental central value represented by the continuous line (exp).

5 Conclusions

The non–mesonic weak decay of s–shell hypernuclei is studied within a finite nucleus approach, using a one–meson–exchange plus two–pion–exchange transition potential.

In the Block–Dalitz phenomenological approach, a contact interaction between the four–baryons is assumed and the nucleon final state interaction are neglected. This approach together with the experimental data allows to extract the spin and isospin behavior of the $\Lambda N \to nN$ interaction without detailing the present interaction mechanisms. Through the finite nucleus calculation we have demonstrated that, despite its simplicity, this approach allows one to set certain conditions and equalities among the partial decay rates for s–shell hypernuclei. Moreover, the Block–Dalitz approach allows one to deduce the four $\Lambda N \to nN$ spin–isospin elementary R_{NJ} rates, and, subsequently, these rates are employed to obtain the decay widths of s–shell hypernuclei. Although this approach predicts the experimental results of the decay rates to a certain degree of agreement, this model is not able to reproduce the value of the asymmetry parameter calculated with a finite nucleus model. FSI and details of the hypernuclear structure make the Block–Dalitz formula an approximate result.

In view of the results obtained, the OME+TPE model modifies moderately the partial decay rates but has a tremendous influence on the asymmetry parameter, due to the change of sign of the negative interference terms A_pE_p, B_pC_p and F_pC_p into positive contributions. Therefore, the OME+TPE model is able to reproduce the positive value of the asymmetry parameter, although it slightly increases Γ_p giving rise to values further away from the experimental ones. For these reasons, more theoretical research is needed together with an improvement of the experimental data, especially in the asymmetry parameter for ${}^{5}_{\Lambda}$He and partial decay rates for four–body hypernuclei, in order to establish the most appropriate model for the non–mesonic weak decay.

The testing of the validity of the $\Delta I = 1/2$ isospin rule has been studied by analysing possible effects of $\Delta I = 3/2$ contributions in the finite nucleus approach using the factorization approximation. We have seen that the $\Lambda N \to nN$ spin–isospin channels with $J = 0$ (i.e., the Block–Dalitz ratio R_{n0}/R_{p0}) becomes especially sensitive to the $\Delta I = 3/2$ transitions. A more accurate experimental determination of this ratio will be of utmost importance in helping to establish the degree of $\Delta I = 1/2$ violation. On the other hand, the ratio R_{n1}/R_{p1} is insensitive to these incorporations due to the fact that in the factorization approximation the K^* and ρ mesons do not contribute to ${}^3S_1 \to {}^1P_1$, that is, the only $\Delta I = 3/2$ with $J = 1$ and $I_f = 1$. Although the asymmetry parameter, Γ_n/Γ_p and the total width $\Gamma_{\rm NM}$ for ${}^{5}_{\Lambda}$He become relatively sensitive to the $\Delta I = 3/2$ contributions, better data for these observables will help in evaluating the validity of the $\Delta I = 1/2$ rule. Unfortunately, the present data do not allow us to establish the relevance of $\Delta I = 3/2$ contributions. Hopefully, these results together with forthcoming J–PARC data on the non–mesonic decay of $\Gamma_n({}^{4}_{\Lambda}\text{He})$

and $\Gamma_n(^4_\Lambda\mathrm{H})$, will allow us to establish the degree of violation of the $\Delta I = 1/2$ rule in non–mesonic weak decay of hypernuclei.

References

[1] M. Danysz and J. Pniewski, Phil. Mag., **44** (1953) 348.

[2] W. M. Alberico and G. Garbarino, Phys. Rep. **369** (2002) 1.

[3] M. Tanabashi et al. (Particle Data Group), Phys. Rev. **D 98** (2018) 030001.

[4] J. F. Donoghue, E. Golowich and B. R. Holstein, *Dynamics of the Standard Model* (Cambridge University Press, Cambridge, England, 1992).

[5] A. Gal, E.V. Hungerford, and D.J. Millener Rev. Mod. Phys. **88** (2016) 035004.

[6] E. Oset and A. Ramos, Prog. Part. Nucl. Phys. **41** (1998) 191.

[7] A. Parreño, Lecture Notes Phys. **724** (2007) 141.

[8] T. Bressani, E. Botta and G. Garbarino, Eur. Phys. J. **A 48** (2012) 41.

[9] G. Garbarino, Nucl. Phys. **A 914** (2013) 170.

[10] A. Parreño, A. Ramos and C. Bennhold, Phys. Rev. **C 56** (1997) 339.

[11] C. Chumillas, G. Garbarino, A. Parreño and A. Ramos, Phys. Lett. **B 657** (2007) 180.

[12] K. Sasaki, T. Inoue and M. Oka, Nucl. Phys. **A 669** (2000) 331; **A 678** (2000) 455(E); **A 707** (2002) 477.

[13] D. Jido, E. Oset and J. E. Palomar, Nucl. Phys. **A 694** (2001) 525.

[14] K. Itonaga, T. Ueda and T. Motoba, Phys. Rev. **C 65** (2002) 034617.

[15] A. Parreño and A. Ramos, Phys. Rev. **C 65** (2002) 015204.

[16] G. Garbarino, A. Parreño and A. Ramos, Phys. Rev. Lett. **91** (2003) 112501; Phys. Rev. **C 69** (2004) 054603.

[17] W.M. Alberico, G. Garbarino, A. Parreño and A. Ramos, Phys. Rev. Lett. **94** (2005) 082501.

[18] K. Itonaga, T. Motoba, T. Ueda and Th. A. Rijken, Phys. Rev. **C 77** (2008) 044605; Int. J. Mod. Phys. **E 19** (2010) 2579.

[19] E. Bauer, G. Garbarino, A. Parreño and A. Ramos, Nucl. Phys. **A 836** (2010) 199.

[20] E. Bauer and G. Garbarino, Phys. Rev. **C 81** (2010) 064315.

[21] E. Bauer and G. Garbarino, Phys. Lett. **B 698** (2011) 306.

[22] E. Bauer, G. Garbarino, A. Parreño and A. Ramos, Phys. Rev. **C 85** (2012) 024321.

[23] E. Bauer and G. Garbarino, Phys. Lett. **B 716** (2012) 249.

[24] S. Okada et al., Phys. Lett. **B 597** (2004) 249.

[25] H. Outa et al., Nucl. Phys. **A 754** (2005) 157c; H. Outa, in *Hadron Physics*, IOS Press, Amsterdam, 2005, p. 219. Edited by T. Bressani, A. Filippi and U. Wiedner. Proceedings of the International School of Physics "Enrico Fermi", Course CLVIII, Varenna (Italy), June 22 – July 2, 2004.

[26] B. H. Kang et al., Phys. Rev. Lett. **96** (2006) 062301.

[27] M. J. Kim et al., Phys. Lett. **B 641** (2006) 28.

[28] T. Maruta, PhD thesis, KEK Report 2006-1, June 2006; Eur. Phys. J. **A 33** (2007) 255.

[29] J.D. Parker et al., Phys. Rev. **C 76** (2007) 035501.

[30] M. Kim et al., Phys. Rev. Lett. **103** (2009) 182502.

[31] M. Agnello et al., Phys. Lett. **B 685** (2010) 247.

[32] M. Agnello et al., Phys. Lett. **B 701** (2011) 556.

[33] M. Oka, Nucl. Phys. **A 754** (2005) 117

[34] A. Pérez-Obiol, A. Parreño and B. Juliá-Díaz, Phys. Rev. **C 84** (2011) 024606

[35] A. Parreño, A. Ramos, C. Bennhold and K. Maltman, Phys. Lett.**B 435** (1998) 1.

[36] W. M. Alberico and G. Garbarino, in *Hadron Physics*, IOS Press, Amsterdam, 2005, p. 125. Edited by T. Bressani, A. Filippi and U. Wiedner. Amsterdam, Proceedings of the International School of Physics "Enrico Fermi", Summer Course on Hadronic Physics.

[37] A. Ramos, E. van Meijgaard, C. Bennhold and B. K. Jennings, Nucl. Phys. **A 544** (1992) 703.

[38] Redmond P.J, Proc. R. Soc. **222** (1954) 84-93.

[39] M. Moshinsky, Nucl. Phys., **13** (1959) 104–116

[40] V.G.J. Stoks and Th.A. Rijken, Phys. Rev. **C 59** (1999) 3009. Th.A. Rijken, V.G.J. Stoks and Y. Yamamoto, Phys. Rev. **C 59** (1999) 21.

[41] B. Holzenkamp, K. Holinde and J. Speth, Nucl. Phys. **A 500** (1989) 485.

[42] C. Barbero, A. P. Galeão and F. Krmpotić, Phys. Rev. **C 72** (2005) 035210.

[43] R. H. Dalitz and G. Rajasekaran, Phys. Lett. **1** (1962) 58; M. M. Block and R. H. Dalitz, Phys. Rev. Lett. **11** (1963) 96.

[44] C. B. Dover, Few–Body Systems Suppl. **2** (1987) 77.

[45] J. Cohen, Phys. Rev. **C 42** (1990) 2724.

[46] R. A. Schumacher, Nucl. Phys. **A 547** (1992) 143c.

[47] W. M. Alberico and G. Garbarino, Phys. Lett. **B 486** (2000) 362.

[48] R. L. Gill, Nucl. Phys. **A 691** (2001) 180c.

[49] K. Sasaki, M. Izaki, and M. Oka, Phys. Rev. **C 71** (2005) 035502.

[50] S. Ajimura et al., *Exclusive study on the ΛN weak interaction in $A = 4$ Λ–Hypernuclei*, Letter of intent for an experiment (E22) at J–PARC (2007).

[51] A. Ramos, E. Oset and L. L. Salcedo, Phys. Rev. **C 50** (1994) 2314.

[52] E. Bauer, G. Garbarino, C. A. Rodríguez Peña, Phys. Rev. **C 96** (2017) 044303.

[53] B. I. Abelev, Science **328** (2010), 58-62

[54] C. Rappold, E. Kim, D. Nakajima, T. R. Saito, O. Bertini, S. Bianchin, V. Bozkurt, M. Kavatsyuk, Y. Ma and F. Maas, Nucl. Phys. **A 913** (2013) 170

[55] L. Adamczyk Phys. Rev. **C 97** (2018) 054909

[56] A. Gal and H. Garcilazo, Phys. Lett. **B 791** (2019) 48-53

[57] S. Acharya, Phys. Lett. **B 797** (2019) 134905

[58] A. Pérez-Obiol, D. Gazda, E. Friedman and A. Gal, Phys. Lett. **B** (2020) 135916.

[59] J. Golak, K. Miyagawa, H. Kamada, H. Witala, W. Gloeckle, A. Parreño, A. Ramos and C. Bennhold, Phys. Rev. **C 55** (1997) 2196

[60] V. J. Zeps, Nucl. Phys. **A 639** (1998) 261c.

[61] H. Outa et al., Nucl. Phys. **A 639** (1998) 251c.

[62] K. Maltman and M. Shmatikov, Phys. Rev. **C 51** (1995) 1576

[63] H. Nabetani, T. Ogaito, T. Sato and T. Kishimoto, Phys. Rev. **C 60** (1999) 017001.

Appendix A The Block–Dalitz non–mesonic decay rates

In this appendix we review the methodology used to isolate the Block–Dalitz amplitudes. First, to study the hypernucleus we will use the weak coupling scheme. As we have already mentioned, the hypernuclear state is the result of the coupling between the Λ and the nuclear core states:

$$|^{A}_{\Lambda}\ Z\rangle =| \Lambda\rangle \otimes |\text{Core}\rangle\ . \tag{104}$$

To study the non–mesonic weak decay, it will be necessary to decouple one of the nucleons of the core, leaving a residual $(A-1)$ nuclear system. Being both, Λ and N, in the lower energy state of the ground state hypernucleus, only two initial ΛN states are possible, the singlet $^1S_0$ and the triplet $^3S_1$ states.

A.1 $^{3}_{\Lambda}$H rate

The hypertriton $^{3}_{\Lambda}$H is a bound state of a proton, a neutron and a Λ with total spin $J_H = 1/2$ and $M_H = \pm 1/2$. The initial state is defined by

$$|^{3}_{\Lambda}\ \text{H}\rangle \equiv| \frac{1}{2}\ M_H\rangle =| \Lambda\rangle\otimes |\ np\rangle\ . \tag{105}$$

As we have already commented, antisymmetry of the final NN system imposes some restrictions to the relevant quantum numbers. The np pair is in total orbital momentum $L = 0$ and therefore, $J = S$. Due to the fact that the Λ is an isosinglet state ($t_\Lambda = 0$) the total isospin of the initial hypernucleus is the same as the nuclear core. Experimentally, there is no evidence of Λnn and Λpp bound states, which would imply that the ΛNN system could form an isotriplet ($I = 1$) state. The np pair, and consequently the hypertriton, are in isospin singlet states ($I = 0$). Therefore, only the $S = 1$ np state is allowed, leading to a total spin and projection of $J = 1$ and $M = \pm 1, 0$. Taking $J_H = 1/2$ and $j_\Lambda = 1/2$ we can write:

$$|\ \frac{1}{2}\ M_H\rangle = \sum_{m_\Lambda, M} \langle \frac{1}{2}\ m_\Lambda\ 1\ M\ |\ \frac{1}{2}\ M_H\rangle\ |\ \frac{1}{2}\ m_\Lambda\rangle_\Lambda\ |\ \ 1\ M\rangle_{np}\ . \tag{106}$$

Without loss of generality, one can impose $M_H = +\frac{1}{2}$ and therefore,
$M_H = \frac{1}{2} = m_\Lambda + M \Rightarrow m_\Lambda = \frac{1}{2} - M$

$$|\ \frac{1}{2}\ \frac{1}{2}\rangle = \sum_{M} \langle \frac{1}{2}\ \frac{1}{2}\ \text{-}\ M\ 1\ M\ |\ \frac{1}{2}\ \frac{1}{2}\rangle\ |\ \frac{1}{2}\ \frac{1}{2}\ \text{-}\ M\rangle_\Lambda\ |\ 1\ M\rangle_{np}\ . \tag{107}$$

Now, we decouple the np pair in the neutron and the proton states.

$$|\ 1\ M\rangle_{np} = \sum_{m_n}\sum_{m_p} = \langle \frac{1}{2}\ m_n\ \frac{1}{2}\ m_p\ |\ \frac{1}{2}\ \frac{1}{2}\rangle\ |\ \frac{1}{2}\ m_n\rangle\ |\ \frac{1}{2}\ m_p\rangle\ ,$$

so, the initial hypernuclear state is rewritten as

$$
\begin{aligned}
|\ \frac{1}{2}\ \frac{1}{2}\rangle = \sum_{M,m_p} \langle \frac{1}{2}\ \frac{1}{2}\ \text{-}\ M\ 1\ M \mid \frac{1}{2}\ \frac{1}{2}\rangle \langle \frac{1}{2}\ M\ \text{-}\ m_p\ \frac{1}{2}\ m_p \mid 1\ M\rangle \\
|\ \frac{1}{2}\ \frac{1}{2}\ \text{-}\ M\rangle_\Lambda \mid \frac{1}{2}\ M\ \text{-}\ m_p\rangle_n \mid \frac{1}{2}\ m_p\rangle_p\ .
\end{aligned}
\tag{108}
$$

To describe the $\Lambda n \to nn$ and $\Lambda p \to np$ transitions, one needs to couple the Λ with a neutron n and with a proton p, respectively. We will denote the coupled ΛN state as $|S_i M_i\rangle$:

$$
\Lambda n :| \frac{1}{2}\ \frac{1}{2}\ \text{-}\ M\rangle_\Lambda \mid \frac{1}{2}\ M\ \text{-}\ m_p\rangle_n = \sum_{S_i,M_i} \langle \frac{1}{2}\ \frac{1}{2} - M\ \frac{1}{2}\ M - m_p \mid S_i M_i\rangle \mid S_i M_i\rangle_{\Lambda n}\ ,
\tag{109}
$$

where $M_i = 1/2 - M + M - m_p = 1/2 - m_p \Rightarrow m_p = 1/2 - M_i$.

$$
\Lambda p :| \frac{1}{2}\ \frac{1}{2}\ \text{-}\ M\rangle_\Lambda \mid \frac{1}{2}\ m_p\rangle_p = \sum_{S_i,M_i} \langle \frac{1}{2}\ \frac{1}{2}\ \text{-}\ M\ \frac{1}{2}\ m_p \mid S_i M_i\rangle \mid S_i\ M_i\rangle_{\Lambda p}\ ,
\tag{110}
$$

where $M_i = 1/2 - M + m_p \Rightarrow m_p = M + M_i - 1/2$

Rewriting the sum in Eq. (108) one obtains:

$$
\begin{aligned}
|\ \frac{1}{2}\ \frac{1}{2}\rangle = \sum_{S_i} \sum_{M_i} \sum_{M} \langle \frac{1}{2}\ \frac{1}{2}\ \text{-}\ M\ 1\ M \mid \frac{1}{2}\ \frac{1}{2}\rangle \langle \frac{1}{2}\ M + M_i\ \text{-}\ 1\ \frac{1}{2}\ \frac{1}{2}\ \text{-}\ M_i \mid 1\ M\rangle \\
\langle \frac{1}{2}\ \frac{1}{2}\ \text{-}\ M\ \frac{1}{2}\ M + M_i - \frac{1}{2} \mid S_i\ M_i\rangle \mid S_i\ M_i\rangle_{\Lambda n} \mid \frac{1}{2}\ \frac{1}{2}\ \text{-}\ M_i\rangle_p\ ,
\end{aligned}
\tag{111}
$$

for the $\Lambda n \to nn$ transition and

$$
\begin{aligned}
|\ \frac{1}{2}\ \frac{1}{2}\rangle = \sum_{S_i} \sum_{M_i} \sum_{M} \langle \frac{1}{2}\ \frac{1}{2}\ \text{-}\ M\ 1\ M \mid \frac{1}{2}\ \frac{1}{2}\rangle \langle \frac{1}{2}\ \frac{1}{2}\ \text{-}\ M_i\ \frac{1}{2}\ M + M_i\ \text{-}\ \frac{1}{2} \mid 1\ M\rangle \\
\langle \frac{1}{2}\ \frac{1}{2}\ \text{-}\ M\ \frac{1}{2}\ M + M_i\ \text{-}\ \frac{1}{2} \mid S_i\ M_i\rangle \mid S_i\ M_i\rangle_{\Lambda p} \mid \frac{1}{2}\ \frac{1}{2}\ \text{-}\ M_i\rangle_n\ ,
\end{aligned}
\tag{112}
$$

for the $\Lambda p \to np$ one.

We focus on the $\Lambda n \to nn$ transition, but the $\Lambda p \to np$ case proceeds analogously. If $S_i = 0 \Rightarrow M_i = 0$ and $M = \pm 1, 0$, the contribution to Eq. (111) reads:

$$
\begin{aligned}
&\sum_M \langle \frac{1}{2}\ \frac{1}{2}\ \text{-}\ M\ 1\ M \mid \frac{1}{2}\ \frac{1}{2}\rangle \langle \frac{1}{2}\ M\ \text{-}\ \frac{1}{2}\ \frac{1}{2}\ \frac{1}{2} \mid 1\ M\rangle \\
&\times \langle \frac{1}{2}\ \frac{1}{2}\ \text{-}\ M\ \frac{1}{2}\ M\ \text{-}\ \frac{1}{2} \mid 0\ 0\rangle \mid 0\ 0\rangle_{\Lambda n} \mid \frac{1}{2}\ \frac{1}{2}\rangle_p \\
&= \langle \frac{1}{2}\ -\frac{1}{2}\ 1\ 1 \mid \frac{1}{2}\ \frac{1}{2}\rangle \langle \frac{1}{2}\ \frac{1}{2}\ \frac{1}{2}\ \frac{1}{2} \mid 1\ 1\rangle \langle \frac{1}{2}\ -\frac{1}{2}\ \frac{1}{2}\ \frac{1}{2} \mid 0\ 0\rangle \mid 0\ 0\rangle_{\Lambda n} \mid \frac{1}{2}\ \frac{1}{2}\rangle_p \\
&+ \langle \frac{1}{2}\ \frac{1}{2}\ 1\ 0 \mid \frac{1}{2}\ \frac{1}{2}\rangle \langle \frac{1}{2}\ -\frac{1}{2}\ \frac{1}{2}\ \frac{1}{2} \mid 1\ 0\rangle \langle \frac{1}{2}\ \frac{1}{2}\ \frac{1}{2}\ -\frac{1}{2} \mid 0\ 0\rangle \mid 0\ 0\rangle_{\Lambda n} \mid \frac{1}{2}\ \frac{1}{2}\rangle_p \\
&+ \langle \frac{1}{2}\ \frac{3}{2}\ 1\ -1 \mid \frac{1}{2}\ \frac{1}{2}\rangle \langle \frac{1}{2}\ -\frac{3}{2}\ \frac{1}{2}\ \frac{1}{2} \mid 1\ -1\rangle \\
&\times \langle \frac{1}{2}\ -\frac{1}{2}\ \frac{1}{2}\ -\frac{3}{2} \mid 0\ 0\rangle \mid 0\ 0\rangle_{\Lambda n} \mid \frac{1}{2}\ \frac{1}{2}\rangle_p \\
&= \left(-\sqrt{\frac{2}{3}} \cdot 1 \cdot \frac{-1}{\sqrt{2}} + \frac{1}{\sqrt{3}} \cdot \frac{1}{\sqrt{2}} \cdot \frac{1}{\sqrt{2}} + 0 \right) \mid 0\ 0\rangle_{\Lambda n} \mid \frac{1}{2}\ \frac{1}{2}\rangle_p \\
&= \frac{\sqrt{3}}{2} \mid 0\ 0\rangle_{\Lambda n} \mid \frac{1}{2}\ \frac{1}{2}\rangle_p \ .
\end{aligned}
\tag{113}
$$

Then, the probability is calculated as follows:

$$
P = \left| \langle \frac{1}{2}\ \frac{1}{2} \mid \frac{1}{2}\ \frac{1}{2}\rangle \right|^2_{S_i=0} = \frac{3}{4} \ . \tag{114}
$$

If $S_i = 1 \Rightarrow M_i = \pm 1, 0$ and $M = \pm 1, 0$, the contribution to Eq. (111) reads:

$$
\begin{aligned}
&\sum_{M_i} \sum_M \langle \frac{1}{2}\ \frac{1}{2}\ \text{-}\ M\ 1\ M \mid \frac{1}{2}\ \frac{1}{2}\rangle \langle \frac{1}{2}\ M + M_i\ \text{-}\ \frac{1}{2}\ \frac{1}{2}\ \frac{1}{2}\ \text{-}\ M_i | 1\ 0\rangle \\
&\langle \frac{1}{2}\ \frac{1}{2}\ \text{-}\ M\ \frac{1}{2}\ M + M_i\ \text{-}\ \frac{1}{2} | 1\ M\rangle | 1\ M_i\rangle | \frac{1}{2}\ \frac{1}{2}\ \text{-}\ M_i\rangle \ .
\end{aligned}
\tag{115}
$$

From the previous equation, we can extract some restrictions:

- The state $|\frac{1}{2}\ \frac{1}{2} - M_i\rangle$ implies that the $M_i = -1$ spin projection is forbidden.
- The CG coefficient $\langle \frac{1}{2}\ \frac{1}{2} - M\ 1\ M | \frac{1}{2}\ \frac{1}{2}\rangle$ implies that the $M = -1$ spin projection is forbidden.
- $M + M_i - \frac{1}{2} = \pm \frac{1}{2} \Rightarrow M + M_i = 1$ or $M + M_i = 0$.

To sum up, if $M_i = 1 \Rightarrow M = 0$ and if $M_i = 0 \Rightarrow M = 0, 1$. Therefore,

$$
\begin{aligned}
&\langle\frac{1}{2}\ \frac{1}{2}\ 1\ 0\mid\frac{1}{2}\ \frac{1}{2}\rangle\langle\frac{1}{2}\ \frac{1}{2}\ \frac{1}{2}\ -\frac{1}{2}\mid 1\ 0\rangle\langle\frac{1}{2}\ \frac{1}{2}\ \frac{1}{2}\ \frac{1}{2}\mid 1\ 1\rangle\mid 1\ 1\rangle\mid\frac{1}{2}\ -\frac{1}{2}\rangle\\
&+\langle\frac{1}{2}\ -\frac{1}{2}\ 1\ 1\mid\frac{1}{2}\ \frac{1}{2}\rangle\langle\frac{1}{2}\ \frac{1}{2}\ \frac{1}{2}\ \frac{1}{2}\mid 1\ 1\rangle\langle\frac{1}{2}\ -\frac{1}{2}\ \frac{1}{2}\ \frac{1}{2}\mid 1\ 0\rangle\mid 1\ 0\rangle\mid\frac{1}{2}\ \frac{1}{2}\rangle\\
&+\langle\frac{1}{2}\ \frac{1}{2}\ 1\ 0\mid\frac{1}{2}\ \frac{1}{2}\rangle\langle\frac{1}{2}\ -\frac{1}{2}\ \frac{1}{2}\ \frac{1}{2}\mid 1\ 0\rangle\langle\frac{1}{2}\ \frac{1}{2}\ \frac{1}{2}\ -\frac{1}{2}\mid 1\ 0\rangle\mid 1\ 0\rangle\mid\frac{1}{2}\ \frac{1}{2}\rangle\\
&=\left(\frac{1}{\sqrt{3}}\cdot\frac{1}{\sqrt{2}}\cdot 1\right)\mid 1\ 1\rangle\mid\frac{1}{2}\ -\frac{1}{2}\rangle\\
&+\left(-\sqrt{\frac{2}{3}}\cdot 1\cdot\frac{1}{\sqrt{2}}+\frac{1}{\sqrt{3}}\cdot\frac{1}{\sqrt{2}}\cdot\frac{1}{\sqrt{2}}\right)\mid 1\ 0\rangle\mid\frac{1}{2}\ \frac{1}{2}\rangle\\
&=\frac{1}{\sqrt{6}}\mid 1\ 1\rangle|\frac{1}{2}-\frac{1}{2}\rangle-\frac{1}{2\sqrt{3}}\mid 1\ 0\rangle\mid\frac{1}{2}\ \frac{1}{2}\rangle\ .
\end{aligned}
\tag{116}
$$

The probability is:

$$
P=\left|\langle\frac{1}{2}\ \frac{1}{2}\mid\frac{1}{2}\ \frac{1}{2}\rangle\right|^2_{S_i=1}=\left(\frac{1}{\sqrt{6}}\right)^2+\left(-\frac{1}{2\sqrt{3}}\right)^2=\frac{1}{4}\ . \tag{117}
$$

As a result, the n–induced and p–induced rates read:

$$
\overline{R}_n=\frac{3}{4}R_{n0}+\frac{1}{4}R_{n1}\ .\qquad \overline{R}_p=\frac{3}{4}R_{p0}+\frac{1}{4}R_{p1}\ . \tag{118}
$$

Finally, if we go back to Eq. (62), the total width for ${}^3_\Lambda$H reads:

$$
\Gamma_{\rm NM}({}^3_\Lambda{\rm H})=\frac{N\overline{R}_n({}^3_\Lambda{\rm H})+Z\overline{R}_p({}^3_\Lambda{\rm H})}{2}\rho_2=(3R_{n0}+R_{n1}+3R_{p0}+R_{p1})\frac{\rho_2}{8}\ .
$$

A.2 ${}^4_\Lambda$H rate

The ${}^4_\Lambda$H is a bound state of a proton, two neutrons and a Λ with total spin $J_H=0$ and $M_H=0$. Assuming a weak coupling scheme, the initial hypernuclear state is defined as

$$
|{}^4_\Lambda\ {\rm H}\rangle\equiv|\ 0\ 0\rangle=|\ \Lambda\rangle\otimes|\ pnn\rangle\ . \tag{119}
$$

The nuclear core composed by three baryons (nnp) can only be coupled to $J_c=1/2$ due to the total angular momentum conservation ($0=1/2_\Lambda\otimes 1/2_{nnp}$). In consequence, the initial hypernuclear state can be treated as

$$
|\ 0\ 0\rangle=|\ \frac{1}{2}\ m_\Lambda\rangle_\Lambda\mid\frac{1}{2}\ M_J\rangle_{nnp}\ , \tag{120}
$$

with $0=m_\Lambda+M_J$.

To define the n–induced and the p–induced transitions, it is necessary to study the nuclear core. Assuming the pairing hypothesis of nuclear physics, the nuclear core can be treated as the coupling between nn and p states.

$$
|\ nnp\rangle=|\ nn\rangle\otimes|\ p\rangle \tag{121}
$$

As we already commented, the total antisymmetric wave function of the nn pair requires $J = 0$. In accordance with these considerations, the initial state described in Eq. (120) can be rewritten as

$$\mid 0\ 0\rangle = \mid \frac{1}{2}\ m_\Lambda\rangle_\Lambda \mid \frac{1}{2}\ m_p\rangle_p \mid 0\ 0\rangle_{nn}\ , \tag{122}$$

where $m_\Lambda + m_p = 0$.

In the first place, we study the p–induced transition. Starting from Eq. (122), the $\Lambda p \to np$ transition is described with the coupling between Λ and p states. We will denote the Λp state with $|S_i\ M_i\rangle$. The angular momentum conservation requires that the Λp pair is in a spin–singlet state ($S_i = 0$) in order to satisfy $J_H = 0$. As a consequence, the probability of this configuration is

$$P(S_i = 0) = 1\ . \tag{123}$$

In the second place, we study the n–induced process. Starting from the initial state defined in Eq. (122), the procedure will be as follows. To describe the $\Lambda n \to nn$ transition it is necessary to uncouple the nn pair and subsequently, to define the $|S_i M_i\rangle$ state coupling the Λ with one n:

$$\begin{aligned} \mid 0\ 0\rangle_{nn} &= \sum_{m_n m'_n} \langle\frac{1}{2}\ m_n\ \frac{1}{2}m'_n \mid 0\ 0\rangle \mid \frac{1}{2}\ m_n\rangle_n \mid \frac{1}{2}\ m'_n\rangle_n \\ &= \sum_{m_n} \langle\frac{1}{2}\ m_n\ \frac{1}{2}\ \text{-}\ m_n \mid 0\ 0\rangle \mid \frac{1}{2}\ m_n\rangle_n \mid \frac{1}{2}\ -m_n\rangle_n\ , \end{aligned} \tag{124}$$

where $0 = m_n + m'_n \Rightarrow m'_n = -m_n$.

Now, we couple the Λn pair in a $|S_i M_i\rangle$ state.

$$\mid \frac{1}{2}\ m_\Lambda\rangle_\Lambda \mid \frac{1}{2}\ m_n\rangle_n = \sum_{S_i M_i} \langle\frac{1}{2}\ m_\Lambda\ \frac{1}{2}\ m_n \mid S_i\ M_i\rangle \mid S_i\ M_i\rangle_{\Lambda n}\ . \tag{125}$$

As a result, the ${}^{4}_{\Lambda}$H hypernuclear state can be written as:

$$\begin{aligned} \mid 0\ 0\rangle = \sum_{m_n} \sum_{S_i M_i} &\langle\frac{1}{2}\ m_n\ \frac{1}{2}\ -m_n \mid 0\ 0\rangle \langle\frac{1}{2}\ m_\Lambda\ \frac{1}{2}\ m_n \mid S_i\ M_i\rangle \\ &\mid \frac{1}{2}\ m_p\rangle_p \mid \frac{1}{2}\ -m_n\rangle_n \mid S_i\ M_i\rangle_{\Lambda n}\ , \end{aligned} \tag{126}$$

where $M_i = m_\Lambda + m_n$.

If $S_i = 0 \Rightarrow M_i = 0$ and $m_\Lambda = -m_n$. Using $m_\Lambda = 1/2$ without loss of generality, the $S_i = 0$ contribution from the above equation reads:

$$\begin{aligned} &\langle\frac{1}{2}\ -\frac{1}{2}\ \frac{1}{2}\ \frac{1}{2} \mid 0\ 0\rangle \langle\frac{1}{2}\ \frac{1}{2}\ \frac{1}{2}\ -\frac{1}{2} \mid 0\ 0\rangle \mid \frac{1}{2}\ -\frac{1}{2}\rangle_p \mid \frac{1}{2}\ \frac{1}{2}\rangle_n \mid 0\ 0\rangle_{\Lambda n} \\ &= \left(-\frac{1}{\sqrt{2}} \cdot \frac{1}{\sqrt{2}}\right) \mid \frac{1}{2}m_p\rangle_p \mid \frac{1}{2}\frac{1}{2}\rangle_n \mid 00\rangle_{\Lambda n} \\ &= -\frac{1}{2} \mid \frac{1}{2}\ -\frac{1}{2}\rangle_p \mid \frac{1}{2}\ \frac{1}{2}\rangle_n \mid 0\ 0\rangle_{\Lambda n}\ . \end{aligned} \tag{127}$$

The probability of this configuration is:

$$P(S_i = 0) = |\langle 0\ 0 \mid 0\ 0\rangle|^2_{S_i=0} = \frac{1}{4}\ , \tag{128}$$

and for completeness,

$$P(S_i = 1) = 1 - P(S_i = 0) = \frac{3}{4}\ . \tag{129}$$

As a result, the n–induced and p–induced rates read:

$$\overline{R}_n = \frac{1}{4}R_{n0} + \frac{3}{4}R_{n1}\ . \qquad \overline{R}_p = R_{p0}\ . \tag{130}$$

Finally, if we go back to Eq. (62), the total width for ${}^{4}_{\Lambda}$H reads:

$$\Gamma_{\rm NM}({}^{4}_{\Lambda}{\rm H}) = \frac{N\overline{R}_n({}^{4}_{\Lambda}{\rm H}) + Z\overline{R}_p({}^{4}_{\Lambda}{\rm H})}{3}\rho_3 = (R_{n0} + 3R_{n1} + 2R_{p0})\frac{\rho_3}{6}\ . \tag{131}$$

A.3 ${}^{4}_{\Lambda}$He rate

This case is completely analogous to the ${}^{4}_{\Lambda}$H, but exchanging the role of the neutrons by that of the protons.

Therefore, the n–induced and p–induced rates read:

$$\overline{R}_n = R_{n0}\ . \qquad \overline{R}_p = \frac{1}{4}R_{p0} + \frac{3}{4}R_{p1}\ . \tag{132}$$

Finally, if we go back to Eq. (62), the total width for ${}^{4}_{\Lambda}$He is

$$\Gamma({}^{4}_{\Lambda}{\rm He}) = \frac{N\overline{R}_n({}^{4}_{\Lambda}{\rm He}) + Z\overline{R}_p({}^{4}_{\Lambda}{\rm He})}{3}\rho_3 = (R_{p0} + 3R_{p1} + 2R_{n0})\frac{\rho_3}{6}\ . \tag{133}$$

A.4 ${}^{5}_{\Lambda}$He rate

The ${}^{5}_{\Lambda}$He is a bound state composed by a Λ, two protons and two neutrons. The total initial angular momentum is $J_H = 1/2$ and we assume $M_H = 1/2$ without loss of generality. So, the initial state is defined as

$$|{}^{5}_{\Lambda}\ {\rm He}\rangle \equiv |\ \frac{1}{2}\ \frac{1}{2}\rangle = |\ \Lambda\rangle \otimes |\ nnpp\rangle\ . \tag{134}$$

As it is well known, the nuclear core is the ^{4}He state and has $J = 0$. Assuming the pairing hypothesis of nuclear physics, we will describe this system from the coupling between nn and pp pairs.

$$|\ nnpp\rangle \equiv |\ {}^{4}{\rm He}\rangle \equiv |nn\rangle \otimes |pp\rangle \tag{135}$$

As we have already commented, the nn and pp pairs are in $L = 0$ and $I = 1$ states, therefore $S = J = 0$. By using these considerations, the total hypernuclear state reads:

$$| \frac{1}{2} \ \frac{1}{2}\rangle = | \frac{1}{2} \ m_\Lambda\rangle_\Lambda \mid 0 \ 0\rangle_{nn} \mid 0 \ 0\rangle_{pp} \ , \tag{136}$$

with $M_H = \frac{1}{2} = m_\Lambda$.

As in the previous cases, the procedure will be as follows. First of all, it will be advisable to decouple the nn and pp pairs in two single nucleon states and then, it will be necessary to couple the Λ with n and the Λ with p states to study the n–induced and the p–induced processes, respectively.

$$| 0 \ 0\rangle_{nn} = \sum_{m_n} \langle \frac{1}{2} \ m_n \ \frac{1}{2} \ -m_n \mid 0 \ 0\rangle \mid \frac{1}{2} \ m_n\rangle_n \mid \frac{1}{2} \ -m_n\rangle_n \ , \tag{137}$$

$$| 0 \ 0\rangle_{pp} = \sum_{m_p} \langle \frac{1}{2} \ m_p \ \frac{1}{2} \ -m_p \mid 0 \ 0\rangle \mid \frac{1}{2} \ m_p\rangle_p \mid \frac{1}{2} \ -m_p\rangle_p \ . \tag{138}$$

We analyse the n–induced process, but the p–induced one proceeds analogously. The initial state is defined as:

$$| \frac{1}{2}\frac{1}{2}\rangle = | \ \Lambda\rangle \otimes \mid 00\rangle_{nn} \otimes \mid 00\rangle_{pp} \ . \tag{139}$$

After decoupling $\mid 00\rangle_{nn}$, as shown in Eq. (137), we couple Λ with n to the $|S_i \ M_i\rangle$ state:

$$| \frac{1}{2} \ m_\Lambda\rangle_\Lambda \mid \frac{1}{2} \ m_p\rangle_n = \sum_{S_i M_i} \langle \frac{1}{2} \ m_\Lambda \ \frac{1}{2} \ m_n \mid S_i \ M_i\rangle \mid S_i \ M_i\rangle_{\Lambda n} \ , \tag{140}$$

where $M_i = m_\Lambda + m_n$.

Therefore, the total initial state read:

$$\begin{aligned} | \frac{1}{2} \ \frac{1}{2}\rangle = \sum_{m_n} \sum_{S_i M_i} & \langle \frac{1}{2} \ m_n \ \frac{1}{2} \ -m_n \mid 0 \ 0\rangle \langle \frac{1}{2} \ m_\Lambda \ \frac{1}{2} \ m_n \mid S_i \ M_i\rangle \\ & \mid \frac{1}{2} \ -m_n\rangle_n \mid S_i \ M_i\rangle_{\Lambda n} \mid 0 \ 0\rangle_{pp} \end{aligned} \tag{141}$$

If $S_i = 0 \Rightarrow M_i = 0$ and $m_\Lambda = -m_n$ with $m_\Lambda = 1/2$. Then, the $S_i = 0$ contribution reads:

$$\begin{aligned} & \langle \frac{1}{2} \ -\frac{1}{2} \ \frac{1}{2} \ \frac{1}{2} \mid 0 \ 0\rangle \langle \frac{1}{2} \ \frac{1}{2} \ \frac{1}{2} \ -\frac{1}{2} \mid 0 \ 0\rangle \mid \frac{1}{2} \ \frac{1}{2}\rangle_n \mid 0 \ 0\rangle_{\Lambda n} \mid 0 \ 0\rangle_{pp} \\ & = -\frac{1}{2} \mid \frac{1}{2} \ \frac{1}{2}\rangle_n \mid 0 \ 0\rangle_{\Lambda n} \mid 0 \ 0\rangle_{pp} \end{aligned} \tag{142}$$

The probability of this configuration is:

$$P(S_i = 0) = \left| \langle \frac{1}{2} \ \frac{1}{2} \mid \frac{1}{2} \ \frac{1}{2}\rangle \right|^2 = \frac{1}{4} \ , \tag{143}$$

and for completeness ,

$$P(S_i = 1) = 1 - P(S_i = 0) = \frac{3}{4} \ . \tag{144}$$

An analogous procedure is followed for the p–induced process. As a result, the n–induced and p–induced rates read:

$$\overline{R}_n = \frac{1}{4} R_{n0} + \frac{3}{4} R_{n1} \ . \qquad \overline{R}_p = \frac{1}{4} R_{p0} + \frac{3}{4} R_{p1} \ . \tag{145}$$

Finally, if we go back to Eq. (62), the total width for ${}^{5}_{\Lambda}\mathrm{He}$ read:

$$\Gamma({}^{5}_{\Lambda}\mathrm{He}) = \frac{N\overline{R}_n({}^{5}_{\Lambda}\mathrm{He}) + Z\overline{R}_p({}^{5}_{\Lambda}\mathrm{He})}{4}\rho_4 = (R_{n0} + 3R_{n1} + R_{p0} + 3R_{p1})\frac{\rho_4}{8} \ . \tag{146}$$

Appendix B Spin matrix elements

For completeness, in this section we show the spin matrix coefficients appearing in the $\Lambda N \to nN$ weak transition potential [10]. We denote the initial pair of ΛN with spin and angular momentum S_0 and L_r and a final NN pair with spin and angular momentum S and L'. The total spin angular momentum and its third projection are denoted by J and M_J, respectively.

B.1 Spin–Spin Transition

$$\langle (L'S)JM_J|\hat{\mathcal{O}}_\alpha|(L_rS_0)JM_J\rangle = (2S(S+1)-3)\delta_{L_rL'}\delta_{S_0S}$$

B.2 Tensor Transition

$$\langle (L'S)JM_J|\hat{\mathcal{O}}_\alpha|(L_rS_0)JM_J\rangle = S^J_{L_rL'}\delta_{L_rL'}\delta_{S_0S}$$

where $S^J_{L_rL'}$ are given in the following table.

$S^J_{L_rL'}$	$L'=J+1$	$L'=J$	$L'=J-1$
$L_r=J+1$	$\frac{-2(J+2)}{2J+1}$	0	$\frac{6\sqrt{J(J+1)}}{2J+1}$
$L_r=J$	0	0	0
$L_r=J-1$	$\frac{6\sqrt{J(J+1)}}{2J+1}$	0	$\frac{-2(J-1)}{2J+1}$

B.3 PV Transition: Pseudoscalar Mesons

$$\langle (L'S)JM_J|\hat{\mathcal{O}}_\alpha|(L_rS_0)JM_J\rangle = (-1)^{J+1-L'}\sqrt{6}\sqrt{2S_0+1}$$
$$\times\sqrt{2S+1}\sqrt{2L_r+1}\langle 10L_r0|L'0\rangle \begin{pmatrix} 1/2 & 1/2 & S_0 \\ S & 1 & 1/2 \end{pmatrix}\begin{pmatrix} L' & L_r & 1 \\ S_0 & S & J \end{pmatrix}$$

B.4 PV Transition: Vector Mesons

$$\langle (L'S)JM_J|\hat{\mathcal{O}}_\alpha|(L_rS_0)JM_J\rangle = \mathrm{i}(-1)^{J-L'+S})6\sqrt{6}\sqrt{2S_0+1}$$
$$\times\sqrt{2S+1}\sqrt{2L_r+1}\langle 10L_r0|L'0\rangle \begin{pmatrix} L' & L_r & 1 \\ S_0 & S & J \end{pmatrix}\begin{pmatrix} 1 & 1 & 1 \\ 1/2 & 1/2 & S \\ 1/2 & 1/2 & S_0 \end{pmatrix}$$

Appendix C The asymmetry parameter

In this section we will obtain the spin observable of the non–mesonic weak decay through the study of the inverse reaction $pn \to p\Lambda$. In the inverse reaction one can employ polarized proton beams in such a way that the polarization of Λ generated in the reaction can be measured from the asymmetry parameter of the $\Lambda \to \pi^- p$ decay. In Ref. [63] they restrict the treatment to s–wave production of $p\Lambda$ states to focus the discussion on the relation to the inverse non–mesonic decay process. By this truncation, the spin structure of the $\hat{T}$–matrix can be written as a function of the matrix elements written in Table 1. Therefore, and following the steps detailed in Ref. [63] the $\hat{T}$-matrix is given as:

$$\begin{aligned}\hat{T} = & a\frac{1-\vec{\sigma_1}\cdot\vec{\sigma_2}}{4} - b\frac{1-\vec{\sigma_1}\cdot\vec{\sigma_2}}{8}(\vec{\sigma_1}-\vec{\sigma_2})\cdot\hat{p} + c\frac{3+\vec{\sigma_1}\cdot\vec{\sigma_2}}{4} \\ & + d\frac{1}{2\sqrt{2}}(3\vec{\sigma_1}\cdot\hat{p}\ \vec{\sigma_2}\cdot\hat{p} - \vec{\sigma_1}\cdot\vec{\sigma_2}) + e\frac{\sqrt{3}(3+\vec{\sigma_1}\cdot\vec{\sigma_2})}{8}(\vec{\sigma_1}-\vec{\sigma_2})\cdot\hat{p} \\ & - f\frac{\sqrt{6}}{4}(\vec{\sigma_1}+\vec{\sigma_2})\cdot\hat{p}\ ,\end{aligned} \tag{147}$$

where $\hat{p} = \vec{p}/|\vec{p}|$ is the momentum carried by the emitted proton.

In order to calculate the polarization observables induced by a Λ with polarization $\vec{p}_\Lambda$, we introduce the following density matrix:

$$\rho_\Lambda = \frac{1+\vec{\sigma}_\Lambda\cdot\vec{p}_\Lambda}{2}\ . \tag{148}$$

The intensity of protons can be calculated by taking the following trace:

$$I_p(\theta) = Tr[\hat{T}\hat{T}^\dagger\rho_\Lambda] = I_0 + I_{\mathcal{A}}(\theta)\ , \tag{149}$$

where I_0 and $I_{\mathcal{A}}$ are defined as

$$I_0 = \frac{1}{2}Tr[\hat{T}\hat{T}^\dagger]\ , \tag{150}$$

$$I_A(\theta) = \frac{1}{2}Tr[\hat{T}\hat{T}^\dagger\vec{\sigma}_\Lambda\cdot\vec{p}_\Lambda]\ . \tag{151}$$

We perform the trace–summation in the last equations, and by using trace properties of Pauli matrices, after some algebra, we have [See C.1–C.6]:

$$I_0 = \frac{1}{2}(|a|^2+|b|^2+3(|c|^2+|d|^2+|e|^2+|f|^2)\ , \tag{152}$$

$$I_A(\theta) = \frac{1}{2}2\sqrt{3}\mathcal{R}e\left[ae^* - \frac{1}{\sqrt{3}}b(c^*-\sqrt{2}d^*) + f(\sqrt{2}c^*+d^*)\right]\vec{q}\cdot\vec{p}_\Lambda, \tag{153}$$

where $\vec{q}$ is the transferred momentum. If we assume the Λ particle at rest, we have $\vec{p} = -\vec{q}$.

From Eq. (149) one can introduce the asymmetry of the angular distribution for the outgoing protons in such a way that

$$I_p(\theta) = I_0 + I_{\mathcal{A}}(\theta) = I_0(1 + \mathcal{A}_y(\theta)) \ , \tag{154}$$

where $\mathcal{A}_y$ is defined as

$$\mathcal{A}_Y(\theta) = \frac{I_{\mathcal{A}}(\theta)}{I_0} = a_\Lambda \vec{q} \cdot \vec{p}_\Lambda \ . \tag{155}$$

Finally, the intrinsic asymmetry parameter reads:

$$a_\Lambda = \frac{2\sqrt{3}\mathcal{R}e\left[ae^* - \frac{1}{\sqrt{3}}b(c^* - \sqrt{2}d^*) + f(\sqrt{2}c^* + d^*)\right]}{|a|^2 + |b|^2 + 3(|c|^2 + |d|^2 + |e|^2 + |f|^2)} \ . \tag{156}$$

TRACE – SUMMATION

On account of the fact that $\hat{T}\hat{T}^\dagger$ presents 6×6 terms and it would not be intuitive to perform a direct trace–summation, the procedure to perform the traces will be the following: Firstly, we will take the first term (terms with a) of the operator $\hat{T}$ and we will multiply it by the first term of the operator $\hat{T}^\dagger$, then the second and so on (denoted as aa, ab, ac, ad, ae and af terms). Secondly, we will do the same for the second term of $\hat{T}$ (the one that contains b) and we will multiplying it for the first term of the operator $\hat{T}^\dagger$, then the second and so on (denoted as ba, bb, bc, bd, be and bf terms). This way until all the combinations are made. In addition, we note that the trace is made on two different spin–spaces, (σ_1) and (σ_2), so that, as an example, $Tr(\sigma_1\sigma_2) = Tr(\sigma_1)Tr(\sigma_2)$.

The main properties of Pauli matrices (σ_i) used to perform the trace–summations are as follows:

$$\begin{aligned}
\sigma_i^\dagger &= \sigma_i \ , && (157)\\
Tr[\sigma_i] &= 0 \ , && (158)\\
Tr[\sigma_i\sigma_j] &= 2\delta_{ij} \ , && (159)\\
Tr[\sigma_i\sigma_j\sigma_k] &= 2i\epsilon_{ijk} \ , && (160)\\
Tr[\sigma_i\sigma_j\sigma_k\sigma_m] &= 2(\delta_{ij}\delta_{km} - \delta_{ik}\delta_{jm} + \delta_{im}\delta_{jk}) \ , && (161)\\
Tr[\sigma_i\sigma_j\sigma_k\sigma_m\sigma_n] &= 2i(\delta_{ij}\epsilon_{kmn} + \delta_{mk}\epsilon_{ijn} + \delta_{nk}\epsilon_{imj} + \delta_{mn}\epsilon_{ijk}) \ . && (162)
\end{aligned}$$

C.1 A terms

C.1.1 aa* combination

$$\begin{aligned}
\hat{T}\hat{T}^\dagger &= \frac{|a|^2}{16}\left(1 - \vec{\sigma_1}\cdot\vec{\sigma_2}\right)\left(1 - \vec{\sigma_1}\cdot\vec{\sigma_2}\right) = \frac{|a|^2}{16}\left(4 - 4\vec{\sigma_1}\cdot\vec{\sigma_2}\right)\\
&= \frac{|a|^2}{4}(1 - \vec{\sigma_1}\cdot\vec{\sigma_2})
\end{aligned} \tag{163}$$

$$Tr[\hat{T}\hat{T}^\dagger] = \frac{|a|^2}{4} \cdot Tr[I_1 I_2 - \sigma_{1i}\sigma_{2i}] = \frac{|a|^2}{4} \cdot Tr[I_1 I_2] = |a|^2 \tag{164}$$

$$Tr[\vec{p}_2 \cdot \vec{\sigma}_2 \hat{T}\hat{T}^\dagger] = \frac{|a|^2}{4} \cdot Tr[p_{2k}\sigma_{2k} I_1 I_2 - P_{2k}\sigma_{2k}\sigma_{2i}\sigma_{1i}] = 0 \tag{165}$$

C.1.2 ab* combination

$$\begin{aligned}
\hat{T}\hat{T}^\dagger &= \frac{ab^*}{32}(1 - \vec{\sigma_1} \cdot \vec{\sigma_2})(\vec{\sigma_1} - \vec{\sigma_2}) \cdot q(1 - \vec{\sigma_1} \cdot \vec{\sigma_2}) \\
&= \frac{ab^*}{32}(1 - \sigma_{1i}\sigma_{2i})(\sigma_{1j} - \sigma_{2j})q_j(1 - \sigma_{1k}\sigma_{2k}) \\
&= \frac{ab^*}{32}(1 - \sigma_{1i}\sigma_{2i})(\sigma_{1j} - \sigma_{2j} - \sigma_{1j}\sigma_{1k}\sigma_{2k} + \sigma_{1k}\sigma_{2j}\sigma_{2k})q_j \\
&= \frac{ab^*}{32}(\sigma_{1j} - \sigma_{2j} - \sigma_{1j}\sigma_{1k}\sigma_{2k} + \sigma_{1k}\sigma_{2j}\sigma_{2k} \\
&- \sigma_{1i}\sigma_{1j}\sigma_{2i} + \sigma_{1i}\sigma_{2i}\sigma_{2j} + \sigma_{1i}\sigma_{1j}\sigma_{1k}\sigma_{2i}\sigma_{2k} - \sigma_{1i}\sigma_{1k}\sigma_{2i}\sigma_{2j}\sigma_{2k})q_j
\end{aligned} \tag{166}$$

$$\begin{aligned}
Tr[\hat{T}\hat{T}^\dagger] &= \frac{ab^*}{32} Tr[(\sigma_{1i}\sigma_{1j}\sigma_{1k}\sigma_{2i}\sigma_{2k} - \sigma_{1i}\sigma_{1j}\sigma_{2i}\sigma_{2j}\sigma_{2k})q_j] \\
&= \frac{ab^*}{32}[(4i\delta_{ij}\epsilon_{ijk} - 4i\delta_{ij}\epsilon_{ijk})q_j] = 0
\end{aligned} \tag{167}$$

$$\begin{aligned}
Tr[\vec{p}_2 \cdot \vec{\sigma}_2 \hat{T}\hat{T}^\dagger] &= \frac{ab^*}{32} \cdot Tr[p_{2l}(-I_1\sigma_{2l}\sigma_{2j} - \sigma_{1j}\sigma_{1k}\sigma_{2l}\sigma_{2k} - \sigma_{1i}\sigma_{1j}\sigma_{2l}\sigma_{2i} \\
&+ \sigma_{1i}\sigma_{1j}\sigma_{1k}\sigma_{2l}\sigma_{2i}\sigma_{2k} - \sigma_{1i}\sigma_{1k}\sigma_{2l}\sigma_{2i}\sigma_{2j}\sigma_{2k})q_j] \\
&= \frac{ab^*}{32}[p_{2l}(-2 \cdot 2\delta_{lj} - 4\delta_{jk}\delta_{lk} - 4\delta_{ij}\delta_{li} + (2i\epsilon_{ijk}2i\epsilon_{lik}) \\
&- 2\delta_{ik}(2(\delta_{li}\delta_{jk} - \delta_{lj}\delta_{ik} + \delta_{lk}\delta_{ij})q_k] \\
&= \frac{ab^*}{32}[p_{2l}(-4\delta_{lj} - 4\delta_{lj} - 4\delta_{lj} - 4 \cdot -2\delta_{lj} \\
&- 4(\delta_{lj} - 3\delta_{lj} + \delta_{lj}))q_j] = 0
\end{aligned} \tag{168}$$

C.1.3 ac* combination

$$\hat{T}\hat{T}^\dagger = \frac{ac^*}{16}(1 - \vec{\sigma_1} \cdot \vec{\sigma_2})(3 + \vec{\sigma_1} \cdot \vec{\sigma_2}) = \frac{ac^*}{16}(3 - 2\vec{\sigma_1} \cdot \vec{\sigma_2} - 3 + 2\vec{\sigma_1} \cdot \vec{\sigma_2}) = 0 \tag{169}$$

$$Tr(\hat{T}\hat{T}^\dagger) = 0 \tag{170}$$

$$Tr[\vec{p}_2 \cdot \vec{\sigma}_2 \hat{T}\hat{T}^\dagger] = 0 \tag{171}$$

C.1.4 ad* combination

$$\begin{aligned}
\hat{T}\hat{T}^\dagger &= \frac{ad^*}{8\sqrt{2}}(1 - \vec{\sigma_1} \cdot \vec{\sigma_2})(3\vec{\sigma_1} \cdot q\vec{\sigma_2} \cdot q - \vec{\sigma_1} \cdot \vec{\sigma_2}) \\
&= \frac{ad^*}{8\sqrt{2}}(1 - \sigma_{1i}\sigma_{2i})(3\sigma_{1j}q_j\sigma_{2k}q_k - \sigma_{1m}\sigma_{2m}) \\
&= \frac{ad^*}{8\sqrt{2}}[(3\sigma_{1j}\sigma_{2k} - 3\sigma_{1i}\sigma_{1j}\sigma_{2i}\sigma_{2k})q_j q_k - \sigma_{1m}\sigma_{2m} + \sigma_{1i}\sigma_{1m}\sigma_{2i}\sigma_{2m}]
\end{aligned} \tag{172}$$

$$
\begin{aligned}
Tr[\hat{T}\hat{T}^\dagger] &= \frac{ad^*}{8\sqrt{2}} Tr[-3\sigma_{1i}\sigma_{1j}\sigma_{2i}\sigma_{2k}q_j q_k + \sigma_{1i}\sigma_{1m}\sigma_{2i}\sigma_{2m}] \\
&= \frac{ad^*}{8\sqrt{2}}[-3\cdot 2\delta_{ij}2\delta_{ik}q_j q_k + 2\delta_{im}2\delta_{im}] \\
&= \frac{ad^*}{8\sqrt{2}}[-12\delta_{jk}q_j q_k + 12] = 0
\end{aligned}
\tag{173}
$$

$$
\begin{aligned}
Tr[\vec{p}_2\cdot\vec{\sigma}_2\hat{T}\hat{T}^\dagger] &= \frac{ad^*}{8\sqrt{2}} Tr[p_{2l}(-3\sigma_{1i}\sigma_{1j}\sigma_{2l}\sigma_{2i}\sigma_{2k}q_j q_k + \sigma_{1i}\sigma_{1m}\sigma_{2l}\sigma_{2i}\sigma_{2m})] \\
&= \frac{ad^*}{8\sqrt{2}}[p_{2l}(-3\cdot 2\delta_{ij}2i\epsilon_{lik}q_j q_k + 2\delta_{im}2i\epsilon_{lim})] \\
&= \frac{ad^*}{8\sqrt{2}}[p_{2l}(-12i\epsilon_{ljk}p_j p_k)] = -\frac{12ad^*}{8\sqrt{2}}[\vec{p}_2\cdot(\vec{q}\times\vec{q})] = 0
\end{aligned}
\tag{174}
$$

C.1.5 ae* combination

$$
\begin{aligned}
\hat{T}\hat{T}^\dagger &= -\frac{\sqrt{3}}{32}ae^*(1-\vec{\sigma_1}\cdot\vec{\sigma_2})(\vec{\sigma_1}-\vec{\sigma_2})\cdot q(3+\vec{\sigma_1}\cdot\vec{\sigma_2}) \\
&= -\frac{\sqrt{3}}{32}ae^*(1-\sigma_{1i}\sigma_{2i})(\sigma_{1j}-\sigma_{2j})q_j(3+\sigma_{1k}\sigma_{2k}) \\
&= -\frac{\sqrt{3}}{8}ae^*(1-\sigma_{1i}\sigma_{2i})(3\sigma_{1j}-3\sigma_{2j}+\sigma_{1j}\sigma_{1k}\sigma_{2k}-\sigma_{1k}\sigma_{2j}\sigma_{2k})q_j \\
&= -\frac{\sqrt{3}}{32}ae^*(3\sigma_{1j}-3\sigma_{2j}+\sigma_{1j}\sigma_{1k}\sigma_{2k}-\sigma_{1k}\sigma_{2j}\sigma_{2k} \\
&- 3\sigma_{1i}\sigma_{1j}\sigma_{2i}+3\sigma_{1i}\sigma_{2i}\sigma_{2j}-\sigma_{1i}\sigma_{1j}\sigma_{1k}\sigma_{2i}\sigma_{2k}+\sigma_{1i}\sigma_{1k}\sigma_{2i}\sigma_{2j}\sigma_{2k})q_j
\end{aligned}
\tag{175}
$$

$$
\begin{aligned}
Tr[\hat{T}\hat{T}^\dagger] &= -\frac{\sqrt{3}}{32}ae^* Tr[-\sigma_{1i}\sigma_{1j}\sigma_{1k}\sigma_{2i}\sigma_{2k}+\sigma_{1i}\sigma_{1k}\sigma_{2i}\sigma_{2j}\sigma_{2k})q_j] \\
&= -\frac{\sqrt{3}}{32}ae^*(-2i\epsilon_{ijk}\delta_{ik}+2i\epsilon_{ijk}\delta_{ik})q_j = 0
\end{aligned}
\tag{176}
$$

$$
\begin{aligned}
Tr[\vec{p}_2\cdot\vec{\sigma}_2\hat{T}\hat{T}^\dagger] &= -\frac{\sqrt{3}}{32}ae^* Tr[p_{2l}(-3I_1\sigma_{2l}\sigma_{2j}+\sigma_{1j}\sigma_{1k}\sigma_{2l}\sigma_{2k}-3\sigma_{1i}\sigma_{1j}\sigma_{2l}\sigma_{2i} \\
&- \sigma_{1i}\sigma_{1j}\sigma_{1k}\sigma_{2l}\sigma_{2i}\sigma_{2k}+\sigma_{1i}\sigma_{1k}\sigma_{2l}\sigma_{2i}\sigma_{2j}\sigma_{2k})q_j] \\
&= -\frac{\sqrt{3}}{32}ae^*[-12\delta_{lj}+4\delta_{jk}\delta_{lk}-12\delta_{ij}\delta_{li}-(2i\epsilon_{ijk}2i\epsilon_{lik}) \\
&+ 2\delta_{ik}2(\delta_{li}\delta_{jk}-\delta_{lj}\delta_{ik}+\delta_{lk}\delta_{ij})p_{2l}q_j] \\
&= -\frac{\sqrt{3}}{32}ae^*[-12\delta_{lj}+4\delta_{lj}-12\delta_{lj}+4(-2\delta_{lj}) \\
&+ 4(\delta_{lj}-3\delta_{lj}+\delta_{lj})P_{2l}q_j] = -\frac{\sqrt{3}}{32}ae^*[-32p_2\cdot q] \\
&= \sqrt{3}ae^*\vec{p}_2\cdot\vec{q}
\end{aligned}
\tag{177}
$$

C.1.6 af* combination

$$\begin{aligned}\hat{T}\hat{T}^\dagger &= \frac{\sqrt{6}}{16}af^*(1-\vec{\sigma_1}\cdot\vec{\sigma_2})(\vec{\sigma_1}+\vec{\sigma_2})\cdot q \\ &= \frac{\sqrt{6}}{16}af^*(1-\sigma_{1i}\sigma_{2i})(\sigma_{1j}+\sigma_{2j})q_j \\ &= \frac{\sqrt{6}}{16}af^*(\sigma_{1j}+\sigma_{2j}-\sigma_{1i}\sigma_{1j}\sigma_{2i}-\sigma_{1i}\sigma_{2i}\sigma_{2j})q_j\end{aligned} \tag{178}$$

$$Tr[\hat{T}\hat{T}^\dagger] = \frac{\sqrt{6}}{16}af^*Tr[\sigma_{1j}I_2+\sigma_{2j}I_1-\sigma_{1i}\sigma_{1j}\sigma_{2i}-\sigma_{1i}\sigma_{2i}\sigma_{2j}] = 0 \tag{179}$$

$$\begin{aligned}Tr[\vec{p}_2\cdot\vec{\sigma}_2\hat{T}\hat{T}^\dagger] &= \frac{\sqrt{6}}{16}af^*Tr[p_{2k}(I_1\sigma_{2k}\sigma_{2j}-\sigma_{1i}\sigma_{1j}\sigma_{2k}\sigma_{2i})q_j] \\ &= \frac{\sqrt{6}}{16}af^*[p_{2k}(2\cdot 2\delta_{kj}-2\delta_{ij}\cdot 2\delta_{ki})q_j] = 0\end{aligned} \tag{180}$$

C.2 B terms

C.2.1 ba* combination

$$\begin{aligned}\hat{T}\hat{T}^\dagger &= \frac{ba^*}{32}(1-\vec{\sigma_1}\cdot\vec{\sigma_2})(\vec{\sigma_1}-\vec{\sigma_2})\cdot q(1-\vec{\sigma_1}\cdot\vec{\sigma_2}) \\ &= \frac{ba^*}{32}(1-\sigma_{1i}\sigma_{2i})(\sigma_{1j}-\sigma_{2j})q_j(1-\sigma_{1k}\sigma_{2k}) \\ &= \frac{ba^*}{32}(\sigma_{1j}-\sigma_{2j}-\sigma_{1i}\sigma_{1j}\sigma_{2i}+\sigma_{1i}\sigma_{2i}\sigma_{2j})(1-\sigma_{1k}\sigma_{2k})q_j \\ &= \frac{ba^*}{32}(\sigma_{1j}-\sigma_{2j}-\sigma_{1i}\sigma_{1j}\sigma_{2i}+\sigma_{1i}\sigma_{2i}\sigma_{2j} \\ &- \sigma_{1j}\sigma_{1k}\sigma_{2k}+\sigma_{1k}\sigma_{2j}\sigma_{2k}+\sigma_{1i}\sigma_{1j}\sigma_{1k}\sigma_{2i}\sigma_{2k}-\sigma_{1i}\sigma_{1k}\sigma_{2i}\sigma_{2j}\sigma_{2k})q_j\end{aligned} \tag{181}$$

$$\begin{aligned}Tr[\hat{T}\hat{T}^\dagger] &= \frac{ba^*}{32}Tr[(\sigma_{1i}\sigma_{1j}\sigma_{1k}\sigma_{2i}\sigma_{2k}-\sigma_{1i}\sigma_{1k}\sigma_{2i}\sigma_{2j}\sigma_{2k})q_j] \\ &= \frac{ba^*}{32}[(2i\epsilon_{ijk}2\delta_{ik}-2\delta_{ik}2i\epsilon_{ijk})q_j] = 0\end{aligned} \tag{182}$$

$$\begin{aligned}Tr[\vec{p}_2\cdot\vec{\sigma}_2\hat{T}\hat{T}^\dagger] &= \frac{ba^*}{32}Tr(P_{2l}(-I_1\sigma_{2l}\sigma_{2j}-\sigma_{1i}\sigma_{1j}\sigma_{2l}\sigma_{2i}-\sigma_{1j}\sigma_{1k}\sigma_{2l}\sigma_{2k} \\ &+ \sigma_{1i}\sigma_{1j}\sigma_{1k}\sigma_{2l}\sigma_{2i}\sigma_{2k}-\sigma_{1i}\sigma_{1k}\sigma_{2l}\sigma_{2i}\sigma_{2j}\sigma_{2k})q_j) \\ &= \frac{ba^*}{32}[p_{2l}(-4\delta_{lj}-4\delta_{lj}-4\delta_{lj}+(2i\epsilon_{ijk}2i\epsilon_{lik}) \\ &- 4\delta_{ik}(\delta_{li}\delta_{jk}-\delta_{lj}\delta_{ik}+\delta_{lk}\delta_{ij}))q_j] \\ &= \frac{ba^*}{32}[p_{2l}(-12\delta_{lj}+4\cdot 2\delta_{lj}-4(\delta_{lj}-3\delta_{lj}+\delta_{lj}))q_j] = 0\end{aligned} \tag{183}$$

C.2.2 bb* combination

$$\begin{aligned}\hat{T}\hat{T}^\dagger &= \frac{|b|^2}{64}(1-\vec{\sigma_1}\cdot\vec{\sigma_2})(\vec{\sigma_1}-\vec{\sigma_2})\cdot q(1-\vec{\sigma_1}\cdot\vec{\sigma_2})(\vec{\sigma_1}-\vec{\sigma_2})\cdot q \\ &= \frac{|b|^2}{64}4(1-\vec{\sigma_1}\cdot\vec{\sigma_2})(\vec{\sigma_1}-\vec{\sigma_2})\cdot q(\vec{\sigma_1}-\vec{\sigma_2})\cdot q \\ &= \frac{|b|^2}{16}(1-\sigma_{1i}\sigma_{2i})(\sigma_{1j}\sigma_{1k}+\sigma_{2j}\sigma_{2k}-\sigma_{1j}\sigma_{2k}-\sigma_{2j}\sigma_{1k})q_jq_k \\ &= \frac{|b|^2}{16}(\sigma_{1j}\sigma_{1k}+\sigma_{2j}\sigma_{2k}-\sigma_{1j}\sigma_{2k}-\sigma_{2j}\sigma_{1k}-\sigma_{1i}\sigma_{1j}\sigma_{1k}\sigma_{2i} \\ &- \sigma_{1i}\sigma_{2i}\sigma_{2j}\sigma_{2k}+\sigma_{1i}\sigma_{1j}\sigma_{2i}\sigma_{2k}+\sigma_{1i}\sigma_{1k}\sigma_{2i}\sigma_{2j})q_jq_k\end{aligned} \tag{184}$$

$$\begin{aligned}Tr[\hat{T}\hat{T}^\dagger] &= \frac{|b|^2}{16}Tr[(\sigma_{1j}\sigma_{1k}I_2+I_1\sigma_{2j}\sigma_{2k} \\ &+ \sigma_{1i}\sigma_{1j}\sigma_{2i}\sigma_{2k}+\sigma_{1i}\sigma_{1k}\sigma_{2i}\sigma_{2j})q_jq_k] \\ &= \frac{|b|^2}{16}(16\delta_{ij})p_ip_j = |b|^2\end{aligned} \tag{185}$$

$$\begin{aligned}Tr[\vec{p}_2\cdot\vec{\sigma}_2\hat{T}\hat{T}^\dagger] &= \frac{|b|^2}{16}Tr[p_{2l}(I_1\sigma_{2l}\sigma_{2j}\sigma_{2k}-\sigma_{1i}\sigma_{1j}\sigma_{1k}\sigma_{2l}\sigma_{2i}+\sigma_{1i}\sigma_{1j}\sigma_{2l}\sigma_{2i}\sigma_{2k} \\ &+ \sigma_{1i}\sigma_{1k}\sigma_{2l}\sigma_{2i}\sigma_{2j})q_jq_k] = \frac{|b|^2}{16}[p_{2l}(2\cdot 2i\epsilon_{ljk}-2i\epsilon_{ijk}2\delta_{li} \\ &+ 2\delta_{ij}2i\epsilon_{lik}+2\delta_{ik}2i\epsilon_{lij})q_jq_k] = \frac{|b|^2}{16}[p_{2l}(4i\epsilon_{ljk}-4i\epsilon_{ljk} \\ &+ 4\epsilon_{ljk}+4i\epsilon_{lkj})q_jq_k] = 0\end{aligned} \tag{186}$$

C.2.3 bc* combination

$$\begin{aligned}\hat{T}\hat{T}^\dagger &= \frac{bc^*}{32}(1-\vec{\sigma_1}\cdot\vec{\sigma_2})(\vec{\sigma_1}-\vec{\sigma_2})\cdot q(3+\vec{\sigma_1}\cdot\vec{\sigma_2}) \\ &= \frac{bc^*}{32}(1-\sigma_{1i}\sigma_{2i})(\sigma_{1j}-\sigma_{2j})q_j(3+\sigma_{1k}\sigma_{2k}) \\ &= \frac{bc^*}{32}(\sigma_{1j}-\sigma_{2j}-\sigma_{1i}\sigma_{1j}\sigma_{2i}+\sigma_{1i}\sigma_{2i}\sigma_{2j})(3+\sigma_{1k}\sigma_{2k})q_j \\ &= \frac{bc^*}{32}(3\sigma_{1j}-3\sigma_{2j}-3\sigma_{1i}\sigma_{1j}\sigma_{2i}+3\sigma_{1i}\sigma_{2i}\sigma_{2j} \\ &+ \sigma_{1j}\sigma_{1k}\sigma_{2k}-\sigma_{1k}\sigma_{2j}\sigma_{2k}-\sigma_{1i}\sigma_{1j}\sigma_{1k}\sigma_{2i}\sigma_{2k}+\sigma_{1i}\sigma_{1k}\sigma_{2i}\sigma_{2j}\sigma_{2k})q_j\end{aligned} \tag{187}$$

$$\begin{aligned}Tr[\hat{T}\hat{T}^\dagger] &= \frac{bc^*}{32}Tr[(-\sigma_{1i}\sigma_{1j}\sigma_{1k}\sigma_{2i}\sigma_{2k}+\sigma_{1i}\sigma_{1k}\sigma_{2i}\sigma_{2j}\sigma_{2k})q_j] \\ &= \frac{bc^*}{32}[(-2i\epsilon_{ijk}2\delta_{ik}+2\delta_{ik}2i\epsilon_{ijk})q_j] = 0\end{aligned} \tag{188}$$

$$
\begin{aligned}
Tr[\vec{p}_2\cdot\vec{\sigma}_2\hat{T}\hat{T}^\dagger] &= \frac{bc^*}{32}Tr[p_{2l}(-3I_1\sigma_{2l}\sigma_{2j}-3\sigma_{1i}\sigma_{1j}\sigma_{2l}\sigma_{2i}+\sigma_{1j}\sigma_{1k}\sigma_{2l}\sigma_{2k}\\
&-\sigma_{1i}\sigma_{1j}\sigma_{1k}\sigma_{2l}\sigma_{2i}\sigma_{2k}+\sigma_{1i}\sigma_{1k}\sigma_{2l}\sigma_{2i}\sigma_{2j}\sigma_{2k})q_j]\\
&= \frac{bc^*}{32}[p_{2l}(-12\delta_{lj}-12\delta_{lj}+4\delta_{lj}+4\epsilon_{ijk}\epsilon_{lik}\\
&+4\delta_{ik}(\delta_{li}\delta_{jk}-\delta_{lj}\delta_{ik}+\delta_{lk}\delta_{ij}))q_j]\\
&= \frac{bc^*}{32}[p_{2l}(-20\delta_{lj}-4\cdot 2\delta_{lj}+4(\delta_{lj}-3\delta_{lj}+\delta_{lj})q_j]\\
&= \frac{bc^*}{32}[p_{2l}(-32\delta_{lj})q_j] = -bc^*\vec{p}_2\cdot\vec{q}
\end{aligned}
\tag{189}
$$

C.2.4 bd* combination

$$
\begin{aligned}
\hat{T}\hat{T}^\dagger &= \frac{bd^*}{16\sqrt{2}}(1-\vec{\sigma_1}\cdot\vec{\sigma_2})(\vec{\sigma_1}-\vec{\sigma_2})\cdot q(3\vec{\sigma_1}\cdot p\vec{\sigma_2}\cdot q-\vec{\sigma_1}\cdot\vec{\sigma_2})\\
&= \frac{bd^*}{16\sqrt{2}}(1-\sigma_{1i}\sigma_{2i})(\sigma_{1j}-\sigma_{2j})q_j(3\sigma_{1k}q_k\sigma_{2m}q_m-\sigma_{1n}\sigma_{2n})\\
&= \frac{bd^*}{16\sqrt{2}}[(3\sigma_{1j}\sigma_{1k}\sigma_{2m}-3\sigma_{1k}\sigma_{2j}\sigma_{2m}-3\sigma_{1i}\sigma_{1j}\sigma_{1k}\sigma_{2i}\sigma_{2m}\\
&+3\sigma_{1i}\sigma_{1k}\sigma_{2i}\sigma_{2j}\sigma_{2m})q_jq_kq_m+(\sigma_{1n}\sigma_{2j}\sigma_{2n}-\sigma_{1j}\sigma_{1n}\sigma_{2n}\\
&+\sigma_{1i}\sigma_{1j}\sigma_{1n}\sigma_{2i}\sigma_{2n}-\sigma_{1i}\sigma_{1n}\sigma_{2i}\sigma_{2j}\sigma_{2n})q_j]
\end{aligned}
\tag{190}
$$

$$
\begin{aligned}
Tr[\hat{T}\hat{T}^\dagger] &= \frac{bd^*}{16\sqrt{2}}Tr[(-3\sigma_{1i}\sigma_{1j}\sigma_{1k}\sigma_{2i}\sigma_{2m}+3\sigma_{1i}\sigma_{1k}\sigma_{2i}\sigma_{2j}\sigma_{2m})q_jq_kq_m\\
&+(\sigma_{1i}\sigma_{1j}\sigma_{1n}\sigma_{2i}\sigma_{2n}-\sigma_{1i}\sigma_{1n}\sigma_{2i}\sigma_{2j}\sigma_{2n})q_j] = 0
\end{aligned}
\tag{191}
$$

$$
\begin{aligned}
Tr[\vec{p}_2\cdot\vec{\sigma}_2\hat{T}\hat{T}^\dagger] &= \frac{bd^*}{16\sqrt{2}}Tr[p_{2l}[(3\sigma_{1j}\sigma_{1k}\sigma_{2l}\sigma_{2m}-3\sigma_{1i}\sigma_{1j}\sigma_{1k}\sigma_{2l}\sigma_{2i}\sigma_{2m}\\
&+3\sigma_{1i}\sigma_{1k}\sigma_{2l}\sigma_{2i}\sigma_{2j}\sigma_{2m})q_jq_kq_m+(-\sigma_{1j}\sigma_{1n}\sigma_{2l}\sigma_{2n}\\
&+\sigma_{1i}\sigma_{1j}\sigma_{1n}\sigma_{2l}\sigma_{2i}\sigma_{2n}-\sigma_{1i}\sigma_{1n}\sigma_{2l}\sigma_{2i}\sigma_{2j}\sigma_{2n})q_j]]\\
&= \frac{bd^*}{16\sqrt{2}}(p_{2l}[(12\delta_{jk}\delta_{lm}+12\epsilon_{ijk}\epsilon_{lim}\\
&+12\delta_{ik}(\delta_{li}\delta_{jm}-\delta_{lj}\delta_{im}+\delta_{lm}\delta_{ij}))q_jq_kq_m\\
&+(-4\delta_{lj}-4\epsilon_{ijn}\epsilon_{lin}-4\delta_{in}(\delta_{li}\delta_{jn}-\delta_{lj}\delta_{in}+\delta_{ln}\delta_{ij}))q_j]]\\
&= \frac{bd^*}{16\sqrt{2}}[p_{2l}[12\delta_{jk}\delta_{lm}-12(\delta_{lj}\delta_{km}-\delta_{jm}\delta_{kl})\\
&+12(\delta_{lk}\delta_{jm}-\delta_{lj}\delta_{km}+\delta_{lm}\delta_{kj}))q_jq_kq_m+8\delta_{lj}q_j]]\\
&= \frac{bd^*}{16\sqrt{2}}[32\vec{p}_2\cdot\vec{q}] = \frac{2}{\sqrt{2}}bd^*\vec{p}_2\cdot\vec{q} = \sqrt{2}bd^*\vec{p}_2\cdot\vec{q}
\end{aligned}
\tag{192}
$$

C.2.5 be* combination

$$\begin{aligned}\hat{T}\hat{T}^\dagger &= -\frac{\sqrt{3}}{64}be^*(1-\vec{\sigma_1}\cdot\vec{\sigma_2})(\vec{\sigma_1}-\vec{\sigma_2})\cdot q(\vec{\sigma_1}-\vec{\sigma_2})\cdot q(3+\vec{\sigma_1}\cdot\vec{\sigma_2})\\ &= -\frac{\sqrt{3}}{64}be^*(1-\sigma_{1i}\sigma_{2i})(\sigma_{1j}-\sigma_{2j})(3\sigma_{1k}-3\sigma_{2k}+\sigma_{1k}\sigma_{1m}\sigma_{2m}\\ &- \sigma_{1m}\sigma_{2k}\sigma_{2m})q_jq_k = -\frac{\sqrt{3}}{64}be^*(1-\sigma_{1i}\sigma_{2i})(3\sigma_{1j}\sigma_{1k}-3\sigma_{1j}\sigma_{2k}\\ &+ \sigma_{1j}\sigma_{1k}\sigma_{1m}\sigma_{2m}-\sigma_{1j}\sigma_{1m}\sigma_{2k}\sigma_{2m}-3\sigma_{1k}\sigma_{2j}+3\sigma_{2j}\sigma_{2k}\\ &- \sigma_{1k}\sigma_{1m}\sigma_{2j}\sigma_{2m}+\sigma_{1m}\sigma_{2j}\sigma_{2k}\sigma_{2m})q_jq_k\end{aligned} \tag{193}$$

$$\begin{aligned}Tr[\hat{T}\hat{T}^\dagger] &= -\frac{\sqrt{3}}{64}be^*Tr[(3\sigma_{1j}\sigma_{1k}I_2-\sigma_{1j}\sigma_{1m}\sigma_{2k}\sigma_{2m}+3I_1\sigma_{2j}\sigma_{2k}\\ &- \sigma_{1k}\sigma_{1m}\sigma_{2j}\sigma_{2m}+3\sigma_{1i}\sigma_{1j}\sigma_{2i}\sigma_{2k}-\sigma_{1i}\sigma_{1j}\sigma_{1k}\sigma_{1m}\sigma_{2i}\sigma_{2m}\\ &+ \sigma_{1i}\sigma_{1j}\sigma_{1m}\sigma_{2i}\sigma_{2k}\sigma_{2m}+3\sigma_{1i}\sigma_{1k}\sigma_{2i}\sigma_{2j}\\ &+ \sigma_{1i}\sigma_{1k}\sigma_{1m}\sigma_{2i}\sigma_{2j}\sigma_{2m}-\sigma_{1i}\sigma_{1m}\sigma_{2i}\sigma_{2j}\sigma_{2k}\sigma_{2m})q_jq_k]\\ &= -\frac{\sqrt{3}}{64}be^*[(12\delta_{jk}-4\delta_{jk}+12\delta_{jk}-4\delta_{jk}+12\delta_{jk}-12\delta_{jk}\\ &- 8\delta_{jk}+12\delta_{jk}-8\delta_{jk}-12\delta_{jk})q_jq_k]=0\end{aligned} \tag{194}$$

$$\begin{aligned}Tr[\vec{p}_2\cdot\vec{\sigma}_2\hat{T}\hat{T}^\dagger] &= -\frac{\sqrt{3}}{64}be^*Tr[p_{2l}(\sigma_{2l}-\sigma_{1i}\sigma_{2l}\sigma_{2i})(3\sigma_{1j}\sigma_{1k}-3\sigma_{1j}\sigma_{2k}\\ &+ \sigma_{1j}\sigma_{1k}\sigma_{1m}\sigma_{2m}-\sigma_{1j}\sigma_{1m}\sigma_{2k}\sigma_{2m}-3\sigma_{1k}\sigma_{2j}+3\sigma_{2j}\sigma_{2k}\\ &- \sigma_{1k}\sigma_{1m}\sigma_{2l}\sigma_{2k}\sigma_{2m}+\sigma_{1m}\sigma_{2j}\sigma_{2k}\sigma_{2m})q_jq_k]\\ &= -\frac{\sqrt{3}}{64}be^*Tr[p_{2l}(\sigma_{1j}\sigma_{1k}\sigma_{1m}\sigma_{2l}\sigma_{2m}\\ &- \sigma_{1j}\sigma_{1m}\sigma_{2l}\sigma_{2k}\sigma_{2m}+3\sigma_{2l}\sigma_{2j}\sigma_{2k}-\sigma_{1k}\sigma_{1m}\sigma_{12l}\sigma_{2j}\sigma_{2m}\\ &- 3\sigma_{1i}\sigma_{1j}\sigma_{1k}\sigma_{2l}\sigma_{2i}+3\sigma_{1i}\sigma_{1j}\sigma_{1k}\sigma_{2l}\sigma_{2i}\\ &- \sigma_{1i}\sigma_{1j}\sigma_{1k}\sigma_{1m}\sigma_{2l}\sigma_{2i}\sigma_{2m}+\sigma_{1i}\sigma_{1j}\sigma_{1m}\sigma_{2l}\sigma_{2i}\sigma_{2k}\sigma_{2m}\\ &+ 3\sigma_{1i}\sigma_{1k}\sigma_{2l}\sigma_{2i}\sigma_{2j}+\sigma_{1i}\sigma_{1k}\sigma_{1m}\sigma_{2l}\sigma_{2i}\sigma_{2j}\sigma_{2m}\\ &- \sigma_{1i}\sigma_{1m}\sigma_{2l}\sigma_{2i}\sigma_{2j}\sigma_{2k}\sigma_{2m})q_jq_k]\\ &= -\frac{\sqrt{3}}{64}be^*[ip_{2l}(4\epsilon_{jkl}-4\epsilon_{lkj}+12\epsilon_{ljk}-4\epsilon_{ljk}-12\epsilon_{ljk}\\ &+ 12\epsilon_{ljk}-4\epsilon_{ljk}+4\epsilon_{lkj}+4\epsilon_{ljk}+4\epsilon_{kjl}+12\epsilon_{lkj}+4\epsilon_{lkj}\\ &+ 4\epsilon_{jkl}-4\epsilon_{jkl}-4\epsilon_{lkj}-4\epsilon_{lkj})q_jq_k]=0\end{aligned} \tag{195}$$

C.2.6 bf* combination

$$\begin{aligned}\hat{T}\hat{T}^\dagger &= \frac{\sqrt{6}}{32}bf^*(1-\vec{\sigma_1}\cdot\vec{\sigma_2})(\vec{\sigma_1}-\vec{\sigma_2})\cdot q(\vec{\sigma_1}+\vec{\sigma_2})\cdot q \\ &= \frac{\sqrt{6}}{32}bf^*(1-\sigma_{1i}\sigma_{2i})(\sigma_{1j}-\sigma_{2j})q_j(\sigma_{1k}+\sigma_{2k})q_k \\ &= \frac{\sqrt{6}}{32}bf^*(\sigma_{1j}-\sigma_{2j}-\sigma_{1i}\sigma_{1j}\sigma_{2i}+\sigma_{1i}\sigma_{2i}\sigma_{2j})(\sigma_{1k}+\sigma_{2k})q_jq_k \\ &= \frac{\sqrt{6}}{32}bf^*(\sigma_{1j}\sigma_{1k}+\sigma_{1j}\sigma_{2k}-\sigma_{2j}\sigma_{1k}-\sigma_{2j}\sigma_{2k}-\sigma_{1i}\sigma_{1j}\sigma_{1k}\sigma_{2i} \\ &\quad -\sigma_{1i}\sigma_{1j}\sigma_{2i}\sigma_{2k}+\sigma_{1i}\sigma_{1k}\sigma_{2i}\sigma_{2j}+\sigma_{1i}\sigma_{2i}\sigma_{2j}\sigma_{2k})q_jq_k\end{aligned} \tag{196}$$

$$\begin{aligned}Tr[\hat{T}\hat{T}^\dagger] &= \frac{\sqrt{6}}{32}bf^*Tr[(\sigma_{1j}\sigma_{1k}I_2 - I_1\sigma_{2j}\sigma_{2k}-\sigma_{1i}\sigma_{1j}\sigma_{2i}\sigma_{2k} \\ &\quad +\sigma_{1i}\sigma_{1k}\sigma_{2i}\sigma_{2j})q_jq_k] = \frac{\sqrt{6}}{32}bf^*[(2\delta_{jk}2-2\cdot 2\delta_{jk}-2\delta_{ij}2\delta_{ik} \\ &\quad +2\delta_{ik}2\delta_{ij})q_jq_k] = 0\end{aligned} \tag{197}$$

$$\begin{aligned}Tr[\vec{p}_2\cdot\vec{\sigma}_2\hat{T}\hat{T}^\dagger] &= \frac{\sqrt{6}}{32}bf^*Tr[P_{2l}(-I_1\sigma_{2l}\sigma_{2j}\sigma_{2k}-\sigma_{1i}\sigma_{1j}\sigma_{1k}\sigma_{2l}\sigma_{2i} \\ &\quad -\sigma_{1i}\sigma_{1j}\sigma_{2l}\sigma_{2i}\sigma_{2k}+\sigma_{1i}\sigma_{1k}\sigma_{2l}\sigma_{2i}\sigma_{2j})q_jq_k] \\ &= \frac{\sqrt{6}}{32}bf^*[p_{2l}(-2\cdot 2i\epsilon_{ljk}-2i\epsilon_{ijk}2\delta_{li} \\ &\quad -2\delta_{ij}2i\epsilon_{lik}+2\delta_{ik}2i\epsilon_{lij})q_lq_k] \\ &= \frac{\sqrt{6}}{32}bf^*[p_{2l}(-16i\epsilon_{ljk})q_jp_k] = -\frac{\sqrt{6}}{2}bf^*\vec{p}_2\cdot(\vec{q}\times\vec{q}) = 0\end{aligned} \tag{198}$$

C.3 C terms

C.3.1 ca* combination

$$\begin{aligned}\hat{T}\hat{T}^\dagger &= \frac{ca^*}{16}(3+\vec{\sigma_1}\cdot\vec{\sigma_2})(1-\vec{\sigma_1}\cdot\vec{\sigma_2}) \\ TT^* &= \frac{ca^*}{16}(3-2\vec{\sigma_1}\cdot\vec{\sigma_2}-3+2\vec{\sigma_1}\cdot\vec{\sigma_2}) = 0\end{aligned} \tag{199}$$

$$Tr[\hat{T}\hat{T}^\dagger] = 0 \tag{200}$$

$$Tr[\vec{p}_2\cdot\vec{\sigma}_2\hat{T}\hat{T}^\dagger] = 0 \tag{201}$$

C.3.2 cb* combination

$$\begin{aligned}\hat{T}\hat{T}^\dagger &= \frac{cb^*}{32}(3+\vec{\sigma_1}\cdot\vec{\sigma_2})(\vec{\sigma_1}-\vec{\sigma_2})\cdot q(1-\vec{\sigma_1}\cdot\vec{\sigma_2}) \\ &= \frac{cb^*}{32}(3+\sigma_{1i}\sigma_{2i})(\sigma_{1j}-\sigma_{2j}-\sigma_{1j}\sigma_{1k}\sigma_{2k}+\sigma_{1k}\sigma_{2j}\sigma_{2k})q_j \\ &= \frac{cb^*}{32}(3\sigma_{1j}-3\sigma_{2j}-3\sigma_{1j}\sigma_{1k}\sigma_{2k}+3\sigma_{1k}\sigma_{2j}\sigma_{2k} \\ &+\sigma_{1i}\sigma_{1j}\sigma_{2i}-\sigma_{1i}\sigma_{2i}\sigma_{2j}-\sigma_{1i}\sigma_{1j}\sigma_{1k}\sigma_{2i}\sigma_{2k}+\sigma_{1i}\sigma_{1k}\sigma_{2i}\sigma_{2j}\sigma_{2k})q_j\end{aligned} \tag{202}$$

$$Tr[\hat{T}\hat{T}^\dagger] = \frac{cb^*}{32}Tr[(-\sigma_{1i}\sigma_{1j}\sigma_{1k}\sigma_{2i}\sigma_{2k}+\sigma_{1i}\sigma_{1k}\sigma_{2i}\sigma_{2j}\sigma_{2k})q_j] = 0 \tag{203}$$

$$\begin{aligned}Tr[\vec{p}_2\cdot\vec{\sigma}_2\hat{T}\hat{T}^\dagger] &= \frac{cb^*}{32}Tr[p_{2l}(-3I_1\sigma_{2l}\sigma_{2j}-3\sigma_{1j}\sigma_{1k}\sigma_{2l}\sigma_{2k}+\sigma_{1i}\sigma_{1j}\sigma_{2l}\sigma_{2i} \\ &-\sigma_{1i}\sigma_{1j}\sigma_{1k}\sigma_{2l}\sigma_{2i}\sigma_{2k}+\sigma_{1i}\sigma_{1k}\sigma_{2l}\sigma_{2i}\sigma_{2j}\sigma_{2k})q_j] \\ &= \frac{cb^*}{32}[p_{2k}(-3\cdot 2\cdot 2\delta_{lj}-3\cdot 2\delta_{jk}2\delta_{lk}+2\delta_{ij}2\delta_{li} \\ &-2i\epsilon_{ijk}2i\epsilon_{lik}+2\delta_{ik}2(\delta_{li}\delta_{jk}-\delta_{lj}\delta_{ik}+\delta_{lk}\delta_{ij}))q_j] \\ &= \frac{cb^*}{32}[p_{2l}(-12\delta_{lj}-12\delta_{lj}+4\delta_{lj}-4\cdot 2\delta_{lj} \\ &+4(\delta_{lj}-3\delta_{lj}+\delta_{lj})q_j)] = -cb^*(\vec{p}_2\cdot\vec{q})\end{aligned} \tag{204}$$

C.3.3 cc* combination

$$\begin{aligned}\hat{T}\hat{T}^\dagger &= \frac{|c|^2}{16}(3+\vec{\sigma_1}\cdot\vec{\sigma_2})(3+\vec{\sigma_1}\cdot\vec{\sigma_2}) \\ &= \frac{|c|^2}{16}(9+6\vec{\sigma_1}\cdot\vec{\sigma_2}+(\vec{\sigma_1}\cdot\vec{\sigma_2})^2) \\ &= \frac{|c|^2}{16}(12+4(\vec{\sigma_1}\cdot\vec{\sigma_2})) = \frac{|c|^2}{4}(3+\vec{\sigma_1}\cdot\vec{\sigma_2})\end{aligned} \tag{205}$$

$$Tr[\hat{T}\hat{T}^\dagger] = \frac{|c|^2}{4}Tr[3+\vec{\sigma_1}\cdot\vec{\sigma_2}] = \frac{|c|^2}{4}Tr[3I_1I_2+\sigma_{1i}\sigma_{2i}] = 3|c|^2 \tag{206}$$

$$Tr[\vec{p}_2\cdot\vec{\sigma}_2\hat{T}\hat{T}^\dagger] = \frac{|c|^2}{4}Tr[p_2(3I_1\sigma_{2k}+\sigma_{1i}\sigma_{2k}\sigma_{2i})] = 0 \tag{207}$$

C.3.4 cd* combination

$$\begin{aligned}\hat{T}\hat{T}^\dagger &= \frac{cd^*}{8\sqrt{2}}(3+\vec{\sigma_1}\cdot\vec{\sigma_2})(3\vec{\sigma_1}\cdot q\vec{\sigma_2}\cdot q-\vec{\sigma_1}\cdot\vec{\sigma_2}) \\ &= \frac{cd^*}{8\sqrt{2}}(3+\sigma_{1i}\sigma_{2i})(3\sigma_{1j}q_j\sigma_{2k}q_k-\sigma_{1m}\sigma_{2m}) \\ &= \frac{cd^*}{8\sqrt{2}}[(9\sigma_{1j}\sigma_{2k}+3\sigma_{1i}\sigma_{1j}\sigma_{2i}\sigma_{2k})q_jq_k-3\sigma_{1m}\sigma_{2m}-\sigma_{1i}\sigma_{1m}\sigma_{2i}\sigma_{2m}]\end{aligned} \tag{208}$$

$$
\begin{aligned}
Tr[\hat{T}\hat{T}^\dagger] &= \frac{cd^*}{8\sqrt{2}} Tr[3\sigma_{1i}\sigma_{1j}\sigma_{2i}\sigma_{2k}q_j q_k - \sigma_{1i}\sigma_{1m}\sigma_{2i}\sigma_{2m}] \\
&= \frac{cd^*}{8\sqrt{2}}[12\delta_{jk}q_j q_k - 4\delta_{im}\delta_{im}] = 0
\end{aligned} \tag{209}
$$

$$
\begin{aligned}
Tr[\vec{p}_2 \cdot \vec{\sigma}_2 \hat{T}\hat{T}^\dagger] &= \frac{cd^*}{8\sqrt{2}} Tr[p_{2l}(3\sigma_{1i}\sigma_{1j}\sigma_{2l}\sigma_{2i}\sigma_{2k}q_j q_k - \sigma_{1i}\sigma_{1m}\sigma_{2l}\sigma_{2i}\sigma_{2m})] \\
&= \frac{cd^*}{8\sqrt{2}}[p_{2l}(12i\delta_{ij}\epsilon_{ljk}q_j q_k - 4i\delta_{im}\epsilon_{lim})] \\
&= \frac{cd^*}{8\sqrt{2}} 12[\vec{p}_2 \cdot (\vec{q} \times \vec{q})] = 0
\end{aligned} \tag{210}
$$

C.3.5 ce* combination

$$
\begin{aligned}
\hat{T}\hat{T}^\dagger &= -\frac{\sqrt{3}}{32} ce^*(3 + \vec{\sigma_1} \cdot \vec{\sigma_2})(\vec{\sigma_1} - \vec{\sigma_2}) \cdot q(3 + \vec{\sigma_1} \cdot \vec{\sigma_2}) \\
&= -\frac{\sqrt{3}}{32} ce^*(3 + \sigma_{1i}\sigma_{2i})(\sigma_{1j} - \sigma_{2j})q_j(3 + \sigma_{1k}\sigma_{2k}) \\
&= -\frac{\sqrt{3}}{32} ce^*(3 + \sigma_{1i}\sigma_{2i})(3\sigma_{1j} - 3\sigma_{2j} + \sigma_{1j}\sigma_{1k}\sigma_{2k} - \sigma_{1k}\sigma_{2j}\sigma_{2k})q_j \\
&= -\frac{\sqrt{3}}{32} ce^*(9\sigma_{1j} - 9\sigma_{2j} + 3\sigma_{1j}\sigma_{1k}\sigma_{2k} - 3\sigma_{1k}\sigma_{2j}\sigma_{2k} \\
&+ 3\sigma_{1i}\sigma_{1j}\sigma_{2i} - 3\sigma_{1i}\sigma_{2i}\sigma_{2j} + \sigma_{1i}\sigma_{1j}\sigma_{1k}\sigma_{2i}\sigma_{2k} - \sigma_{1i}\sigma_{1k}\sigma_{2i}\sigma_{2j}\sigma_{2k})q_j
\end{aligned} \tag{211}
$$

$$
Tr[\hat{T}\hat{T}^\dagger] = -\frac{\sqrt{3}}{32} ce^* Tr[(\sigma_{1i}\sigma_{1j}\sigma_{1k}\sigma_{2i}\sigma_{2k} - \sigma_{1i}\sigma_{1k}\sigma_{2i}\sigma_{2j}\sigma_{2k})q_j] = 0 \tag{212}
$$

$$
\begin{aligned}
Tr[\vec{p}_2 \cdot \vec{\sigma}_2 \hat{T}\hat{T}^\dagger] &= -\frac{\sqrt{3}}{32} ce^* Tr[p_{2l}(-9I_1\sigma_{2l}\sigma_{2j} + 3\sigma_{1j}\sigma_{1k}\sigma_{2l}\sigma_{2k} + 3\sigma_{1i}\sigma_{1j}\sigma_{2l}\sigma_{2i} \\
&+ \sigma_{1i}\sigma_{1j}\sigma_{1k}\sigma_{2l}\sigma_{2i}\sigma_{2k} - \sigma_{1i}\sigma_{1k}\sigma_{2l}\sigma_{2i}\sigma_{2j}\sigma_{2k})q_j] \\
&= -\frac{\sqrt{3}}{32} ce^*[p_{2l}(-9 \cdot 2 \cdot 2\delta_{lj} + 3 \cdot 2\delta_{jk}2\delta_{lk} + 3 \cdot 2\delta_{ij}2\delta_{li} \\
&+ 2i\epsilon_{ijk}2i\epsilon_{lik} - 2\delta_{ik}2(\delta_{li}\delta_{jk} - \delta_{lj}\delta_{ik} + \delta_{lk}\delta_{ij})q_j] \\
&= -\frac{\sqrt{3}}{32} ce^*[p_{2l}(-36\delta_{lj} + 12\delta_{lj} + 12\delta_{lk} + 8\delta_{lj} \\
&- 4(\delta_{lj} - 3\delta_{lj} + \delta_{lj}))q_j] = 0
\end{aligned} \tag{213}
$$

C.3.6 cf* combination

$$
\begin{aligned}
\hat{T}\hat{T}^\dagger &= \frac{\sqrt{6}}{16} cf^*(3 + \vec{\sigma_1} \cdot \vec{\sigma_2})(\vec{\sigma_1} + \vec{\sigma_2}) \cdot q \\
&= \frac{\sqrt{6}}{16} cf^*(3 + \sigma_{1i}\sigma_{2i})(\sigma_{1j} + \sigma_{2j})q_j \\
&= \frac{\sqrt{6}}{16} cf^*(3\sigma_{1j} + 3\sigma_{2j} + \sigma_{1i}\sigma_{1j}\sigma_{2i} + \sigma_{1i}\sigma_{2i}\sigma_{2j})q_j
\end{aligned} \tag{214}
$$

$$Tr[\hat{T}\hat{T}^\dagger] = 0 \tag{215}$$

$$\begin{aligned} Tr[\vec{p}_2 \cdot \vec{\sigma}_2 \hat{T}\hat{T}^\dagger] &= \frac{\sqrt{6}}{16} c f^* Tr[p_{2k}(3I_1\sigma_{2l}\sigma_{2j} + \sigma_{1i}\sigma_{1j}\sigma_{2l}\sigma_{2i})q_j] \\ &= \frac{\sqrt{6}}{16} c f^* [p_{2k}(3 \cdot 2 \cdot 2\delta_{kj} + 2\delta_{ij}2\delta_{ki})q_j] \\ &= \frac{\sqrt{6}}{16} c f^* [p_{2k}(16\delta_{kj})q_j] = \sqrt{6} c f^* (\vec{p}_2 \cdot \vec{q}) \end{aligned} \tag{216}$$

C.4 D terms

C.4.1 da* combination

$$\begin{aligned} \hat{T}\hat{T}^\dagger &= \frac{da^*}{8\sqrt{2}}(3\vec{\sigma_1} \cdot q\vec{\sigma_2} \cdot q - \vec{\sigma_1} \cdot \vec{\sigma_2})(1 - \vec{\sigma_1} \cdot \vec{\sigma_2}) \\ &= \frac{da^*}{8\sqrt{2}}(3\sigma_{1i}q_i\sigma_{2j}q_j - \sigma_{1k}\sigma_{2k})(1 - \sigma_{1m}\sigma_{2m}) \\ &= \frac{da^*}{8\sqrt{2}}[(3\sigma_{1i}\sigma_{2j} - 3\sigma_{1i}\sigma_{1m}\sigma_{2j}\sigma_{2m})q_iq_j - \sigma_{1k}\sigma_{2k} \\ &+ \sigma_{1k}\sigma_{1m}\sigma_{2k}\sigma_{2m}] \end{aligned} \tag{217}$$

$$\begin{aligned} Tr[\hat{T}\hat{T}^\dagger] &= \frac{ad^*}{8\sqrt{2}} Tr[-3\sigma_{1i}\sigma_{1m}\sigma_{2j}\sigma_{2m}q_iq_j + \sigma_{1k}\sigma_{1m}\sigma_{2k}\sigma_{2m}] \\ &= \frac{ad^*}{8\sqrt{2}}[-3 \cdot 2\delta_{im}2\delta_{jm}q_iq_j + 2\delta_{km}2\delta_{km}] \\ &= \frac{ad^*}{8\sqrt{2}}[-12\delta_{ij}q_iq_j + 4\delta_{km}\delta_{km}] = 0 \end{aligned} \tag{218}$$

$$\begin{aligned} Tr[\vec{p}_2 \cdot \vec{\sigma}_2 \hat{T}\hat{T}^\dagger] &= \frac{ad^*}{8\sqrt{2}} Tr[P_{2l}(-3\sigma_{1i}\sigma_{1m}\sigma_{2l}\sigma_{2j}\sigma_{2m}q_iq_j + \sigma_{1k}\sigma_{1m}\sigma_{2l}\sigma_{2k}\sigma_{2m})] \\ &= \frac{ad^*}{8\sqrt{2}}[p_{2l}(-3 \cdot 2\delta_{im}2i\epsilon_{ljm}q_iq_j + 2\delta_{km}2i\epsilon_{ikm})] \\ &= \frac{ad^*}{8\sqrt{2}}[p_{2l}(-12i\epsilon_{lji}q_iq_j)] = -\frac{ad^*}{8\sqrt{2}}12[\vec{p}_2 \cdot (\vec{q} \times \vec{q})] = 0 \end{aligned} \tag{219}$$

C.4.2 db* combination

$$\begin{aligned} \hat{T}\hat{T}^\dagger &= \frac{db^*}{16\sqrt{2}}(3\vec{\sigma_1} \cdot q\vec{\sigma_2} \cdot q - \vec{\sigma_1} \cdot \vec{\sigma_2})(\vec{\sigma_1} - \vec{\sigma_2}) \cdot \vec{q}(1 - \vec{\sigma_1} \cdot \vec{\sigma_2}) \\ &= \frac{db^*}{16\sqrt{2}}(3\sigma_{1i}\sigma_{2j}q_iq_j - \sigma_{1k}\sigma_{2k})(\sigma_{1m} - \sigma_{2m})(1 - \sigma_{1n}\sigma_{2n})q_m \\ &= \frac{db^*}{16\sqrt{2}}[(3\sigma_{1i}\sigma_{1m}\sigma_{2j} - 3\sigma_{1i}\sigma_{2j}\sigma_{2m} - 3\sigma_{1i}\sigma_{1m}\sigma_{1n}\sigma_{2j}\sigma_{2n} \\ &+ 3\sigma_{1i}\sigma_{1n}\sigma_{2j}\sigma_{2m}\sigma_{2n})q_iq_jq_m + (-\sigma_{1k}\sigma_{1m}\sigma_{2k} + \sigma_{1k}\sigma_{2k}\sigma_{2m} \\ &+ \sigma_{1k}\sigma_{1m}\sigma_{1n}\sigma_{2k}\sigma_{2n} - \sigma_{1k}\sigma_{1n}\sigma_{2k}\sigma_{2m}\sigma_{2n})q_m] \end{aligned} \tag{220}$$

$$
\begin{aligned}
Tr[\hat{T}\hat{T}^\dagger] &= \frac{db^*}{16\sqrt{2}} Tr[(-3\sigma_{1i}\sigma_{1m}\sigma_{1n}\sigma_{2j}\sigma_{2n} + 3\sigma_{1i}\sigma_{1n}\sigma_{2j}\sigma_{2m}\sigma_{2n})q_i q_j q_m \\
&+ (\sigma_{1k}\sigma_{1m}\sigma_{1n}\sigma_{2k}\sigma_{2n} - \sigma_{1k}\sigma_{1n}\sigma_{2k}\sigma_{2m}\sigma_{2n})q_m] \\
&= \frac{db^*}{16\sqrt{2}}[(-12i\epsilon_{imn}\delta_{jn} + 12i\epsilon_{jmn}\delta_{in})q_i q_j q_m \\
&+ (4i\epsilon_{kmn}\delta_{kn} - 4i\epsilon_{kmn}\delta_{kn})q_m] = 0
\end{aligned} \tag{221}
$$

$$
\begin{aligned}
Tr[\vec{p}_2 \cdot \vec{\sigma}_2 \hat{T}\hat{T}^\dagger] &= \frac{db^*}{16\sqrt{2}} Tr[p_{2l}[(3\sigma_{1i}\sigma_{1m}\sigma_{2l}\sigma_{2j} - 3\sigma_{1i}\sigma_{1m}\sigma_{1n}\sigma_{2l}\sigma_{2j}\sigma_{2n} \\
&+ 3\sigma_{1i}\sigma_{1n}\sigma_{2l}\sigma_{2j}\sigma_{2m}\sigma_{2n})q_i q_j q_m + (-\sigma_{1k}\sigma_{1m}\sigma_{2l}\sigma_{2k} \\
&+ \sigma_{1k}\sigma_{1m}\sigma_{1n}\sigma_{2l}\sigma_{2k}\sigma_{2n} - \sigma_{1k}\sigma_{1n}\sigma_{2l}\sigma_{2k}\sigma_{2m}\sigma_{2n})q_m]] \\
&= \frac{db^*}{16\sqrt{2}}[p_{2l}[(12\delta_{im}\delta_{lj} + 12(\delta_{il}\delta_{mj} - \delta_{ij}\delta_{ml}) \\
&+ 12\delta_{in}(\delta_{lj}\delta_{mn} - \delta_{lm}\delta_{jn} + \delta_{ln}\delta_{jm}))q_i q_j q_m] \\
&+ (-4\delta_{lm} + 8\delta_{lm} + 4\delta_{lm})q_m \\
&= \frac{db^*}{16\sqrt{2}}[(24q^2 + 8)\vec{p}_2 \cdot \vec{q}] = \sqrt{2}db^*(\vec{p}_2 \cdot \vec{q})
\end{aligned} \tag{222}
$$

C.4.3 $\mathbf{dc^*}$ combination

$$
\begin{aligned}
\hat{T}\hat{T}^\dagger &= \frac{dc^*}{8\sqrt{2}}(3\vec{\sigma_1} \cdot q\vec{\sigma_2} \cdot q - \vec{\sigma_1} \cdot \vec{\sigma_2})(3 + \vec{\sigma_1} \cdot \vec{\sigma_2}) \\
&= \frac{dc^*}{8\sqrt{2}}(3\sigma_{1i}q_i\sigma_{2j}q_j - \sigma_{1k}\sigma_{2k})(3 + \sigma_{1m}\sigma_{2m}) \\
&= \frac{dc^*}{8\sqrt{2}}[(9\sigma_{1i}\sigma_{2j} + 3\sigma_{1i}\sigma_{1m}\sigma_{2j}\sigma_{2m})q_i q_j - 3\sigma_{1k}\sigma_{2k} - \sigma_{1k}\sigma_{1m}\sigma_{2k}\sigma_{2m}]
\end{aligned} \tag{223}
$$

$$
\begin{aligned}
Tr[\hat{T}\hat{T}^\dagger] &= \frac{dc^*}{8\sqrt{2}} Tr[3\sigma_{1i}\sigma_{1m}\sigma_{2j}\sigma_{2m}q_i q_j - \sigma_{1k}\sigma_{1m}\sigma_{2k}\sigma_{2m}] \\
&= \frac{dc^*}{8\sqrt{2}}[12\delta_{ij}q_i q_j - 4\delta_{km}\delta_{km}] = 0
\end{aligned} \tag{224}
$$

$$
\begin{aligned}
Tr[\vec{p}_2 \cdot \vec{\sigma}_2 \hat{T}\hat{T}^\dagger] &= \frac{dc^*}{8\sqrt{2}} Tr[p_{2l}(3\sigma_{1i}\sigma_{1m}\sigma_{2l}\sigma_{2j}\sigma_{2m}q_i q_j - \sigma_{1k}\sigma_{1m}\sigma_{2l}\sigma_{2k}\sigma_{2m})] \\
&= \frac{dc^*}{8\sqrt{2}}[p_{2l}(12i\delta_{im}\epsilon_{ljm} - 4i\delta_{km}\epsilon_{lkm})] = 0
\end{aligned} \tag{225}
$$

C.4.4 dd* combination

$$\begin{aligned}\hat{T}\hat{T}^\dagger &= \frac{|d|^2}{8}(S_{12}(p))^2 = \frac{|d|^2}{8}(4S^2 - 2S_{12}) \\ &= \frac{|d|^2}{8}(4(\frac{3}{2} + \frac{\vec{\sigma_1}\cdot\vec{\sigma_2}}{2}) - 2(3\vec{\sigma_1}\cdot p\vec{\sigma_2}\cdot p - \vec{\sigma_1}\cdot\vec{\sigma_2}) \\ &= \frac{|d|^2}{8}(6 + 4\vec{\sigma_1}\cdot\vec{\sigma_2} - 6\vec{\sigma_1}\cdot p\vec{\sigma_2}\cdot p)\end{aligned} \tag{226}$$

$$Tr[\hat{T}\hat{T}^\dagger] = \frac{|d|^2}{8}Tr(6) = \frac{3}{4}|d|^2 Tr(I) = 3|d|^2 \tag{227}$$

$$Tr[\vec{p_2}\cdot\vec{\sigma}_2\hat{T}\hat{T}^\dagger] = 0 \tag{228}$$

C.4.5 de* combination

$$\begin{aligned}\hat{T}\hat{T}^\dagger &= -\frac{\sqrt{3}}{\sqrt{2}}\frac{de^*}{16}(3\vec{\sigma_1}\cdot q\vec{\sigma_2}\cdot q - \vec{\sigma_1}\cdot\vec{\sigma_2})(\vec{\sigma_1} - \vec{\sigma_2})\cdot q(3 + \vec{\sigma_1}\cdot\vec{\sigma_2}) \\ &= -\frac{\sqrt{3}}{\sqrt{2}}\frac{de^*}{16}(3\sigma_{1i}q_i\sigma_{2j}q_j - \sigma_{1k}\sigma_{2k}) \\ &\times (3\sigma_{1m} - 3\sigma_{2m} + \sigma_{1m}\sigma_{1n}\sigma_{2n} - \sigma_{1n}\sigma_{2m}\sigma_{2n})q_m \\ &= -\frac{\sqrt{3}}{\sqrt{2}}\frac{de^*}{16}[(9\sigma_{1i}\sigma_{1m}\sigma_{2j} - 9\sigma_{1i}\sigma_{2j}\sigma_{2m} + 3\sigma_{1i}\sigma_{1m}\sigma_{1n}\sigma_{2j}\sigma_{2n} \\ &- 3\sigma_{1i}\sigma_{1n}\sigma_{2j}\sigma_{2m}\sigma_{2n})q_iq_jq_m + (3\sigma_{1k}\sigma_{2k}\sigma_{2m} - 3\sigma_{1k}\sigma_{1m}\sigma_{2k} \\ &- \sigma_{1k}\sigma_{1m}\sigma_{1n}\sigma_{2k}\sigma_{2n} + \sigma_{1k}\sigma_{1n}\sigma_{2k}\sigma_{2m}\sigma_{2n})q_m]\end{aligned} \tag{229}$$

$$\begin{aligned}Tr[\hat{T}\hat{T}^\dagger] &= -\frac{\sqrt{3}}{\sqrt{2}}\frac{de^*}{16}Tr[(3\sigma_{1i}\sigma_{1m}\sigma_{1n}\sigma_{2j}\sigma_{2n} - 3\sigma_{1i}\sigma_{1n}\sigma_{2j}\sigma_{2m}\sigma_{2n})q_iq_jq_m \\ &+ (-\sigma_{1k}\sigma_{1m}\sigma_{1n}\sigma_{2k}\sigma_{2n} + \sigma_{1k}\sigma_{1n}\sigma_{2k}\sigma_{2m}\sigma_{2n})q_m] \\ &= -\frac{\sqrt{3}}{\sqrt{2}}\frac{de^*}{16}[(12i\epsilon_{imn}\delta_{jn} - 12i\epsilon_{jmn}\delta_{in})q_iq_jq_m \\ &+ (-4i\delta_{kn}\epsilon_{kmn} + 4i\delta_{kn}\epsilon_{kmn})q_m] = 0\end{aligned} \tag{230}$$

$$
\begin{aligned}
Tr[\vec{p}_2\cdot\vec{\sigma}_2\hat{T}\hat{T}^\dagger] &= -\frac{\sqrt{3}}{\sqrt{2}}\frac{de^*}{16}Tr[p_{2l}[(9\sigma_{1i}\sigma_{1m}\sigma_{2l}\sigma_{2j}+3\sigma_{1i}\sigma_{1m}\sigma_{1n}\sigma_{2l}\sigma_{2j}\sigma_{2n}\\
&-3\sigma_{1i}\sigma_{1n}\sigma_{2l}\sigma_{2j}\sigma_{2m}\sigma_{2n})q_iq_jq_m+(-3\sigma_{1k}\sigma_{1m}\sigma_{2l}\sigma_{2k}\\
&-\sigma_{1k}\sigma_{1m}\sigma_{1n}\sigma_{2l}\sigma_{2k}\sigma_{2n}+\sigma_{1k}\sigma_{1n}\sigma_{2l}\sigma_{2k}\sigma_{2m}\sigma_{2n})q_m]]\\
&= -\frac{\sqrt{3}}{\sqrt{2}}\frac{de^*}{16}[p_{2l}[(36\delta_{im}\delta_{lj}-12(\delta_{il}\delta_{mj}-\delta_{ij}\delta_{ml})\\
&-12\delta_{in}(\delta_{lj}\delta_{mn}-\delta_{lm}\delta_{jn}+\delta_{ln}\delta_{jm})q_iq_jq_m]\\
&+(-12\delta_{lm}-8\delta_{lm}-4\delta_{lm})q_m]\\
&= -\frac{\sqrt{3}}{\sqrt{2}}\frac{de^*}{16}[24q^2\vec{p}_2\cdot\vec{q}-24\vec{p}_2\cdot\vec{q}]=0
\end{aligned}
\tag{231}
$$

C.4.6 df* combination

$$
\begin{aligned}
\hat{T}\hat{T}^\dagger &= \frac{\sqrt{3}}{8}df^*(3\vec{\sigma_1}\cdot q\vec{\sigma_2}\cdot q-\vec{\sigma_1}\cdot\vec{\sigma_2})(\vec{\sigma_1}+\vec{\sigma_2})\cdot q\\
&= \frac{\sqrt{3}}{8}df^*(3\sigma_{1i}p_i\sigma_{2j}p_j-\sigma_{1k}\sigma_{2k})(\sigma_{1m}+\sigma_{2m})p_m\\
&= \frac{\sqrt{3}}{8}df^*[(3\sigma_{1i}\sigma_{1m}\sigma_{2j}+3\sigma_{1i}\sigma_{2j}\sigma_{2m})p_ip_jp_m\\
&-(\sigma_{1k}\sigma_{1m}\sigma_{2k}+\sigma_{1k}\sigma_{2k}\sigma_{2m})p_m]
\end{aligned}
\tag{232}
$$

$$
Tr[\hat{T}\hat{T}^\dagger]=0 \tag{233}
$$

$$
\begin{aligned}
Tr[\vec{p}_2\cdot\vec{\sigma}_2\hat{T}\hat{T}^\dagger] &= \frac{\sqrt{3}}{8}df^*Tr[P_{2l}(3\sigma_{1i}\sigma_{1m}\sigma_{2l}\sigma_{2j}p_ip_jp_m-\sigma_{1k}\sigma_{1m}\sigma_{2l}\sigma_{2k}p_m)]\\
&= \frac{\sqrt{3}}{8}df^*[p_{2l}(12\delta_{im}\delta_{lj}p_ip_jp_m-4\delta_{km}\delta_{lm}p_m)]\\
&= \frac{\sqrt{3}}{8}df^*[12q^2\vec{p}_2\cdot\vec{q}-4\vec{p}_2\cdot\vec{q}]\\
&= \sqrt{3}df^*(\vec{p}_2\cdot\vec{q})
\end{aligned}
\tag{234}
$$

C.5 E terms

C.5.1 ea* combination

$$\begin{aligned}\hat{T}\hat{T}^\dagger &= -\frac{\sqrt{3}}{32}ea^*(3+\vec{\sigma_1}\cdot\vec{\sigma_2})(\vec{\sigma_1}-\vec{\sigma_2})q(1-\vec{\sigma_1}\cdot\vec{\sigma_2})\\ &= -\frac{\sqrt{3}}{32}ea^*(3+\sigma_{1i}\sigma_{2i})(\sigma_{1j}-\sigma_{2j})q_j(1-\sigma_{1k}\sigma_{2k})\\ &= -\frac{\sqrt{3}}{32}ea^*(3\sigma_{1j}-3\sigma_{2j}+\sigma_{1i}\sigma_{1j}\sigma_{2i}-\sigma_{1i}\sigma_{2i}\sigma_{2j})(1-\sigma_{1k}\sigma_{2k})q_j\\ &= -\frac{\sqrt{3}}{32}ea^*(3\sigma_{1j}-3\sigma_{2j}+\sigma_{1i}\sigma_{1j}\sigma_{2i}-\sigma_{1i}\sigma_{2i}\sigma_{2j}\\ &-3\sigma_{1j}\sigma_{1k}\sigma_{2k}+3\sigma_{1k}\sigma_{2j}\sigma_{2k}-\sigma_{1i}\sigma_{1j}\sigma_{1k}\sigma_{2i}\sigma_{2k}+\sigma_{1i}\sigma_{1k}\sigma_{2i}\sigma_{2j}\sigma_{2k})q_j\end{aligned} \tag{235}$$

$$Tr[\hat{T}\hat{T}^\dagger] = -\frac{\sqrt{3}}{32}ea^*Tr[(-\sigma_{1i}\sigma_{1j}\sigma_{1k}\sigma_{2i}\sigma_{2k}+\sigma_{1i}\sigma_{1k}\sigma_{2i}\sigma_{2j}\sigma_{2k})q_j] = 0 \tag{236}$$

$$\begin{aligned}Tr[\vec{p}_2\cdot\vec{\sigma}_2\hat{T}\hat{T}^\dagger] &= -\frac{\sqrt{3}}{32}ea^*Tr[p_{2l}(-3I_1\sigma_{2l}\sigma_{2j}+\sigma_{1i}\sigma_{1j}\sigma_{2l}\sigma_{2i}-3\sigma_{1j}\sigma_{1k}\sigma_{2l}\sigma_{2k}\\ &-\sigma_{1i}\sigma_{1j}\sigma_{1k}\sigma_{2l}\sigma_{2i}\sigma_{2k}+\sigma_{1i}\sigma_{1k}\sigma_{2l}\sigma_{2i}\sigma_{2j}\sigma_{2k})q_j]\\ &= -\frac{\sqrt{3}}{32}ea^*[p_{2l}(-3\cdot 2\cdot 2\delta_{lj}+2\delta_{ij}2\delta_{li}-3\cdot 2\delta_{jk}2\delta_{lk}\\ &-2i\epsilon_{ijk}2i\epsilon_{lik}+2\delta_{ik}2(\delta_{li}\delta_{jk}-\delta_{lk}\delta_{ik}+\delta_{lk}\delta_{ij}))q_j]\\ &= -\frac{\sqrt{3}}{32}ea^*[p_{2l}(-12\delta_{lj}+4\delta_{lj}-12\delta_{lj}-4\cdot 2\delta_{lj}\\ &+4(\delta_{lj}-3\delta_{lj}+\delta_{lj}))p_j] = -\frac{\sqrt{3}}{32}ea^*[p_{2l}(-32\delta_{lj})q_j]\\ &= \sqrt{3}ea^*(\vec{p}_2\cdot\vec{q})\end{aligned} \tag{237}$$

C.5.2 eb* combination

$$\begin{aligned}\hat{T}\hat{T}^\dagger &= \frac{\sqrt{3}}{64}eb^*(3+\vec{\sigma_1}\cdot\vec{\sigma_2})(\vec{\sigma_1}-\vec{\sigma_2})\cdot q(\vec{\sigma_1}-\vec{\sigma_2})\cdot q(1-\vec{\sigma_1}\cdot\vec{\sigma_2})\\ &= \frac{\sqrt{3}}{64}eb^*(3+\sigma_{1i}\sigma_{2i})(\sigma_{1j}-\sigma_{2j})(\sigma_{1k}-\sigma_{2k}-\sigma_{1k}\sigma_{1m}\sigma_{2m}\\ &+\sigma_{1m}\sigma_{2k}\sigma_{2m})q_jq_k = \frac{\sqrt{3}}{64}eb^*(3+\sigma_{1i}\sigma_{2i})(\sigma_{1j}\sigma_{1k}-\sigma_{1j}\sigma_{2k}\\ &-\sigma_{1j}\sigma_{1k}\sigma_{1m}\sigma_{2m}+\sigma_{1j}\sigma_{1m}\sigma_{2k}\sigma_{2m}-\sigma_{1k}\sigma_{2j}\\ &+\sigma_{2j}\sigma_{2k}+\sigma_{1k}\sigma_{1m}\sigma_{2j}\sigma_{2m}-\sigma_{1m}\sigma_{2j}\sigma_{2k}\sigma_{2m})q_jq_k\end{aligned} \tag{238}$$

$$
\begin{aligned}
Tr[\hat{T}\hat{T}^\dagger] = \frac{\sqrt{3}}{64} eb^* Tr[(&3\sigma_{1j}\sigma_{1k}I_2 + 3\sigma_{1j}\sigma_{1m}\sigma_{2k}\sigma_{2m} + 3I_1\sigma_{2j}\sigma_{2k} \\
&+ 3\sigma_{1k}\sigma_{1m}\sigma_{2j}\sigma_{2m} - \sigma_{1i}\sigma_{1j}\sigma_{2i}\sigma_{2k} - \sigma_{1i}\sigma_{1j}\sigma_{1k}\sigma_{1m}\sigma_{2i}\sigma_{2m} \\
&+ \sigma_{1i}\sigma_{1j}\sigma_{1m}\sigma_{2i}\sigma_{2k}\sigma_{2m} - \sigma_{1i}\sigma_{1k}\sigma_{2i}\sigma_{2j} + \sigma_{1i}\sigma_{1k}\sigma_{1m}\sigma_{2i}\sigma_{2j}\sigma_{2m} \\
&- \sigma_{1i}\sigma_{1m}\sigma_{2i}\sigma_{2j}\sigma_{2k}\sigma_{2m})q_j q_k] \\
= \frac{\sqrt{3}}{64} eb^* [&12\delta_{jk} + 12\delta_{jk} + \delta_{jk} - 4\delta_{jk} - 12\delta_{jk} - 8\delta_{jk} - 4\delta_{jk} \\
&- 8\delta_{jk} - 12\delta_{jk}] = 0
\end{aligned}
\tag{239}
$$

$$
\begin{aligned}
Tr[\vec{p}_2 \cdot \vec{\sigma}_2 \hat{T}\hat{T}^\dagger] = \frac{\sqrt{3}}{64} eb^* Tr[p_{2l}(&-3\sigma_{1j}\sigma_{1k}\sigma_{1m}\sigma_{2l}\sigma_{2m} + 3\sigma_{1j}\sigma_{1m}\sigma_{2l}\sigma_{2k}\sigma_{2m} \\
&+ 3\sigma_{2l}\sigma_{2j}\sigma_{2k} + 3\sigma_{1k}\sigma_{1m}\sigma_{2l}\sigma_{2j}\sigma_{2m} + \sigma_{1i}\sigma_{1j}\sigma_{1k}\sigma_{2l}\sigma_{2i} \\
&- \sigma_{1i}\sigma_{1j}\sigma_{2l}\sigma_{2i}\sigma_{2k} - \sigma_{1i}\sigma_{1j}\sigma_{1k}\sigma_{1m}\sigma_{2l}\sigma_{2i}\sigma_{2m} \\
&+ \sigma_{1i}\sigma_{1j}\sigma_{1m}\sigma_{2l}\sigma_{2i}\sigma_{2k}\sigma_{2m} - \sigma_{1i}\sigma_{1k}\sigma_{2l}\sigma_{2i}\sigma_{2j} \\
&+ \sigma_{1i}\sigma_{1k}\sigma_{1m}\sigma_{2l}\sigma_{2i}\sigma_{2j}\sigma_{2m} - \sigma_{1i}\sigma_{1m}\sigma_{2l}\sigma_{2i}\sigma_{2j}\sigma_{2k}\sigma_{2m})q_j q_k] \\
= \frac{\sqrt{3}}{64} eb^* [ip_{2l}(&-12\epsilon_{jkl} + 12\epsilon_{jkj} + 12\epsilon_{ljk} + 12\epsilon_{ljk} + 4\epsilon_{ljk} \\
&- 4\epsilon_{ljk} - 4\epsilon_{ljk} + 4\epsilon_{lkj} + 4\epsilon_{ljk} + 4\epsilon_{kjl} - 4\epsilon_{lkj} + 4\epsilon_{lkj} \\
&+ 4\epsilon_{jkl} - 4\epsilon_{jkl} - 4\epsilon_{lkj} - 4\epsilon_{lkj})q_j q_k] = 0
\end{aligned}
\tag{240}
$$

C.5.3 ec^* combination

$$
\begin{aligned}
\hat{T}\hat{T}^\dagger &= -\frac{\sqrt{3}}{32}(ec^*)(3 + \vec{\sigma_1} \cdot \vec{\sigma_2})(\vec{\sigma_1} - \vec{\sigma_2})q(3 + \vec{\sigma_1} \cdot \vec{\sigma_2}) \\
&= -\frac{\sqrt{3}}{32}(ec^*)(3 + \sigma_{1i}\sigma_{2i})(\sigma_{1j} - \sigma_{2j})q_j(3 + \sigma_{1k}\sigma_{2k}) \\
&= -\frac{\sqrt{3}}{32}(ec^*)(3\sigma_{1j} - 3\sigma_{2j} + \sigma_{1i}\sigma_{1j}\sigma_{2i} - \sigma_{1i}\sigma_{2i}\sigma_{2j})(3 + \sigma_{1k}\sigma_{2k})q_j \\
&= -\frac{\sqrt{3}}{32}(ec^*)(9\sigma_{1j} - 9\sigma_{2j} + 3\sigma_{1i}\sigma_{1j}\sigma_{2i} - 3\sigma_{1i}\sigma_{2i}\sigma_{2j} + 3\sigma_{1j}\sigma_{1k}\sigma_{2k} \\
&\quad - 3\sigma_{1k}\sigma_{2j}\sigma_{2k} + \sigma_{1i}\sigma_{1j}\sigma_{1k}\sigma_{2i}\sigma_{2k} - \sigma_{1i}\sigma_{1k}\sigma_{2i}\sigma_{2j}\sigma_{2k})q_j
\end{aligned}
\tag{241}
$$

$$
Tr[\hat{T}\hat{T}^\dagger] = -\frac{\sqrt{3}}{32}(ec^*)Tr[(\sigma_{1i}\sigma_{1j}\sigma_{1k}\sigma_{2i}\sigma_{2k} - \sigma_{1i}\sigma_{1k}\sigma_{2i}\sigma_{2j}\sigma_{2k})p_j] = 0 \tag{242}
$$

$$
\begin{aligned}
Tr[\vec{p}_2\cdot\vec{\sigma}_2\hat{T}\hat{T}^\dagger] &= -\frac{\sqrt{3}}{32}(ec^*)Tr[p_{2l}(-9I_1\sigma_{2l}\sigma_{2j}+3\sigma_{1i}\sigma_{1j}\sigma_{2l}\sigma_{2i}+3\sigma_{1j}\sigma_{1k}\sigma_{2l}\sigma_{2k}\\
&+\sigma_{1i}\sigma_{1j}\sigma_{1k}\sigma_{2l}\sigma_{2i}\sigma_{2k}-\sigma_{1i}\sigma_{1k}\sigma_{2l}\sigma_{2i}\sigma_{2j}\sigma_{2k})q_j]\\
&= -\frac{\sqrt{3}}{32}(ec^*)[p_{2l}(-9\cdot 2\cdot 2\delta_{lj}+3\cdot 2\delta_{ij}2\delta_{li}+3\cdot 2\delta_{jk}2\delta_{lk}\\
&+2i\epsilon_{ijk}2i\epsilon_{lik}-2\delta_{ik}2(\delta_{li}\delta_{jk}-\delta_{lj}\delta_{ik}+\delta_{lk}\delta_{ij}))q_j]\\
&= -\frac{\sqrt{3}}{32}(ec^*)[p_{2l}(-36\delta_{lj}+12\delta_{lj}+12\delta_{lj}+8\delta_{lj}\\
&-4(\delta_{lj}-3\delta_{lj}+\delta_{lj}))q_j]=0
\end{aligned}
\tag{243}
$$

C.5.4 ed* combination

$$
\begin{aligned}
\hat{T}\hat{T}^\dagger &= -\sqrt{\frac{3}{2}}\frac{ed^*}{16}(3+\vec{\sigma_1}\cdot\vec{\sigma_2})(\vec{\sigma_1}-\vec{\sigma_2})q(3\vec{\sigma_1}\cdot q\vec{\sigma_2}\cdot q-\vec{\sigma_1}\cdot\vec{\sigma_2})\\
&= -\sqrt{\frac{3}{2}}\frac{ed^*}{16}(3+\sigma_{1i}\sigma_{2i})(\sigma_{1j}-\sigma_{2j})q_j(3\sigma_{1k}q_k\sigma_{2m}q_m-\sigma_{1n}\sigma_{2n})\\
&= -\sqrt{\frac{3}{2}}\frac{ed^*}{16}(3\sigma_{1j}-3\sigma_{2j}+\sigma_{1i}\sigma_{1j}\sigma_{2i}-\sigma_{1i}\sigma_{2i}\sigma_{2j})q_j\\
&\times(3\sigma_{1k}q_k\sigma_{2m}q_m-\sigma_{1n}\sigma_{2n})\\
&= -\sqrt{\frac{3}{2}}\frac{ed^*}{16}[(9\sigma_{1j}\sigma_{1k}\sigma_{2m}-9\sigma_{1k}\sigma_{2j}\sigma_{2m}+3\sigma_{1i}\sigma_{1j}\sigma_{1k}\sigma_{2i}\sigma_{2m}\\
&-3\sigma_{1i}\sigma_{1k}\sigma_{2i}\sigma_{2j}\sigma_{2m})q_jq_kq_m+(-3\sigma_{1j}\sigma_{1n}\sigma_{2n}+3\sigma_{1n}\sigma_{2j}\sigma_{2n}\\
&-\sigma_{1i}\sigma_{1j}\sigma_{1n}\sigma_{2i}\sigma_{2n}+\sigma_{1i}\sigma_{1n}\sigma_{2i}\sigma_{2j}\sigma_{2n})q_j]
\end{aligned}
\tag{244}
$$

$$
\begin{aligned}
Tr[\hat{T}\hat{T}^\dagger] &= -\sqrt{\frac{3}{2}}\frac{ed^*}{16}Tr[(3\sigma_{1i}\sigma_{1j}\sigma_{1k}\sigma_{2i}\sigma_{2m}-3\sigma_{1i}\sigma_{1k}\sigma_{2i}\sigma_{2j}\sigma_{2m})q_jq_kq_m\\
&+(-\sigma_{1i}\sigma_{1j}\sigma_{1n}\sigma_{2i}\sigma_{2n}+\sigma_{1i}\sigma_{1n}\sigma_{2i}\sigma_{2j}\sigma_{2n})q_j]\\
&= -\sqrt{\frac{3}{2}}\frac{ed^*}{16}[(3\cdot 2i\epsilon_{ijk}2\delta_{im}-3\cdot 2\delta_{ik}2i\epsilon_{ijm})q_jq_kq_m\\
&+(-2i\epsilon_{ijn}2\delta_{in}+2\delta_{in}2i\epsilon_{ijn})q_j]\\
&= -\sqrt{\frac{3}{2}}\frac{ed^*}{16}[(12i\epsilon_{mjk}-12i\epsilon_{kjm})q_jq_kq_m]\\
&= -\sqrt{\frac{3}{2}}\frac{24}{16}ed^*[i\vec{q}\cdot(\vec{q}\times\vec{q})]=0
\end{aligned}
\tag{245}
$$

$$
\begin{aligned}
Tr[\vec{p}_2\vec{\sigma}_2\hat{T}\hat{T}^\dagger] &= -\sqrt{\frac{3}{2}}\frac{ed^*}{16}Tr[p_{2l}[(9\sigma_{1j}\sigma_{1k}\sigma_{2l}\sigma_{2m}+3\sigma_{1i}\sigma_{1j}\sigma_{1k}\sigma_{2l}\sigma_{2i}\sigma_{2m}\\
&-3\sigma_{1i}\sigma_{1k}\sigma_{2l}\sigma_{2i}\sigma_{2j}\sigma_{2m})q_jq_kq_m+(-3\sigma_{1j}\sigma_{1n}\sigma_{2l}\sigma_{2n}\\
&-\sigma_{1i}\sigma_{1j}\sigma_{1n}\sigma_{2l}\sigma_{2i}\sigma_{2n}+\sigma_{1i}\sigma_{1n}\sigma_{2l}\sigma_{2i}\sigma_{2j}\sigma_{2n})q_j]]\\
&= -\sqrt{\frac{3}{2}}\frac{ed^*}{16}[p_{2l}[(36\delta_{jk}\delta_{lm}-12\epsilon_{ijk}\epsilon_{lim}\\
&-12\delta_{ik}(\delta_{li}\delta_{jm}-\delta_{lj}\delta_{im}+\delta_{lm}\delta_{ij}))q_jq_kq_m]\\
&+(-12\delta_{lj}+4\epsilon_{ijn}\epsilon_{lin}+4\delta_{in}(\delta_{li}\delta_{jn}-\delta_{lj}\delta_{in}+\delta_{ln}\delta_{ij}))q_j]\\
&= -\sqrt{\frac{3}{2}}\frac{ed^*}{16}[p_{2l}[36\delta_{jk}\delta_{lm}+12(\delta_{jl}\delta_{km}-\delta_{jm}\delta_{kl})\\
&-12(\delta_{lk}\delta_{jm}-\delta_{lj}\delta_{km}+\delta_{lm}\delta_{kj})]q_jq_kq_m\\
&+(-12\delta_{lj}-8\delta_{lj}-4\delta_{lj})q_j]\\
&= -\sqrt{\frac{3}{2}}\frac{ed^*}{16}(24)p_{2l}[(\delta_{jk}\delta_{lm}+\delta_{lj}\delta_{km}-\delta_{lk}\delta_{jm})q_jq_kq_m\\
&-\delta_{lk}\delta_{jm}q_j] = -\sqrt{\frac{3}{2}}\frac{ed^*}{16}(24)\cdot 2q^2[\vec{p}_2\cdot\vec{q}-\vec{p}_2\cdot\vec{q}] = 0
\end{aligned}
\tag{246}
$$

C.5.5 ee* combination

$$
\begin{aligned}
\hat{T}\hat{T}^\dagger &= \frac{3}{64}|e|^2(3+\vec{\sigma_1}\cdot\vec{\sigma_2})(\vec{\sigma_1}-\vec{\sigma_2})q(3+\vec{\sigma_1}\cdot\vec{\sigma_2})(\vec{\sigma_1}-\vec{\sigma_2})q\\
&= \frac{3}{64}|e|^2(12+4\sigma_{1i}\sigma_{2i})(\sigma_{1j}\sigma_{1k}+\sigma_{2j}\sigma_{2k}-\sigma_{1j}\sigma_{2k}-\sigma_{2j}\sigma_{1k})q_jq_k\\
&= \frac{3}{64}|e|^2(12(\sigma_{1j}\sigma_{1k}+\sigma_{2j}\sigma_{2k}-\sigma_{1j}\sigma_{2k}-\sigma_{2j}\sigma_{1k})+4(\sigma_{1i}\sigma_{1j}\sigma_{1k}\sigma_{2i}\\
&+\sigma_{1i}\sigma_{2i}\sigma_{2j}\sigma_{2k}-\sigma_{1i}\sigma_{1j}\sigma_{2i}\sigma_{2k}-\sigma_{1i}\sigma_{1k}\sigma_{2i}\sigma_{2k})q_jq_k)\\
&= \frac{3}{16}|e|^2(3\sigma_{1j}\sigma_{1k}+3\sigma_{2j}\sigma_{2k}-3\sigma_{1j}\sigma_{2k}-3\sigma_{2j}\sigma_{1k}+\sigma_{1i}\sigma_{1j}\sigma_{1k}\sigma_{2i}\\
&+\sigma_{1i}\sigma_{2i}\sigma_{2j}\sigma_{2k}-\sigma_{1i}\sigma_{1j}\sigma_{2i}\sigma_{2k}-\sigma_{1i}\sigma_{1k}\sigma_{2i}\sigma_{2j})q_jq_k
\end{aligned}
\tag{247}
$$

$$
\begin{aligned}
Tr[\hat{T}\hat{T}^\dagger] &= \frac{3}{16}|e|^2Tr[(3\sigma_{1j}\sigma_{1k}I_2+3I_1\sigma_{2j}\sigma_{2k}\\
&-\sigma_{1i}\sigma_{1j}\sigma_{2i}\sigma_{2k}-\sigma_{1i}\sigma_{1k}\sigma_{2i}\sigma_{2j})q_jq_k]\\
&= \frac{3}{16}|e|^2[3\cdot 2\cdot 2\delta_{jk}+3\cdot 2\delta_{jk}\cdot 2-2\delta_{ij}2\delta_{ik}-2\delta_{ik}\delta_{ij}]q_jq_k\\
&= 3|e|^2
\end{aligned}
\tag{248}
$$

$$
\begin{aligned}
Tr[\vec{p}_2\cdot\vec{\sigma}_2\hat{T}\hat{T}^\dagger] &= \frac{3}{16}|e|^2 Tr[p_{2l}(3I_1\sigma_{2l}\sigma_{2j}\sigma_{2k}+\sigma_{1i}\sigma_{1j}\sigma_{1k}\sigma_{2l}\sigma_{2i}\\
&-\sigma_{1i}\sigma_{1j}\sigma_{2l}\sigma_{2i}\sigma_{2k}-\sigma_{1i}\sigma_{1k}\sigma_{2l}\sigma_{2i}\sigma_{2j})q_jq_k]\\
&=\frac{3}{16}|e|^2[p_{2l}(3\cdot 2\cdot 2i\epsilon_{ljk}+2i\epsilon_{ijk}2\delta_{li}-2\delta_{ij}2i\epsilon_{lik}\\
&-2\delta_{ik}2i\epsilon_{lij})p_jp_k]=\frac{3}{16}|e|^2[p_{2l}(12i\epsilon_{ljk}+4i\epsilon_{ljk}\\
&-4i\epsilon_{ljk}-4i\epsilon_{lkj})q_jq_k]=\frac{3}{16}|e|^2[p_{2l}(16i\epsilon_{ljk})q_jq_k]\\
&=3|e|^2\vec{p}_2\cdot(\vec{q}\times\vec{q})=0
\end{aligned}
\tag{249}
$$

C.5.6 ef* combination

$$
\begin{aligned}
\hat{T}\hat{T}^\dagger &= \frac{\sqrt{18}}{32}(-ef^*)(3+\vec{\sigma_1}\cdot\vec{\sigma_2})(\vec{\sigma_1}-\vec{\sigma_2})\cdot q(\vec{\sigma_1}+\vec{\sigma_1})\cdot q\\
&=\frac{\sqrt{18}}{32}(-ef^*)(3+\sigma_{1i}\sigma_{2i})(\sigma_{1j}-\sigma_{2j})q_j(\sigma_{1k}+\sigma_{2k})q_k\\
&=\frac{\sqrt{18}}{32}(-ef^*)(3\sigma_{1j}-3\sigma_{2j}+\sigma_{1i}\sigma_{1j}\sigma_{2i}-\sigma_{1i}\sigma_{2i}\sigma_{2j})(\sigma_{1k}+\sigma_{2k})q_jq_k\\
&=\frac{\sqrt{18}}{32}(-ef^*)(3\sigma_{1j}\sigma_{1k}-3\sigma_{2j}\sigma_{1k}+\sigma_{1i}\sigma_{1j}\sigma_{1k}\sigma_{2i}-\sigma_{1i}\sigma_{1k}\sigma_{2i}\sigma_{2j}\\
&+3\sigma_{1j}\sigma_{2k}-3\sigma_{2j}\sigma_{2k}+\sigma_{1i}\sigma_{1j}\sigma_{2i}\sigma_{2k}-\sigma_{1i}\sigma_{2i}\sigma_{2j}\sigma_{2k})q_jq_k
\end{aligned}
\tag{250}
$$

$$
\begin{aligned}
Tr[\hat{T}\hat{T}^\dagger] = \frac{\sqrt{18}}{32}(-ef^*)Tr[&3\sigma_{1j}\sigma_{1k}I_2-\sigma_{1i}\sigma_{1k}\sigma_{2i}\sigma_{2j}\\
&-3I_1\sigma_{2j}\sigma_{2k}+\sigma_{1i}\sigma_{1j}\sigma_{2i}\sigma_{2k}]=0
\end{aligned}
\tag{251}
$$

$$
\begin{aligned}
Tr[\vec{p}_2\cdot\vec{\sigma}_2\hat{T}\hat{T}^\dagger] &= \frac{\sqrt{18}}{32}(-ef^*)Tr[p_{2l}(\sigma_{1i}\sigma_{1j}\sigma_{1k}\sigma_{2l}\sigma_{2i}-\sigma_{1i}\sigma_{1k}\sigma_{2l}\sigma_{2i}\sigma_{2j}\\
&-3I_1\sigma_{2l}\sigma_{2j}\sigma_{2k}+\sigma_{1i}\sigma_{1j}\sigma_{2l}\sigma_{2i}\sigma_{2k})q_jq_k]\\
&=\frac{\sqrt{18}}{32}(-ef^*)Tr[p_{2l}(2i\epsilon_{ijk}2\delta_{li}-2\delta_{ik}2i\epsilon_{lij}\\
&-3\cdot 2\cdot 2i\epsilon_{ljk}+2\delta_{ij}2i\epsilon_{lik})q_jq_k]\\
&=\frac{\sqrt{18}}{32}(-ef^*)[p_{2l}(4i\epsilon_{ljk}+4i\epsilon_{lkj}-12i\epsilon_{ljk}+4i\epsilon_{ljk})q_jq_k]\\
&=0
\end{aligned}
\tag{252}
$$

C.6 F terms

C.6.1 fa* combination

$$\begin{aligned}\hat{T}\hat{T}^\dagger &= \frac{\sqrt{6}}{16} f a^* (\vec{\sigma_1} + \vec{\sigma_2}) \cdot q (1 - \vec{\sigma_1} \cdot \vec{\sigma_2}) \\ &= \frac{\sqrt{6}}{16} f a^* (\sigma_{1i} + \sigma_{2i}) q_i (1 - \sigma_{1j}\sigma_{2j}) \\ &= \frac{\sqrt{6}}{16} f a^* (\sigma_{1i} + \sigma_{2i} - \sigma_{1i}\sigma_{1j}\sigma_{2j} + \sigma_{1i}\sigma_{2i}\sigma_{2j}) q_i\end{aligned} \tag{253}$$

$$Tr[\hat{T}\hat{T}^\dagger] = \frac{\sqrt{6}}{16} f a^* Tr[\sigma_{1i} + \sigma_{2i} - \sigma_{1i}\sigma_{1j}\sigma_{2j} + \sigma_{1i}\sigma_{2i}\sigma_{2j}) q_i] = 0 \tag{254}$$

$$\begin{aligned}Tr[\vec{p}_2 \cdot \vec{\sigma}_2 \hat{T}\hat{T}^\dagger] &= \frac{\sqrt{6}}{16} f a^* Tr[p_{2k}(I_1 \sigma_{2l}\sigma_{2i} - \sigma_{1i}\sigma_{1j}\sigma_{2l}\sigma_{2j}) q_i] \\ &= \frac{\sqrt{6}}{16} f a^* [p_{2l}(2 \cdot 2\delta_{li} - 2\delta_{ij} 2\delta_{lj}) q_i] = 0\end{aligned} \tag{255}$$

C.6.2 fb* combination

$$\begin{aligned}\hat{T}\hat{T}^\dagger &= \frac{\sqrt{6}}{32} f b^* (\vec{\sigma_1} + \vec{\sigma_2}) \cdot q (\vec{\sigma_1} - \vec{\sigma_2}) \cdot q (1 - \vec{\sigma_1} \cdot \vec{\sigma_2}) \\ &= \frac{\sqrt{6}}{32} f b^* (\sigma_{1i} + \sigma_{2i}) q_i (\sigma_{1j} - \sigma_{2j}) q_j (1 - \sigma_{1k}\sigma_{2k}) \\ &= \frac{\sqrt{6}}{32} f b^* (\sigma_{1i} + \sigma_{2i})(\sigma_{1j} - \sigma_{2j} - \sigma_{1j}\sigma_{1k}\sigma_{2k} + \sigma_{1k}\sigma_{2j}\sigma_{2k}) q_i q_j \\ &= \frac{\sqrt{6}}{32} f b^* (\sigma_{1i}\sigma_{1j} - \sigma_{1i}\sigma_{2j} - \sigma_{1i}\sigma_{1j}\sigma_{1k}\sigma_{2k} + \sigma_{1i}\sigma_{1k}\sigma_{2j}\sigma_{2k} \\ &+ \sigma_{1j}\sigma_{2i} - \sigma_{2i}\sigma_{2j} - \sigma_{1j}\sigma_{1k}\sigma_{2i}\sigma_{2k} + \sigma_{1k}\sigma_{2i}\sigma_{2j}\sigma_{2k}) q_i q_j\end{aligned} \tag{256}$$

$$\begin{aligned}Tr[\hat{T}\hat{T}^\dagger] = \frac{\sqrt{6}}{32} f b^* Tr[&(\sigma_{1i}\sigma_{1j} I_2 + \sigma_{1i}\sigma_{1k}\sigma_{2j}\sigma_{2k} \\ &- I_1 \sigma_{2i}\sigma_{2j} - \sigma_{1j}\sigma_{1k}\sigma_{2i}\sigma_{2k}) q_i q_j] \\ &= \frac{\sqrt{6}}{32} f b^* [4\delta_{ij} + 4\delta_{ij} - 4\delta_{ij} - 4\delta_{ij}] q_i q_j = 0\end{aligned} \tag{257}$$

$$\begin{aligned}Tr[\vec{p}_2 \cdot \vec{\sigma}_2 \hat{T}\hat{T}^\dagger] = \frac{\sqrt{6}}{32} f b^* Tr[&p_{2l}(-\sigma_{1i}\sigma_{1j}\sigma_{1k}\sigma_{2l}\sigma_{2j} + \sigma_{1i}\sigma_{1j}\sigma_{2l}\sigma_{2j}\sigma_{2k} \\ &- I_1 \sigma_{2l}\sigma_{2i}\sigma_{2k} - \sigma_{1j}\sigma_{1k}\sigma_{2l}\sigma_{2i}\sigma_{2j}) q_i q_k] \\ &= \frac{\sqrt{6}}{32} f b^* [p_{2l}(-2i\epsilon_{ijk} 2\delta_{lj} + 2\delta_{ij} 2i\epsilon_{ljk} \\ &- 2 \cdot 2i\epsilon_{lik} - 2i\epsilon_{jkl} 2\delta_{ij}) q_i q_k] \\ &= \frac{\sqrt{6}}{32} f b^* [p_{2l}(-4i\epsilon_{ilk} + 4i\epsilon_{lik} - 4i\epsilon_{lik} - 4i\epsilon_{ikl}) q_i q_k] = 0\end{aligned} \tag{258}$$

C.6.3 fc* combination

$$\begin{aligned}\hat{T}\hat{T}^\dagger &= \frac{\sqrt{6}}{16} fc^*(\vec{\sigma_1}+\vec{\sigma_2})\cdot q(3+\vec{\sigma_1}\cdot\vec{\sigma_2}) \\ &= \frac{\sqrt{6}}{16} fc^*(\sigma_{1i}+\sigma_{2i})p_i(3+\sigma_{1j}\sigma_{2j}) \\ &= \frac{\sqrt{6}}{16} fc^*(3\sigma_{1i}+3\sigma_{2i}+\sigma_{1i}\sigma_{1j}\sigma_{2j}+\sigma_{1j}\sigma_{2i}\sigma_{2j})q_i\end{aligned} \tag{259}$$

$$Tr[\hat{T}\hat{T}^\dagger] = 0 \tag{260}$$

$$\begin{aligned}Tr[\vec{p}_2\cdot\vec{\sigma}_2\hat{T}\hat{T}^\dagger] &= \frac{\sqrt{6}}{16} fc^* Tr[p_{2k}(3I_1\sigma_{2k}\sigma_{2i}+\sigma_{1i}\sigma_{1j}\sigma_{2k}\sigma_{2j})q_i] \\ &= \frac{\sqrt{6}}{16} fc^*[p_{2k}(3\cdot 2\cdot 2\delta_{ki}+2\delta_{ij}2\delta_{kj})q_i] \\ &= \frac{\sqrt{6}}{16} fc^*[p_{2k}(12\delta_{ik}+4\delta_{ik})q_i] = \sqrt{6} fc^*(\vec{p}_2\cdot\vec{q})\end{aligned} \tag{261}$$

C.6.4 fd* combination

$$\begin{aligned}TT^* &= \frac{\sqrt{3}fd^*}{8}(\vec{\sigma_1}+\vec{\sigma_2})\cdot q(3\vec{\sigma_1}\cdot q\vec{\sigma_2}\cdot q-\vec{\sigma_1}\cdot\vec{\sigma_2}) \\ &= \frac{\sqrt{3}fd^*}{8}(\sigma_{1i}+\sigma_{2i})q_i(3\sigma_{1j}q_j\sigma_{2k}q_k-\sigma_{1m}\sigma_{2m}) \\ &= \frac{\sqrt{3}fd^*}{8}(3\sigma_{1i}\sigma_{1j}\sigma_{2k}q_iq_jq_k-\sigma_{1i}\sigma_{1m}\sigma_{2m}q_i \\ &+ 3\sigma_{1j}\sigma_{2i}\sigma_{2k}q_iq_jq_k-\sigma_{1m}\sigma_{2i}\sigma_{2m}q_i)\end{aligned} \tag{262}$$

$$Tr[\hat{T}\hat{T}^\dagger] = 0 \tag{263}$$

$$\begin{aligned}Tr[\vec{p}_2\cdot\vec{\sigma}_2\hat{T}\hat{T}^\dagger] &= \frac{\sqrt{3}fd^*}{8} Tr[p_2l(3\sigma_{1i}\sigma_{1j}\sigma_{2l}\sigma_{2k}q_iq_jq_k-\sigma_{1i}\sigma_{1m}\sigma_{2l}\sigma_{2m}q_i)] \\ &= \frac{\sqrt{3}fd^*}{8}[p_{2l}(3\cdot 2\delta_{ij}2\delta_{lk}q_iq_jq_k-2\delta_{im}2\delta_{lm}q_i)] \\ &= \frac{\sqrt{3}fd^*}{8}[12q^2p_{2l}q_l-4P_{2l}q_l] \\ &= \sqrt{3}fd^*(\vec{p}_2\cdot\vec{q})\end{aligned} \tag{264}$$

C.6.5 fe* combination

$$\begin{aligned}\hat{T}\hat{T}^\dagger &= -\frac{\sqrt{18}}{32} f e^* (\vec{\sigma_1} + \vec{\sigma_2}) \cdot q (\vec{\sigma_1} - \vec{\sigma_2}) \cdot q (3 + \vec{\sigma_1} \cdot \vec{\sigma_2}) \\ &= -\frac{\sqrt{18}}{32} f e^* (\sigma_{1i} + \sigma_{2i}) q_i (\sigma_{1j} - \sigma_{2j}) q_j (3 + \sigma_{1k}\sigma_{2k}) \\ &= -\frac{\sqrt{18}}{32} f e^* (\sigma_{1i} + \sigma_{2i})(3\sigma_{1j} - 3\sigma_{2j} + \sigma_{1j}\sigma_{1k}\sigma_{2k} - \sigma_{1k}\sigma_{2j}\sigma_{2k}) q_i q_j \\ &= -\frac{\sqrt{18}}{32} f e^* (3\sigma_{1i}\sigma_{1j} - 3\sigma_{1i}\sigma_{2j} + \sigma_{1i}\sigma_{1j}\sigma_{1k}\sigma_{2k} - \sigma_{1i}\sigma_{1k}\sigma_{2j}\sigma_{2k} \\ &+ 3\sigma_{1j}\sigma_{2i} - 3\sigma_{2i}\sigma_{2j} + \sigma_{1j}\sigma_{1k}\sigma_{2i}\sigma_{2k} - \sigma_{1k}\sigma_{2i}\sigma_{2j}\sigma_{2k}) q_i q_j \end{aligned} \tag{265}$$

$$\begin{aligned} Tr[\hat{T}\hat{T}^\dagger] = -\frac{\sqrt{18}}{32} f e^* Tr[&(3\sigma_{1i}\sigma_{1j} I_2 - \sigma_{1i}\sigma_{1k}\sigma_{2j}\sigma_{2k} \\ &- 3 I_1 \sigma_{2i}\sigma_{2j} + \sigma_{1j}\sigma_{1k}\sigma_{2i}\sigma_{2k}) q_i q_j] = 0 \end{aligned} \tag{266}$$

$$\begin{aligned} Tr[\vec{p}_2 \cdot \vec{\sigma}_2 \hat{T}\hat{T}^\dagger] &= -\frac{\sqrt{18}}{32} f e^* Tr[p_{2l}(\sigma_{1i}\sigma_{1j}\sigma_{1k}\sigma_{2l}\sigma_{2k} - \sigma_{1i}\sigma_{1k}\sigma_{2l}\sigma_{2j}\sigma_{2k} \\ &- 3 I_1 \sigma_{2l}\sigma_{2i}\sigma_{2j} + \sigma_{1j}\sigma_{1k}\sigma_{2l}\sigma_{2i}\sigma_{2k}) q_i q_j] \\ &= -\frac{\sqrt{18}}{32} f e^* [p_{2l}(2i\epsilon_{ijk} 2\delta_{lk} - 2\delta_{ik} 2i\epsilon_{ljk} \\ &- 3 \cdot 2 \cdot 2i\epsilon_{lij} + 2\delta_{jk} 2i\epsilon_{lij}) q_i q_j] \\ &= -\frac{\sqrt{18}}{8} f e^* [p_{2l}(i\epsilon_{ijl} - i\epsilon_{lji} - 3i\epsilon_{lij} + i\epsilon_{lij}) q_i q_j] = 0 \end{aligned} \tag{267}$$

C.6.6 ff* combination

$$\begin{aligned}\hat{T}\hat{T}^\dagger &= \frac{6}{16}|f|^2 (\vec{\sigma_1} + \vec{\sigma_2}) \cdot q (\vec{\sigma_1} + \vec{\sigma_2}) \cdot q \\ &= \frac{6}{16}|f|^2 (\sigma_{1i} + \sigma_{2i}) q_i (\sigma_{1j} + \sigma_{2j}) q_j \\ &= \frac{6}{16}|f|^2 (\sigma_{1i}\sigma_{1j} + \sigma_{2i}\sigma_{2j} + \sigma_{1i}\sigma_{2j} + \sigma_{2i}\sigma_{1j}) p_i p_j \end{aligned} \tag{268}$$

$$\begin{aligned} Tr[\hat{T}\hat{T}^\dagger] &= \frac{6}{16}|f|^2 Tr[(\sigma_{1i}\sigma_{1j} I_2 + I_1 \sigma_{2i}\sigma_{2j})] \\ &= \frac{6}{16}|f|^2 [(2 \cdot 2\delta_{ij} + 2 \cdot 2\delta_{ij}) q_i q_j] = 3|f|^2 \end{aligned} \tag{269}$$

$$\begin{aligned} Tr[\vec{p}_2 \cdot \vec{\sigma}_2 \hat{T}\hat{T}^\dagger] &= \frac{6}{16}|f|^2 Tr[p_{2l}(I_1 \sigma_{2l}\sigma_{2i}\sigma_{2j}) q_i q_j] \\ &= \frac{6}{16}|f|^2 [p_{2l}(2 \cdot 2i\epsilon_{lij} q_i q_j)] \\ &= \frac{6}{4}|f|^2 [\vec{p}_2 \cdot (\vec{q} \times \vec{q})] = 0 \end{aligned} \tag{270}$$